Natural Resources Canada | Ressources naturelles Canada

GEOLOGICAL SURVEY OF CANADA
OPEN FILE 7748

Quaternary geology and till composition north of Wager Bay, Nunavut: results from the GEM Wager Bay Surficial Geology Project

I. McMartin, J.E. Campbell, L.A. Dredge, A.N. LeCheminant, M.W. McCurdy and N. Scromeda

2015

Canada

GEOLOGICAL SURVEY OF CANADA
OPEN FILE 7748

Quaternary geology and till composition north of Wager Bay, Nunavut: results from the GEM Wager Bay Surficial Geology Project

I. McMartin, J.E. Campbell, L.A. Dredge, A.N. LeCheminant, M.W. McCurdy and N. Scromeda

2015

doi:10.4095/296419

This publication is available for free download through GEOSCAN (http://geoscan.nrcan.gc.ca).

Recommended citation
McMartin, I., Campbell, J.E., Dredge, L.A., LeCheminant, A.N., McCurdy, M.W., and Scromeda, N., 2015. Quaternary geology and till composition north of Wager Bay, Nunavut: results from the GEM Wager Bay Surficial Geology Project; Geological Survey of Canada, Open File 7748, 1 .zip file. doi:10.4095/296419

Publications in this series have not been edited; they are released as submitted by the author.

TABLE OF CONTENTS

Appendices
The Readme file provides the complete list of files and sub-directories containing the datasets:

1. Field site location and description
2. Ice-movement indicator location and description
3. Sample location and description
4. Till geochemistry, <0.063 mm, ICP-MS, aqua regia digestion
5. Till geochemistry, <0.063 mm, ICP-MS, 4-acids digestion
6. Till geochemistry, <0.063 mm, ICP-ES/MS, lithium borate fusion
7. Till matrix color and sand-silt-clay distribution
8. Till matrix carbon and carbonate contents, <0.063 mm
9. Till pebble counts, 8-30 mm, % counted
10. Gold grain and indicator mineral counts (0.25-2 mm)
11. Electron microprobe analysis of selected grains
12. Analysis of ultramafic lamprophyre boulder

List of tables

List of figures

Isabelle McMartin, Janet E. Campbell, Lynda A. Dredge, Tony N. LeCheminant, Martin W. McCurdy and Nicole Scromeda
Geological Survey of Canada, 601 Booth Street, Ottawa, ON K1A 0E8

QUATERNARY GEOLOGY AND TILL COMPOSITION NORTH OF WAGER BAY, NUNAVUT: RESULTS FROM THE GEM WAGER BAY SURFICIAL GEOLOGY PROJECT

I. McMartin, J.E. Campbell, L.A. Dredge, A.N. LeCheminant, M.W. McCurdy and N. Scromeda

ABSTRACT

This report presents the field database and analytical results from the Geological Survey of Canada's 2010 to 2012 surficial geology mapping and till sampling campaign in the north Wager Bay project area, mainland Nunavut. An overview of the Quaternary geology of this area is provided together with an interpretation of till provenance, as well as a discussion on the implications for mineral exploration. Field observations and surficial geological mapping indicate the region is key for the glacial history reconstruction of the northeastern part of the Keewatin Sector of the Laurentide Ice Sheet. Most of the study area was located within an extensive onset zone of a large ice stream flowing north into Committee Bay during the last glaciation and early deglaciation, from an ice divide located over and/or south of Wager Bay. Major ice-flow reversals into Repulse Bay and Wager Bay, as a result of drawdown into the opening marine waters in Hudson Bay, are indicated for the latest deglaciation phases. Cold-based ice remnant masses over the uplands north of Wager Bay preserved relict, weathered and fresh glacial landscapes at the end of deglaciation. Although there is evidence of multiple ice-flow directions in the study area, the main ice-flow phase, which converges north (NNE to NNW) towards Committee Bay, is the predominant direction of glacial transport and shaped most prominent streamlined landforms. The carbonate clast content and Al_2O_3 concentrations in surface till indicates relatively long glacial transport distances linked to glacial dispersal by the ice stream.

Mg-rich olivine, many having $>Fo_{90}$ and high NiO contents, are abundant in till in the center of the study area where a frost-shattered ultramafic lamprophyre boulder was found at the surface. Location of the boulder, its distinctive composition, and the olivine in till distribution in conjunction with the glacial transport history, suggest an ultramafic bedrock source other than kimberlite fields known in the region. In the western part of the study area south of Walker Lake, forsteritic olivine and chromite grains in till, locally coincident with ultramafic boulders, form a 35 km-long NNE dispersal train. This dispersal plume points to olivine-rich crustal rocks within undifferentiated Archean supracrustal rocks, and suggests these rocks have potential to host Ni-Cu-PGE mineralization. In addition to known Penhryn Group rocks and extensions of this belt to the southwest, there are suspected but poorly mapped strands of supracrustal rocks between Beach Pt and Wager Bay which show potential for base- and/or precious-metal mineralization. More detailed till sampling, prospecting and bedrock mapping is required to better assess mineral potential in these areas.

INTRODUCTION

The Wager Bay region of mainland Nunavut west of Repulse Bay (Fig. 1) is covered by extensive Quaternary glacial and post-glacial sediments underlain by permafrost yet only reconnaissance scale surficial geology maps with limited field-based observations are available for this area (Prest et al., 1968; Aylsworth and Shilts, 1989a). While this region lies within the western Churchill Geological Province

where active diamond, gold and base metal exploration is ongoing, its central part is protected from mineral exploration and development within the Ukkusiksalik National Park. In order to provide a Quaternary geological framework that would contribute to effective management of the terrain and evaluation of mineral and park resources, the Geological Survey of Canada (GSC) initiated in 2010 a surficial geological mapping activity as part of the Geo-mapping for Energy and Minerals (GEM-1) Program. The project focused on surficial geological mapping at 1:100 000 scale to fill in a major gap in map coverage, the completion of a regional-scale till sampling survey (10-km spacing) to document glacial transport characteristics, and the study of glacial and post-glacial histories, in support of mineral exploration, sustainable resource development and land-use management. This report releases the complete field database and analytical results from the 2010, 2011 and 2012 field seasons (superseding GSC OF 7288; McMartin et al., 2013a) and provides an overview of the Quaternary geology and economic implications for surface mineral exploration in the north Wager Bay project area (Fig. 1). Current work includes surficial geology mapping (Campbell et al., 2013a-d; Campbell and McMartin, 2014; Dredge et al., 2013a-c, in prep.; McMartin et al., 2015) and remote predictive mapping of surficial materials (Campbell et al., 2013e; Wityk, 2014; Wityk et al., 2011, 2012, 2013a-b) which are augmenting the Quaternary geological knowledge base for reconstructing glacial and post-glacial histories of the area (Campbell and McMartin, 2010, 2011; Campbell et al., 2011, 2013f; McMartin et al., 2012, 2013b).

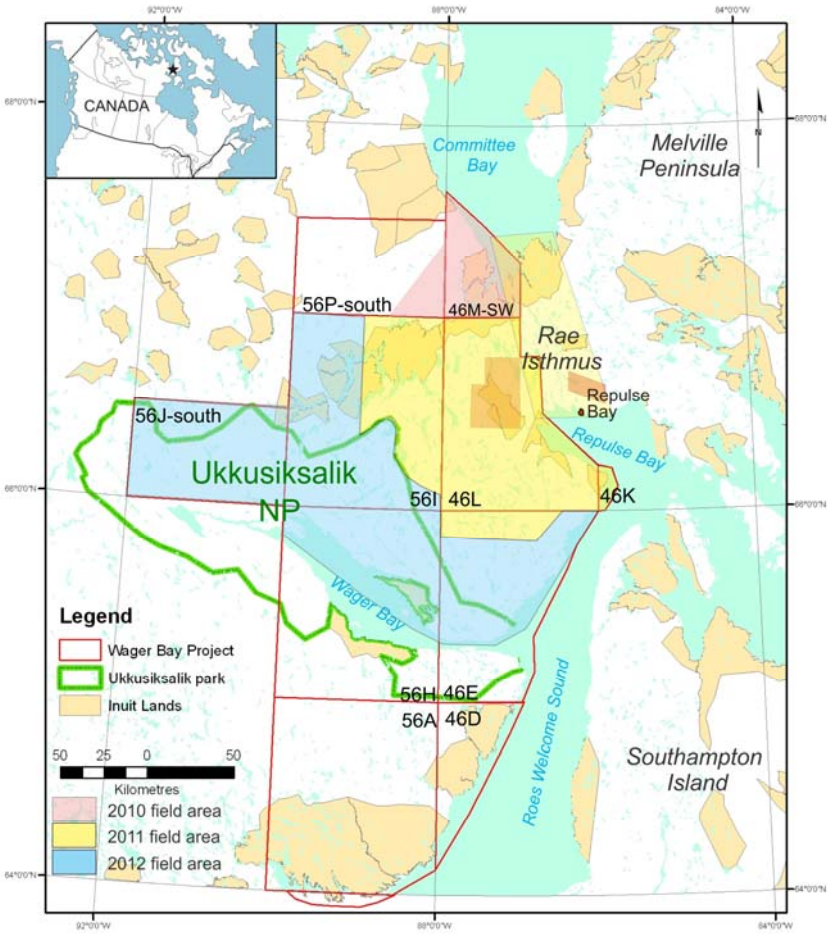

Figure 1. Location of Wager Bay project area showing NTS map sheets (outlined in red) and each field season's areal coverage. Targeted field data were also collected south of Wager Bay in 2012 as part of the Geo-mapping Frontiers' Tehery-Cape Dobbs project (McMartin et al., 2013c).

Location and physiography

The project area lies both north and south of Wager Bay in central Nunavut, between latitudes 64° and 68° and longitudes 86° and 92°, and immediately west of the community of Repulse Bay (Fig. 1). It covers three complete NTS map sheets at 1:250 000 scale (NTS 56A, 56H, 56I) and parts of 6 others (NTS 46D-mainland, 46E-mainland, 46K-southwest, 46L-south and -west, 46M-southwest, and 56J-south). NTS 56P-south, previously field mapped and sampled during the GSC's Committee Bay TGI-1 Project in 2002 (e.g. McMartin et al., 2003a-b; Little, 2004), is also included because surficial geology maps were revised, edited and released as part of the current GEM-1 project (Campbell et al., 2013a-d). Field activities in 2010, 2011 and 2012 were concentrated north of Wager Bay and covered approximately 30,000 km^2 (Fig. 2). South of Wager Bay, targeted till sampling in 2012 was completed as part of the GEM-1 Geo-mapping Frontier's Tehery-Cape Dobbs project (McMartin et al., 2013c) while reconnaissance surficial geology maps based primarily on air photo interpretation were compiled for the Daly Bay (NTS 56A) and Yellow Bluffs (NTS 46D) map sheets (Dredge et al., 2013a-c).

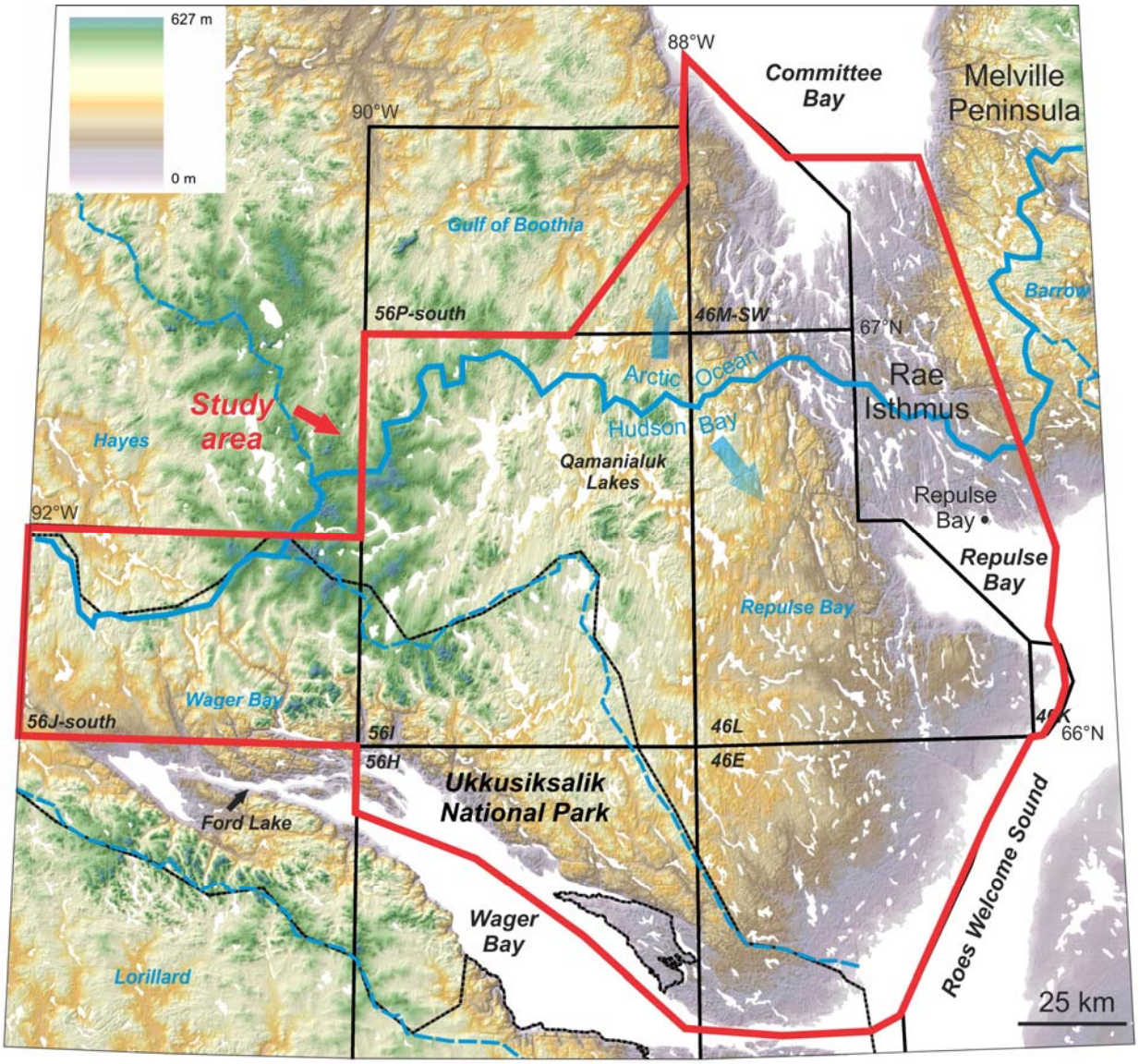

Figure 2. DEM generated from CDED 1:50K topography. Area with 2010, 2011 and 2012 data reported in this Open File is outlined in red ("Study area"). Regional watershed limits are shown in blue and dashed blue.

The Wager Bay north study area lies in the Kazan Physiographic Region of Canada within the Wager Plateau Division (Bostock, 1967). Elevations range from sea level rising westward to 520 m asl in the Qamanialuk Lakes area and northward to 627 m asl in uplands north of Ford Lake. Rae Isthmus forms low-lying terrain at less than 125 m asl connecting the Wager Plateau to Melville Peninsula. Drainage is predominantly towards Hudson Bay via rivers that drain into Repulse Bay and Roes Welcome Sound, and into Wager Bay (Fig. 2). The northernmost parts of the study area drain towards the Arctic Ocean via Committee Bay and Hayes River. Physiography consists of generally low relief with gently rolling hills interspersed by glacially scoured lakes, shallow valleys and depressions, and generally minor bedrock ridges and plateaus. Relief is somewhat more pronounced in the Qamanialuk Lakes area where Proterozoic rocks of the Penhryn Group form prominent ENE-WSW trending bedrock ridges, and along the northwestern shores of Wager Bay and north of Ford Lake where deep U-shaped valleys dissect high plateaus that extend inland for a few 10s of km.

The area lies within the Wager Plateau Ecoregion of Canada (#30) having a mean annual temperature of approximately -11°C (summer mean of 4.5°C; winter mean of -26.5°C) and a mean annual precipitation of 200-300 mm (http://ecozones.ca/english/region/30.html). It is characterized by continuous permafrost with low ice content and a discontinuous tundra vegetation cover. Turbic and Static Cryosols developed on sandy diamicton and glaciofluvial deposits are the dominant soils, while large areas of Regosolic Static Cryosols are associated with thick marine deposits along the coast of Committee Bay.

Geological setting and previous work

Bedrock geology

The study area lies within the 2.7-2.6 Ga Rae craton of the western Churchill Geological Province. It is underlain by a variety of Archean through Paleoproterozoic supracrustal and intrusive rocks, and, except for the Committee Bay supracrustal belt area over NTS 56P-south, has had little geological field mapping since the 1960's (Heywood, 1967) (Fig. 3). Interest by Parks Canada in the development of a national park in the Wager Bay area prompted a mineral-resource assessment by the GSC that resulted in thematic studies and detailed bedrock geology mapping within the proposed park boundaries around Wager Bay (cf. Jefferson et al., 1991, 1993; Chandler et al., 1993).

Bedrock geology north of Wager Bay comprises the Committee Bay supracrustal belt in NTS 56P-south, composed of Prince Albert Group (PAG) rocks dominated by semipelite and psammite with lesser iron-formation, quartzite, komatiite, komatiitic basalt and felsic metavolcanic rocks (i.e. Skulski et al., 2003; Sandeman et al., 2004). These rocks are intruded by diverse Archean plutonic bodies including granodiorite and monzogranite. To the south and east of this belt, rocks that comprise part of the southern Walker Lake intrusive complex consist of foliated, ca. 2.61 Ga magnetite-bearing, K-feldspar-megacrystic granodiorite and monzogranite, older granodiorite gneiss, and younger ca. 1.82 Ga biotite-fluorite Hudsonian monzogranite (Peterson et al., 2002). These younger granites are abundant throughout the northeastern Rae domain and extend to the SW towards Ford Lake (e.g., Ford Lake batholith; LeCheminant et al., 1987). Most of the southeastern portion of the study area is underlain by mixed gneisses (amphibolite gneiss, homblende-biotite gneiss, granitoid gneiss and migmatite; in part derived from sedimentary and volcanic rocks) and generally foliated to gneissic granitoid rocks (undifferentiated) (Heywood, 1967; Jefferson et al., 1991; Skulski et al., unpublished). Some of these rocks engulf Archean supracrustal screens of komatiite, quartzite, banded iron formation (BIF), amphibolite, and semipelite. Metamorphosed Paleoproterozoic cover sequence rocks, part of the Penrhyn Group, outcrop in a narrow

ENE-trending belt north and west of Repulse Bay. These Penrhyn Group rocks contain unsubdivided pelitic gneiss, marble and metawacke gneiss and schist, with minor metabasalt, gabbro and thin quartzite. Areas offshore in Repulse Bay and Roes Welcome Sound are underlain by undifferentiated Paleozoic Hudson Platform sequence carbonate rocks.

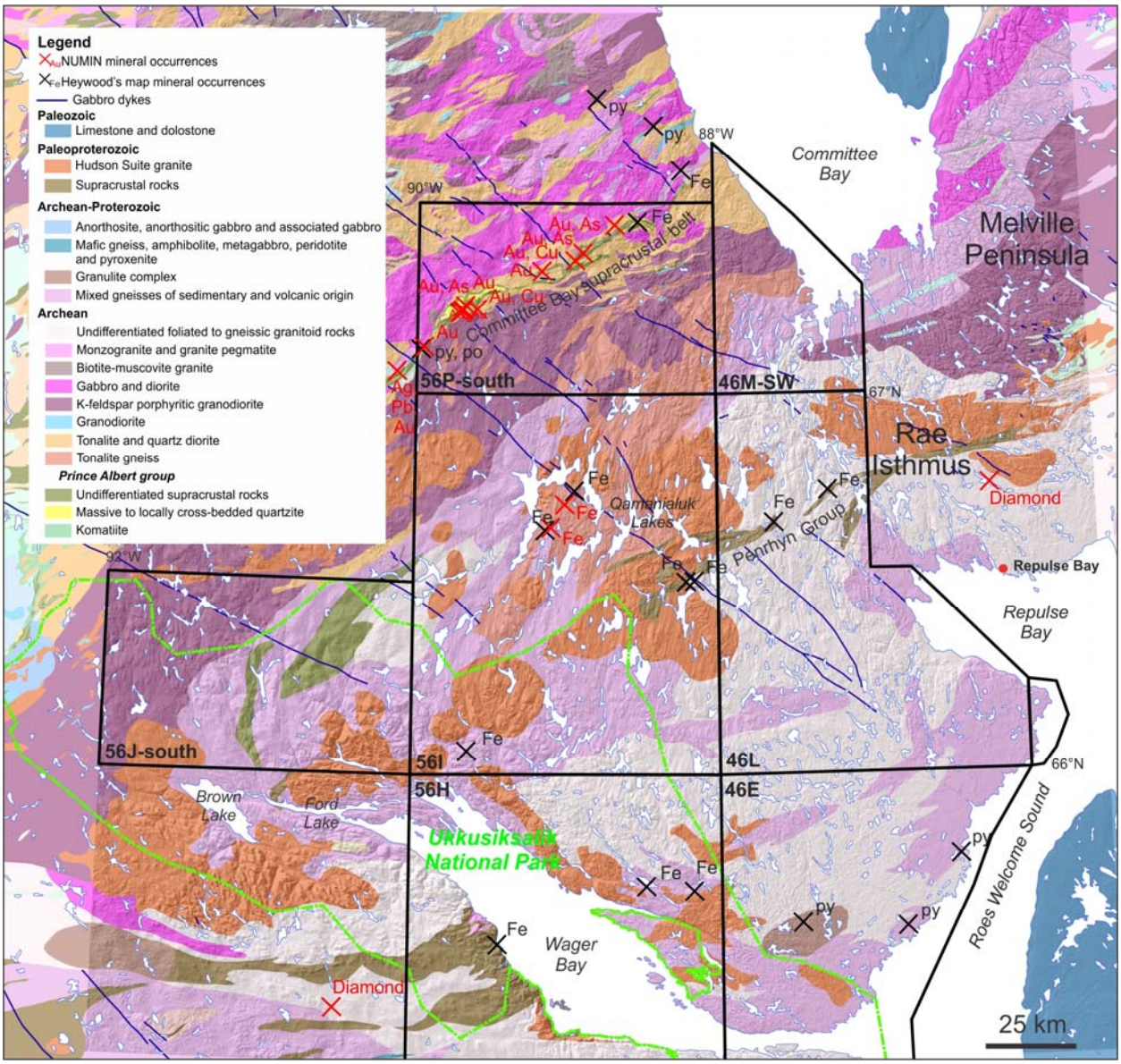

Figure 3. Geology of the Wager Bay North region (after Skulski et al., unpublished) showing mineral occurrences (from Heywood, 1967 and NUMIN: http://nunavutgeoscience.ca/pages/en/numin.html).

From a metallogenic perspective, supracrustal rocks of the PAG contain a number of proven (Au in iron formation) and possible commodities (Ni, Cu, PGE's in mafic and ultramafic volcanic and intrusive rocks) (Deyell and Sherlock, 2003; Sherlock and Deyell, 2003; Skulski et al., 2003). Recently, an emerald occurrence was found in drill core in the Anuri gold prospect area in the southeast part of the Committee Bay greenstone belt (http://northcountrygold.com/). Slivers and screens of equivalents of PAG rocks outcrop to the south of the Committee Bay greenstone belt and have similar mineral potential. Paleoproterozoic sediments of the Penhryn Group have potential for base metals (Pb-Zn ± Co, Cu, Ni, U,

Mo), Au and Ag (Heywood, 1967; Jefferson et al., 1991; Tremblay et al., 2010). Intrusive rocks, including the 1.84-1.80 Ga Hudson granite suite, have potential for Mo, Sn, W, U-REE, Pb-Zn and Cu (LeCheminant et al., 1987; Jefferson et al., 1991). Numerous diamondiferous kimberlites are known to outcrop and subcrop in the region (i.e. Nanuq, Qilalugaq, Aviat, Amaruk) which suggests there is potential for diamonds in the study area.

Quaternary Geology

During the last glaciation (Late Wisconsin), the Wager Bay region was affected mainly by Keewatin Sector Ice of the Laurentide Ice Sheet and its interplay with Foxe Ice Sector on Melville Peninsula (e.g. Dyke and Prest, 1987; Dredge, 2002). The region lay under the northeastern part of a major ice divide in Keewatin (Lee et al., 1957; Aylsworth and Shilts, 1989b; McMartin and Henderson, 2004). The Glacial Map of Canada depicts a handful of superimposed streamlined forms north of Wager Bay, ice-flow indicators that converge northward into Rae Isthmus, and others that diverge on either side of the Chantrey Moraine System which consists of a series of east-west ridges southwest of Committee Bay (Prest et al., 1968). Decreasing marine limit elevations from 240 m asl to 100-110 m asl southward are shown within the project area. The 1:1 million scale map compilation of Aylsworth and Shilts (1989a) depicts the study area with few surficial features except for eskers and small areas of streamlined landforms forming a distribution pattern that is roughly opposite on either side of Wager Bay, indicating northward ice flow north of the bay, and southeastward ice flow south of the bay (Fig. 4). Northward esker systems are shown to begin abruptly in NTS maps 56I-north and 56J-south, while eastward trending eskers are depicted within NTS 46L-south and 46E.

Smith's (1990) work in the proposed national park area brought to light a complex late glacial history for the immediate areas surrounding Wager Bay. Much of her work was based on the interpretation of glacial geomorphology, in particular till landforms and meltwater channels. North of Wager Bay within the Park's boundaries, patches of ribbed moraine and other glacial features such as glacial flutings and ice-scoured bedrock were interpreted as early ice flowing toward the south and southeast. A significant ice flow to the north from an ice divide lying south of Wager Bay was indicated by the presence of hundreds of crag-and-tail landforms, preserving some old landforms in frozen valleys. Glacial retreat was thought by Smith to be largely northward and characterized by breaking up of small remnant ice masses recorded by nested meltwater channels. Relative timing of the landforms and associated ice-flow phases were poorly constrained.

Drift lineations and other glacial landforms were compiled at different scales in the study area and adjacent regions based on remotely sensed data such as satellite imageries and digital elevation models (Boulton and Clark, 1990; Clark, 1997; De Angelis, 2007; De Angelis and Kleman, 2005, 2007, 2008; Kleman et al., 2002, 2010; Shaw et al. 2010a-b; Margold et al., 2015). These studies revealed cross-cutting drift lineations, areas of cold-based ice, end moraines and ice-streaming events. For some of these compilations, the lack of ground truthing resulted in misinterpretation of certain landforms (i.e. nature, sense of ice flow, relative chronology), or over-simplification (i.e. continuity, generalization in areas of complex ice flow).

Quaternary geology studies, surficial geological mapping and till sampling have been completed in adjacent areas; to the east of the study area over Melville Peninsula (e.g. Dredge, 1990, 1995, 2000, 2001, 2002, 2009; Tremblay and Paulen, 2012), to the north in the Committee Bay supracrustal belt area

(e.g. Ozyer and Hicock, 2002; Little et al., 2003; Giangioppi et al., 2003; McMartin et al., 2003a-b; Little, 2004; Utting et al., 2009), and to the southwest in NTS map sheet 56G (e.g. Dredge et al., 2005, 2006; McMartin and Dredge, 2005; Dredge and McMartin, 2007).

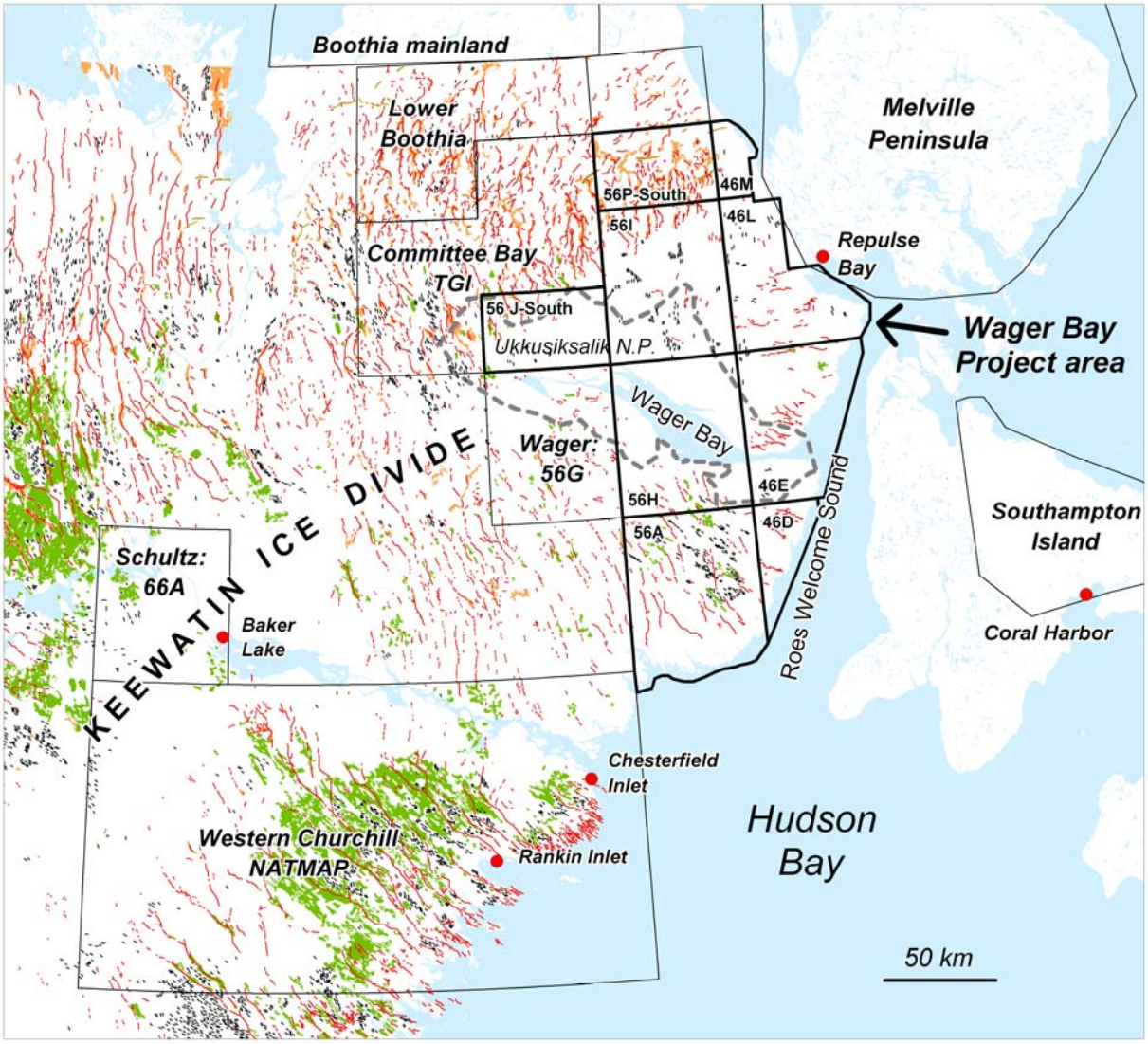

Figure 4. Regional Quaternary geology map showing location of eskers (red), streamlined landforms (black lines),ribbed moraine (green), glaciofluvial deposits (orange) and moraines (brown)(derived from Aylsworth and Shilts, 1989a). Wager Bay Project area (thick black lines) and recent government surficial mapping (field-based) project areas (thin black lines) are outlined.

METHODS

Field procedures

Field data collection

Field work was completed from July 16th to 28th in 2010, July 3rd to 25th in 2011, and June 28th to August 3rd in 2012 by Janet Campbell and Isabelle McMartin (GSC) with assistance from students and local hires, and visits from GSC and CNGO colleagues (L. Dredge, D. Corrigan and T. Tremblay). Access was primarily by helicopter from the town of Repulse Bay, but also from North Country Gold Corp. Hayes River Camp for a short period in 2012. Field work involved surficial mapping from

helicopter and foot traverses, field observations of surficial sediments and landforms, ice-flow indicator mapping, till sampling, and ground truthing of preliminary remote predictive maps. A total of 699 sites were visited (Fig. 5) and are described in Appendix 1.

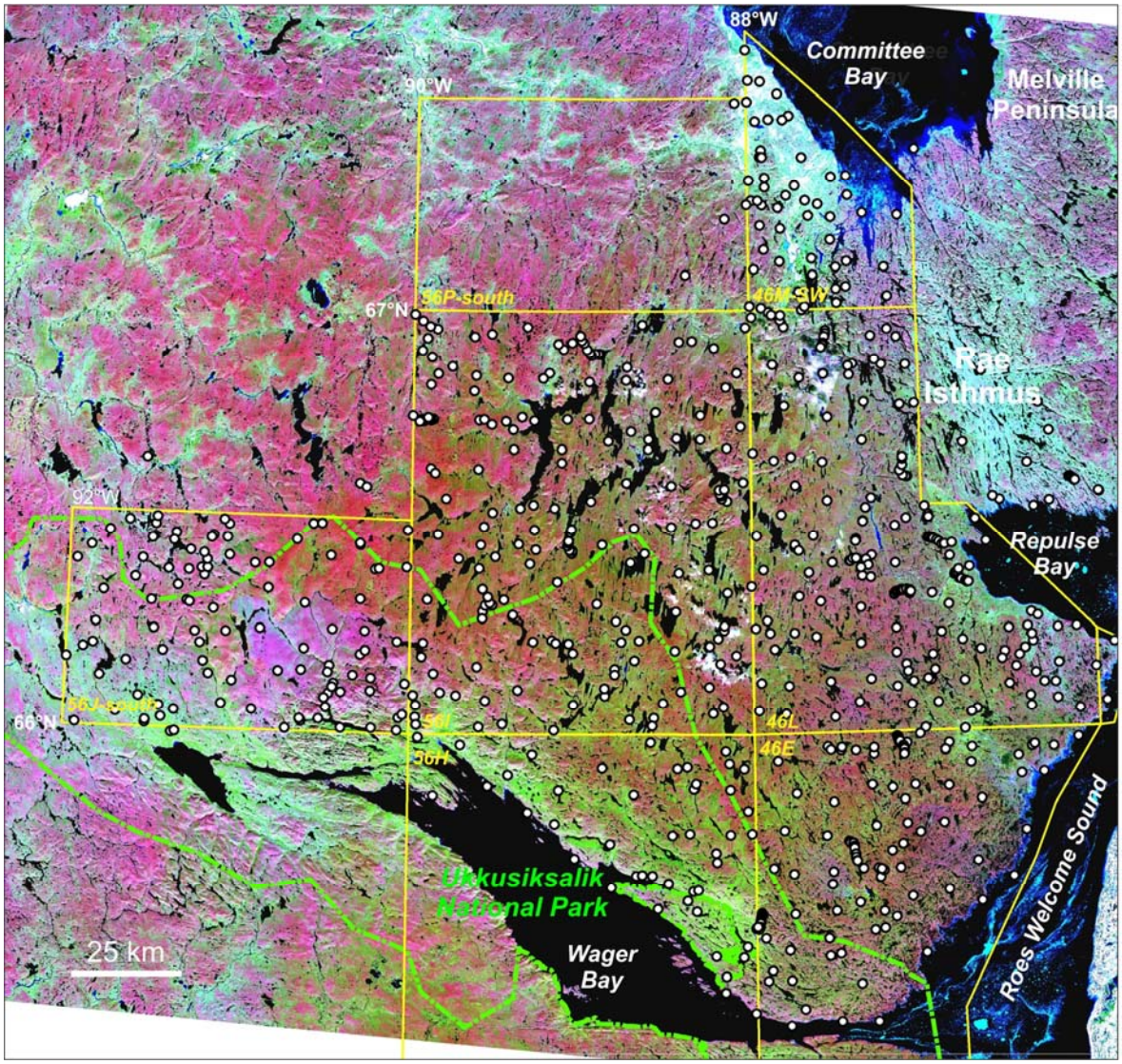

Figure 5. Location of field observation sites (white dots) in the Wager Bay North study area. Landsat TM 7 mosaic imagery using bands 742 appears in the background. Field site locations and descriptions are given in Appendix 1.

Ice-flow indicator mapping

The orientation and sense of 777 small-scale glacial erosional features on bedrock were measured from 345 sites (Fig. 6). Indicators of past ice flow include striations (deep and fine), microstriae, grooves, nail-head striae, reverse nail-head striae, rat tails, chattermarks, crescentic fractures and gouges, stoss and lee forms, whaleback forms, and roches moutonnées (Figs. 7&8). The sense of ice-flow movement was derived from nail-head striae, rat tails, crescentic fractures, and roches moutonnées, or from stoss and lee topography. Relative ages of striated facets were established at 224 sites (Fig. 6). Most sites were located on outcrops nearby till sampling sites, including many from bedrock crags and lakeshores. Several sites were also located along the rocky shorelines of Wager Bay, Roes Welcome Sound and Repulse Bay. Ice-flow indicator measurement locations and descriptions are provided in Appendix 2.

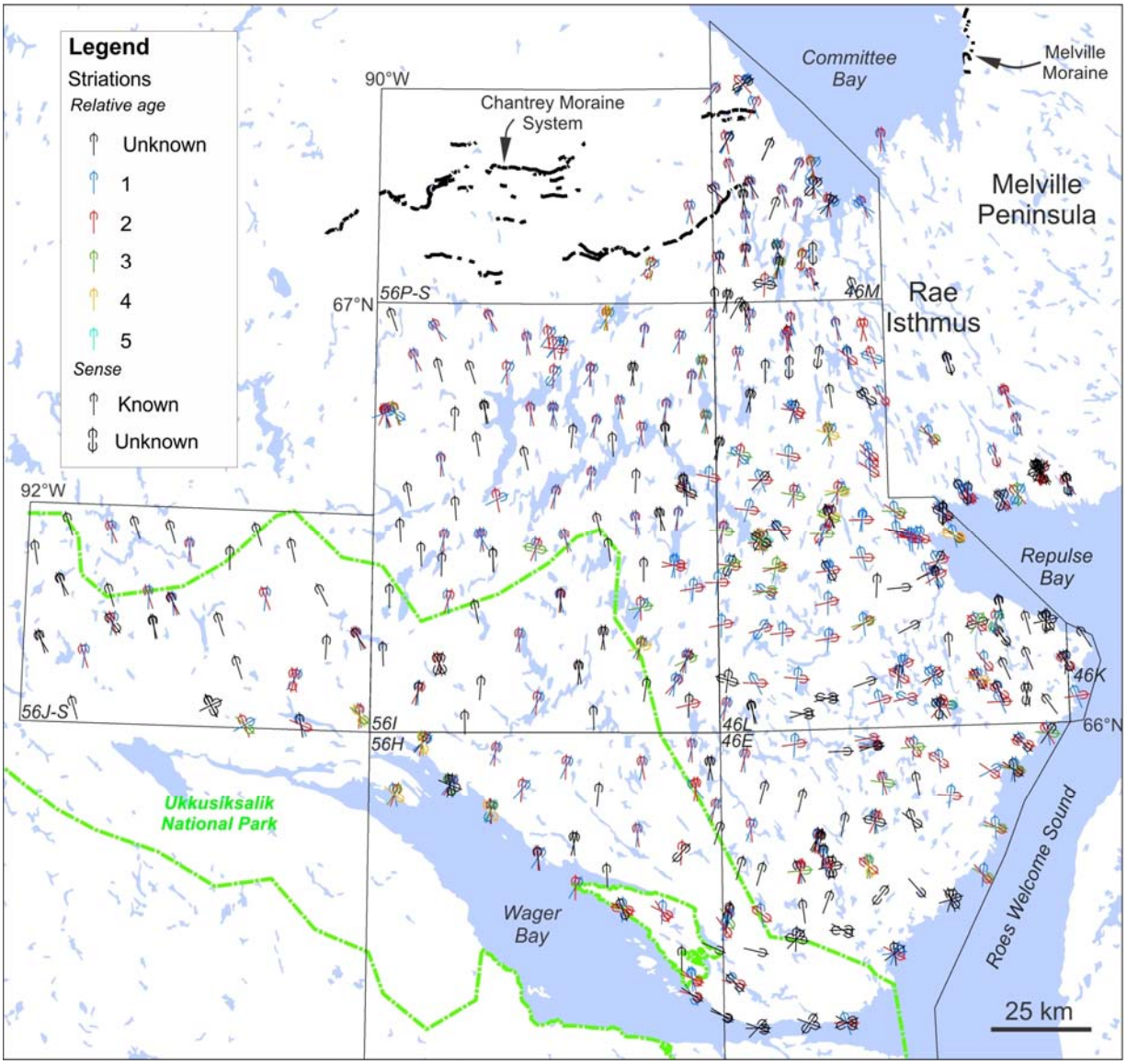

Figure 6. Map of small erosional ice-flow indicators (mainly striations) showing trends and relative ages at each site. Detailed field descriptions and locations of the ice-flow indicators are given in Appendix 2.

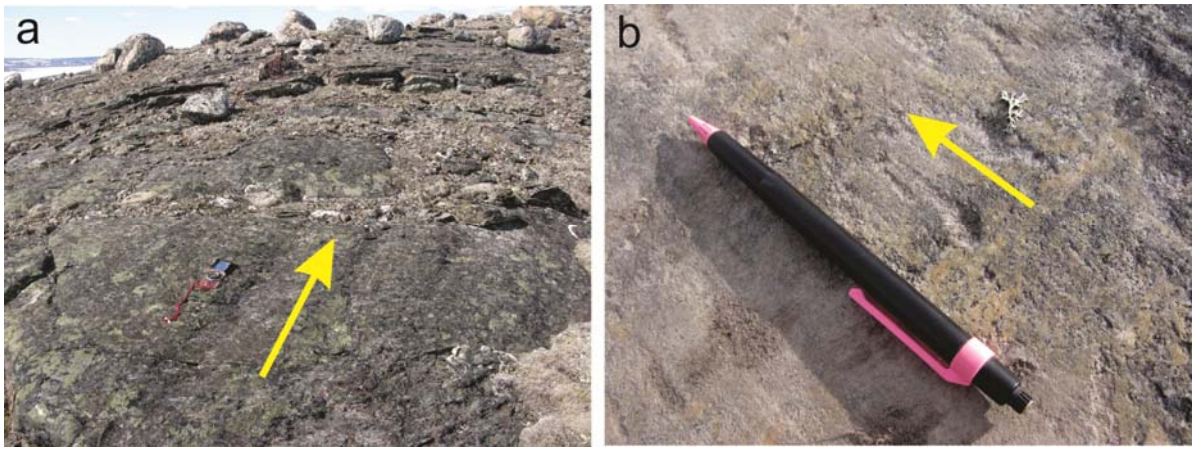

Figure 7. Photographs of deep grooves (a) and reverse nail-head striae (b). Arrow indicates sense of flow.

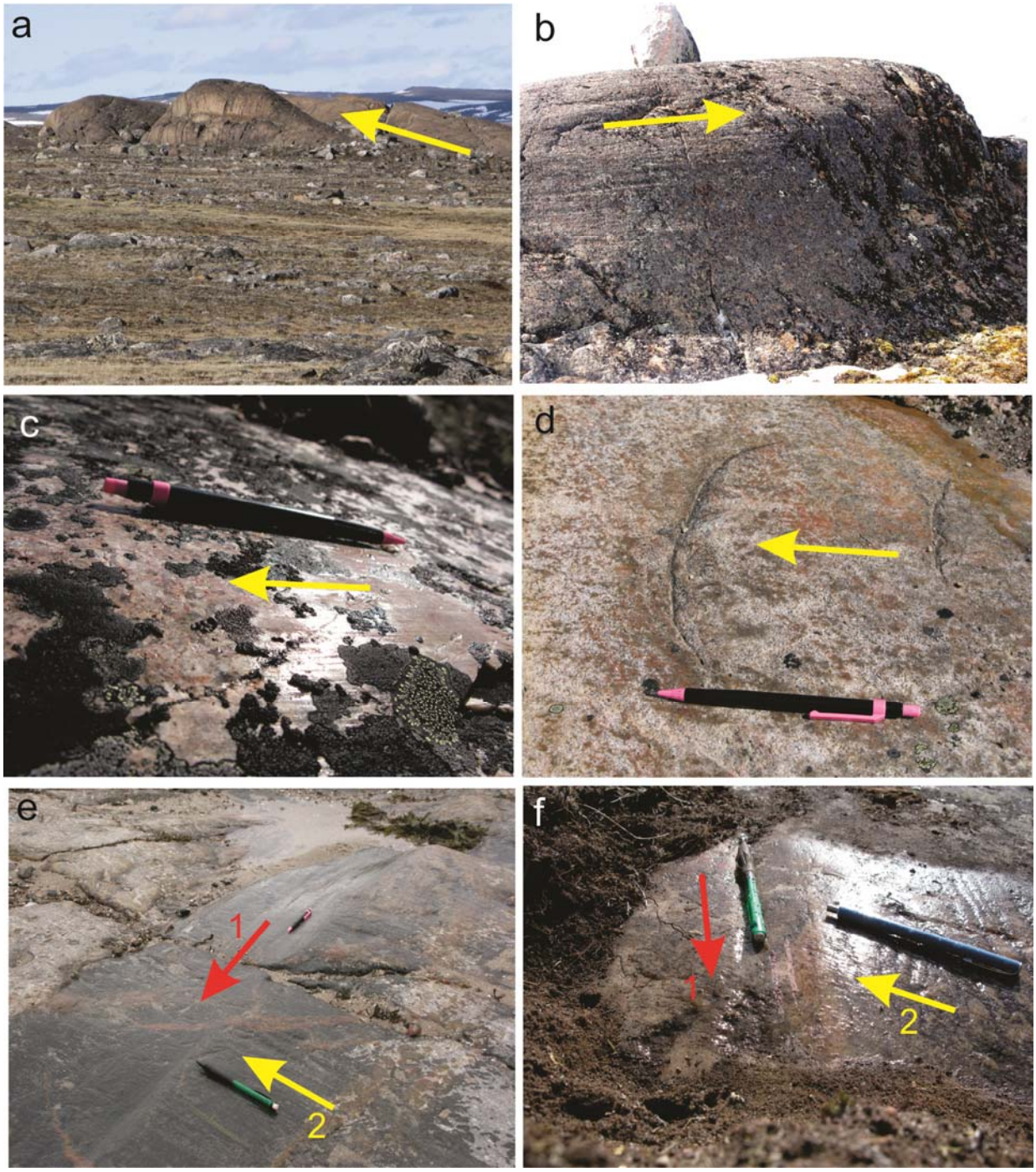

Figure 8. Photographs of various glacial erosional features measured on bedrock: a) whaleback forms; b) roche moutonnée and deep striae; c) microstriae; d) crescentic gouges; e) and f) northward striae and groove (1) preserved on the lee side of surfaces marked with eastward and southeastward striae (2). Arrows indicate sense of flow with relative ages where determined.

Till and marine shell sampling

Regional-scale till samples were collected for geochemistry, carbon content, texture, indicator mineral analyses, gold and platinum group minerals grain counts and pebble lithology counts. Survey design was devised to obtain evenly spaced samples (average of 10-km spacing). Samples were carefully collected on flat till surfaces in Cy-horizon material from hand dug pits in active frost boils, at an average

depth of 32 cm, to obtain relatively unweathered material (Fig. 9). Except where indicated in Appendix 3, most sample sites were from thick till areas over streamlined landforms or till plain, and from undisturbed till surfaces (not winnowed or reworked). Below the limit of post-glacial marine incursion, frost boils developed in fine grained marine sediments were not sampled. Special care was taken to exclude layers or lens of organic material, disaggregated clasts or oxidized sediments, except for one sample collected in weathered relict terrain (see discussion under Relict and cold-based landscapes section). Till sampling protocols for GEM projects in postglacial marine and glaciolacustrine environments, and in permafrost terrain, are further discussed in Spirito et al. (2011) and McClenaghan et al. (2013).

In total, 298 till samples were collected in the study area (Fig. 10). At the majority of sites, one small sample (~3 kg) and one large sample (mean=13 kg; range=9-19 kg) were collected. The sampling exceptions are as follows: 1) a clayey diamicton layer present below the regional till at six sites in the central part of the study area was sampled for geochemical analysis only; 2) a small till sample containing erratic shell fragments at two sites south of Repulse Bay above the marine limit was collected for geochemical analysis only; and 3) one beach sand sample in an area along the coast where till was not available was collected for indicator minerals only. A field duplicate was collected at one randomly chosen site for every block of about 20 sample sites to test site variability (less than 10 m apart). The routine sample and corresponding field duplicate were labelled with the same sample code except for one digit (e.g. 10MOB-I071A01 for the routine sample and 10MOB-I071A02 for the field duplicate). The location and description of all samples are presented in Appendix 3.

Figure 9. Photographs of a) active frost boil from which relatively fresh till samples are collected; b) sample hand-dug pit in a frost boil with small (3 kg) and large (~13 kg) samples besides hole.

Marine mollusc samples were collected at 18 sites within the study area (Fig. 10) between 30 and 187 m asl. Only one site had articulated shells in living position in marine fine sands, and two sites had complete shells in situ but not in living position. The rest of the samples (completed shells or fragments) were collected from the surface or within frost boils developed in marine sediments or in till. Most sites were below the limit of the Holocene marine incursion but five sites on a plateau south of Repulse Bay were above it (see discussion in Marine incursion section). Radiocarbon ages were determined by AMS dating on samples from 16 of these sites at Beta Analytic Inc. Laboratories in Florida and at Keck Carbon Cycle AMS Facility in California. Field duplicate samples collected at one site and laboratory duplicate samples collected at two sites were submitted for analysis. The location, detailed description of the shell samples and nature of inclosing sediments are provided in Appendix 3.

Analytical procedures for till samples

Sample preparation

A 2-kg split of all ~3-kg samples was air-dried and dry-sieved in GSC's Sedimentology Laboratory, Ottawa using a stainless steel US standard No. 230 mesh screen to obtain the <0.063 mm size fraction using procedures outlined in Girard et al. (2004). The remainder (<800 g) of each 3-kg till sample was archived at the GSC, Ottawa. The large (~13-kg) till samples were shipped to Overburden Drilling Management Ltd (ODM), Ottawa, for processing and the production of heavy mineral concentrates. Samples were processed in the order that they are listed in the ODM raw data file in Appendix 10. Sample were disaggregated in water and screened at 2 mm to produce a non-ferromagnetic heavy mineral concentrate for picking indicator minerals involving a two-step process with a shaking table and heavy liquids. The oversize (>2 mm) was wet-sieved to collect the 4-8 mm and 8-30 mm fractions for lithological analysis. Sample preparation and analytical procedures for all till samples are summarized in Figure 11. The analytical and QA/QC procedures follow the protocols for till samples collected as part of GEM projects (Spirito et al., 2011; McClenaghan et al., 2013).

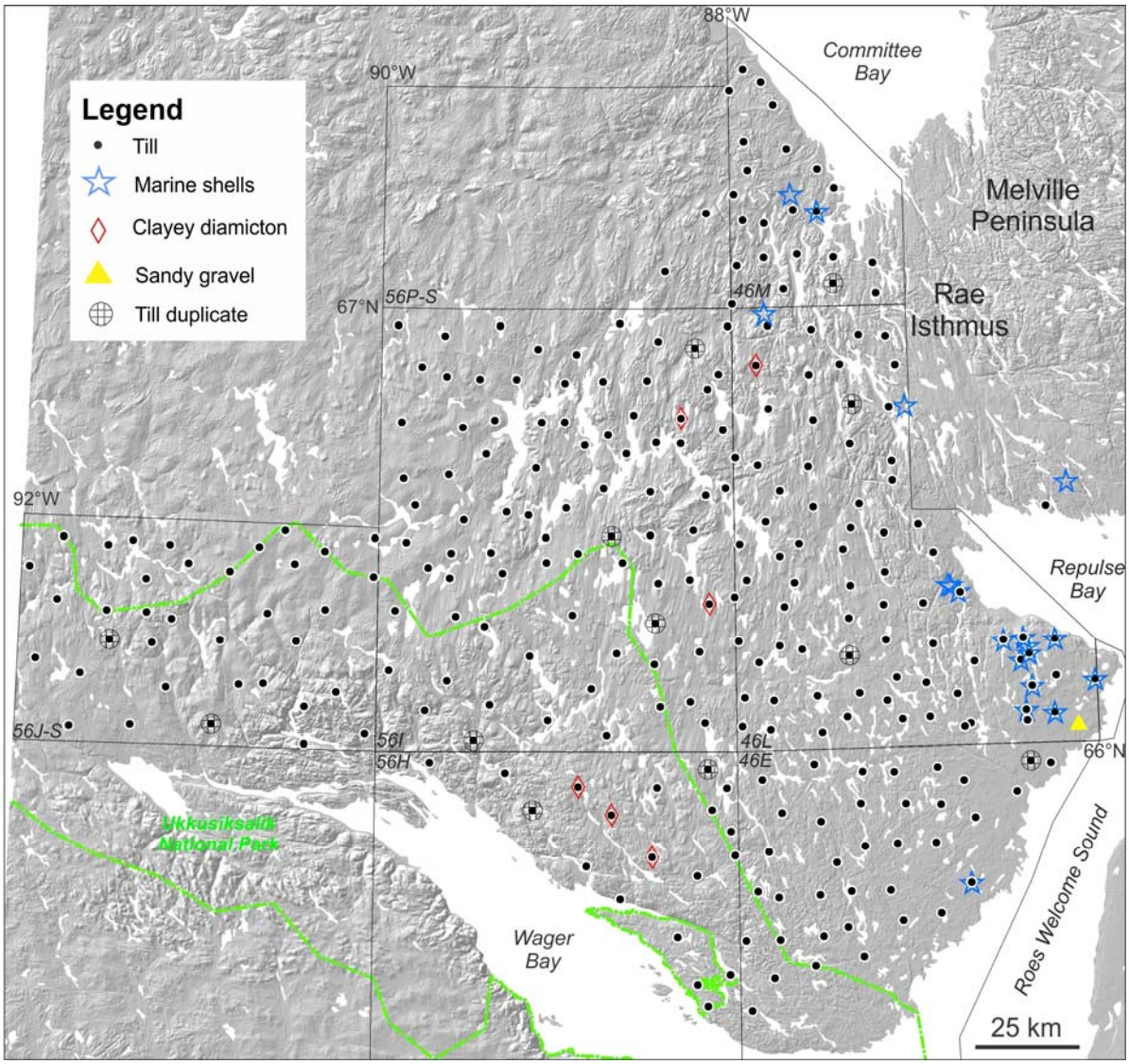

Figure 10. Sample location map. Detailed description and location of the samples are given in Appendix 3.

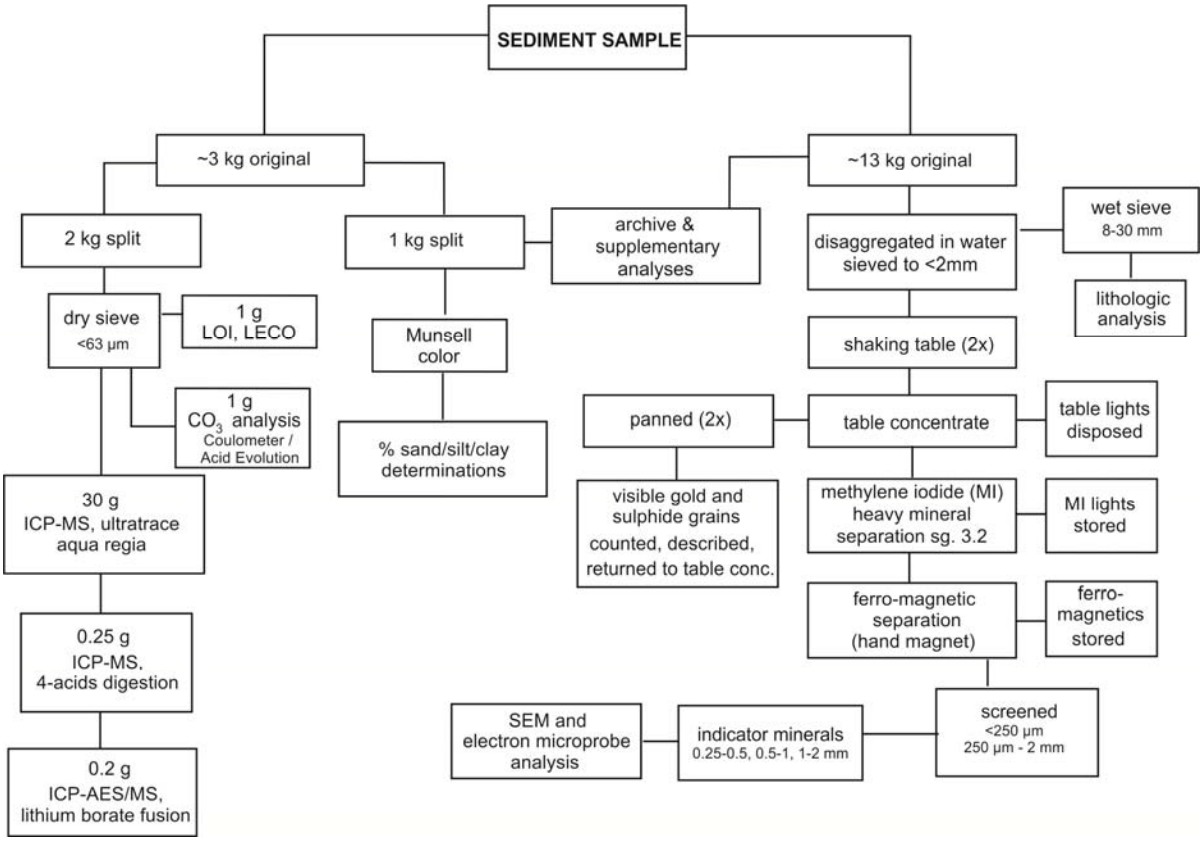

Figure 11. Flow sheet showing steps in till sample processing.

Till matrix geochemistry

Approximately 30 g of the silt+clay-sized fraction (<0.063 mm) of till were analyzed at Acme Analytical Laboratories Ltd. (now Bureau Veritas Mineral Laboratories), Vancouver, for a suite of trace, major and rare earth elements using ultratrace ICP-MS, following a modified aqua regia digestion (HCl-HNO_3, 1:1; 95°C) (Group 1F06-1F09: 65 elements). In addition, a separate 0.25 g split of the same fraction was analyzed at Acme Labs using ultratrace ICP-MS, 4-acids digestion (HNO_3-$HClO_4$-HF dissolved in HCl: Group 1T-MS: 43 + REE elements). Another separate 0.2 g split was analyzed for whole rock plus Cu, Mo, Ni, Pb, Sc and Zn analysis by ICP-ES, and for trace elements by ICP-MS following a lithium metaborate/tetraborate fusion and dilute nitric digestion (Extended Group 4A-4B: 52 elements). Carbon and S were analyzed by LECO as part of the same package. Detection limits and geochemical results are presented by the respective analytical methods in Appendices 4, 5 and 6.

QA/QC analysis of geochemical determinations

Reliability (accuracy or 'trueness', and precision) of analytical data returned from commercial laboratories was determined by including analytical ('blind') duplicates, primary standards and silica blanks within the sample suites submitted to the analytical laboratory. Analytical duplicates were prepared from the field duplicate samples in the laboratory after sieving and were labelled with the same sample code as the sample from which they are derived except for one letter (e.g. 11MOB-C018A02 and 11MOB-C018B02). To monitor potential cross-contamination during the sieving process and to purge the sieves, silicic acid blanks (i.e. qtz-J29623) were sieved at the beginning of each block of about 20 samples

and submitted for geochemical analysis as part of the block. Field duplicates were submitted to provide a measure of the variance due to sediment heterogeneity within a site versus between sites. The QA/QC statistics and plots discussed below are included in the respective appendices for the geochemical results.

Precision

Analysis of laboratory duplicate samples is used to monitor analytical precision of the geochemical results. In every analytical batch (2010, 2011 and 2012), one duplicate was inserted at the beginning of each block of 20 samples for a total of 15 laboratory duplicates. The results for the laboratory duplicate samples indicate that the analytical precision is good to very good for many elements analyzed by ICP-MS after a modified aqua regia digestion (Relative standard deviation: RSD≤10%). This method is somewhat less precise for Gd, Hf, Lu, Nb, Ni and Sn (RSD=10-20%), and even less so for Ag and Mo (RSD>20%). Arsenic, Au, B, Be, Bi, Cd, Ge, Hg, In, Pd, Pt, Re, S, Sb, Se, Ta, Te, Tl and W levels are near or below the lower detection limit in laboratory duplicates, therefore the precision cannot be properly evaluated. For the 4-acid digestion ICP-MS analyses, laboratory duplicates indicate that the analytical precision is very good to excellent for most elements, but less precise in 2010 for Ho and Li (RSD=10-15%), in 2011 for Cd, Cr, Cs, Cu, Dy, K, Mo and Rb (RSD=10-34%) and in 2012 for Cd and Ce (13-26%). This method is consistently not precise for Ag and As (RSD=19-71%). Gold, Be, Bi, In, Lu, Re, S, Sb, Se, Tm and W levels in laboratory duplicates are near or below the detection limit for this method, therefore the precision cannot be properly evaluated for these elements. For lithium borate fusion and dilute nitric digestion ICP-ES/MS analyses, reproducibility is good for most elements (RSD<10%). This method is somewhat less precise for P_2O_5 (2010), Nb (2011), Ta (2010), V, Yb (2011) and Zn (RSD=10-20%), and not very reliable for Cu, Pb (2010) or V (RSD>20%). Precision improved significantly for Pb in 2011 and 2012 (RSD=11.5% and 5% respectively) and for Zn in 2012 (RSD=3%). Precision for Be, Cs, Cr_2O_3, MnO, Mo, Ni, Sn, W cannot be properly evaluated since the results of the laboratory duplicate analysis are below or close to the lower detection limit. Carbon by LECO is reproducible (RSD<10%) while S is below the detection limit. LOI determinations are low therefore poorly precise in till (RSD = 16.5-42.2%).

Accuracy

Analysis of primary standards was used to monitor analytical accuracy of the geochemical results. In every analytical batch, one standard was inserted randomly within each block of 20 samples (CANMET Standard Till 4). The accuracy in the ICP-MS analysis after the modified aqua regia digestion is good for most elements as results are generally within 10% of the mean of values from the provisional or informational analysis available for Till 4. Values above 10% of the mean are shown in red in the QA/QC report Till 4 sheets included in the Matrix Geochemistry Appendices 4 through 6. Silver, As (2010), Bi (2012), Cr (2012), Mn (2012), Pb (2012), and particularly Hg, are less accurate using this method. The accuracy in the ICP-MS analysis by 4-acid digestion is generally acceptable except for Ag, Al, Ba, Cd, Hf, Nb, Rb determinations which are less accurate, mainly in the 2011 batch. Major elements are also irregularly less accurate in the 2011 batch. The accuracy in the analysis by lithium metaborate/tetraborate fusion and dilute nitric digestion is generally good for most elements except for Be (2012), Er (2010), Mo (2012), Pb, Sr, Ta, Tb, W (2012) and Y (2012). The silica blank qtz-J29623 returned average values of 88.8% SiO_2 and 11.1% LOI over the 3 years, which is consistent with previously reported values for this material (e.g. McClenaghan et al., 2015). Aqua regia values for Silica Sand4 in the 2012 batch were elevated for Pt (6 ppb), above the expected value of <2 ppb. Borate fusion/ICP-ES values reported for Silica Sand6 in the 2011 batch and Silica Sand3 in the 2012 batch were

elevated for Pb, above the expected value of <1 ppm (10 and 11 ppm respectively). None of the samples analyzed before or after those silica blanks were particularly high in Pb or Pt suggesting that the spurious values in the blanks are likely the result of analytical errors and that no cross-contamination from metal-rich samples occurred within these batches.

Analysis of variance

The variability of geochemical data between survey sites must exceed sampling and analytical variability in order to generate meaningful maps of element concentrations in sample media (Garrett, 1969, 1983). An estimate of the variance components, i.e. how much of the total variability is 'between' and 'within' the duplicate measurements, is determined using geochemical data from field duplicate pairs and the 'anova1' or 'anova2' function in the 'rgr' package running under the R system (Garrett, 2015). This random effects ANOVA (analysis of variance) model estimates whether the combined sampling and analytical variability between duplicate pairs is significantly smaller than the variability between the till sites where the duplicates were collected. The variance ratio, F, is calculated in ANOVA to gauge whether the variance 'within' is significantly smaller than the variation 'between'. As a 'rule of thumb' this ratio should exceed 4.0 for sampling and analytical errors to be significantly smaller at the 95% confidence level. The p-value is a measure of the exact level of confidence in the results. Generally an acceptable p-value is less than 0.05 (>95th percentile), i.e. there is a <5% probability the observed F ratio could have occurred due to chance alone.

A logarithmic transformation of the geochemical data was carried out in recognition that the data are drawn from constant sum compositions (Filzmoser et al., 2009; Garrett, 2013), and in order to minimize the effects of heteroscedasticity, i.e. where the variance of the duplicate pairs varies as a function of the means of the pairs across the range of the data. Homogeneity of variance, lack of heteroscedasticity, is a fundamental assumption of the ANOVA procedure (Garrett, 1983). Results of the analysis of variance (ANOVA) are presented in each appendix reporting geochemical results.

1. Modified Aqua Regia – ICP-MS

The variability 'between' sites of a majority (49) of the 65 elements determined in 12 field duplicate pairs by a modified aqua regia digestion followed by ICP-MS analysis exceeds variability introduced by sampling and analytical procedures. The F-test results and the associated p-values (Appendix 04, Worksheet 'ANOVA') indicate that these percentages are highly significant and that maps can be prepared with confidence. All values returned for two elements, Ta and S, were below detection limit and their variability could not be estimated. An additional 13 elements (Pd, W, Re, Pt, Hg, In, Se, B, Ge, As, Sb, and Tb) returned values at or just above detection levels, with the percentage of values below detection limit exceeding 50%, and variability could not be estimated. Three elements, Ag, Na and Be have a combined sampling and analytical variability exceeding that between sites, suggesting that the results of mapping these elements should be viewed with caution.

2. 4-acid – ICP-ES/MS

The variability between sites for a majority (46) of the 55 elements determined in 11 field duplicate pairs (8 pairs for In, Re, Se, Te and Tl) by a multi-acid digestion followed by ICP-MS analysis exceeds variability introduced by sampling and analytical variability and can thus be reasonably expected to result in reliable maps. The F-test results and the associated p-values (Appendix 05, Worksheet 'ANOVA') indicate that these percentages are highly significant and that maps can be prepared with confidence. All values for Au and S were below detection limits and variability could not be estimated.

Four elements (Re, Se, Sb and Te) returned values at or just above detection levels, with the percentage of values below detection limit exceeding 50%, and variability could not be estimated. Three elements, In, Be and As, have a combined sampling and analytical variability exceeding that between sites, suggesting that mapping these elements could be misleading.

3. $LiBO_2$ – Quenched Fusion

Variability of a majority of the 51 elements and oxides (46) determined in 11 field duplicate pairs by $LiBO_2$ fusion-ICP-MS/ES analysis exceeds variability introduced by sampling and analytical variability. The F-test results and the associated p-values (Appendix 06, Worksheet 'ANOVA') indicate that these percentages are highly significant and that maps can be prepared with confidence. All values for Total Sulphur ('Total S') were below laboratory lower detection limits and variability was not estimated. Three elements (Ni, Mo and W) returned values at or just above detection levels, with the percentage of values below detection limit exceeding 50%, and variability could not be estimated. One element, Be, has a combined sampling and analytical variability exceeding that between sites, suggesting that mapping this element could be misleading.

Matrix color and texture

Munsell color codes were determined on dry samples at the GSC Sedimentology Laboratory using a spectrophotometer. For textural analysis of the matrix, approximately 200-300 g from each 3-kg till sample was dry-sieved to obtain the <2 mm (-10 mesh) fraction of the samples. The size classes greater than 0.063 mm were determined using wet sieving followed by dynamic digital image processing using a CAMSIZER Particle Size Analysis System. The classes of sizes smaller than 0.063 mm were determined using a Lecotrac LT-100 Particle Size Analyser. The results of the matrix colour and textural determinations for the >2 mm size fraction, sand (2-0.063 mm), silt (0.063-0.002 mm) and clay (<0.002 mm) fractions are presented in Appendix 7.

Matrix carbon, carbonate and organic contents

Loss-on-ignition (LOI), an approximation of total organic content, was determined on the <0.063 mm fraction of all 2010 and 2011 samples after heating a small portion at 500°C for one hour in an ashing furnace (Girard et al., 2004). The LOI results are expressed as % weight loss of the dry weight of the fraction analyzed. Inorganic carbon was determined on the loss on ignition residue with a LECO CR-412 Carbon Analyzer instrument (1350°C) (Girard et al. 2004). Total carbon by LECO was analyzed only on the 2010 and 2011 samples that had inorganic C > 0.10%. For the 2012 samples, total carbon was first determined on the <0.063 mm fraction by LECO (1350°C), and only the samples with Total C > 0.10% were analyzed for LOI and inorganic carbon afterwards.

About 1 g of the <0.063 mm fraction of samples was analyzed to determine carbonate mineralogy using the CM 5015 Coulometer/Acid Evolution Method at the GSC Sedimentology Laboratory (Girard et al., 2004). Total CO_2 was not determined when inorganic C analyzed by LECO was <0.10% for the 2010 and 2011 samples. Calcite and dolomite were not determined when total CO_2 was < 0.05%. Laboratory duplicates as well as in-house and CANMET standards were inserted for the till matrix carbon and carbonate analysis. All results for the inorganic and total C, LOI and carbonate analysis are given in Appendix 8.

Clast lithology

The >2.0 mm material from the large till samples (~13 kg) was wet-sieved to separate the 8-30 mm fraction for lithological analysis. For comparison with results from surrounding surveys (TGI-1 Committee Bay and Wager Bay Project - NTS 56G), the 4-8 mm fraction was also prepared on a few samples collected in 2010. Since the results between the 4-8 mm and 8-30 mm fractions were proven to be comparable, only the 8-30 mm fraction was prepared in 2011 and 2012. Pebbles were visually examined using a binocular microscope (maximum 200 clasts) by Dominique Paré (Consorminex Inc.) and Ariane Castagner (geology student at U. of Ottawa), and subsequently verified and reclassified (if necessary) by the project geologists. Pebbles were grouped into the following general lithological classes: 1) intrusive rocks (mainly granitoids and felsic intrusive and gneissic rocks); 2) basalts; 3) ultramafic rocks; 4) metavolcanic and metasedimentary rocks (undifferentiated); 5) Paleozoic (dolomitic limestones mainly, minor sandstones); and 6) any other distinctive lithologies (e.g., quartzite and/or quartzite veins, gossanous clasts, k-feldspar minerals, clasts with clean contact between two lithologies of uncertain origin). In the 2012 batch, intrusive clasts were further subdivided into granitic (non-foliated), syenitic, foliated to gneissic felsic intrusive, foliated to gneissic intermediate intrusive, and mafic intrusive rocks. The objective of this sub-classification was to distinguish undeformed granitic rocks (younger Hudson and/or Nueltin Suite) from deformed or foliated intrusive rocks. Results presented in Appendix 9 include the number of clasts and the percentage (%) of the total in each category. High resolution scanned images of the classified pebbles in each sample are provided in this appendix for future reference.

Heavy mineral processing

The large till samples (~13 kg) were processed at ODM for recovery of the heavy mineral fraction and indicator mineral counting, including gold grains (e.g. Plouffe et al., 2013a). Samples were processed simply in numerical order as the potential for mineralization was unknown in the area and all samples had equal potential to cross contaminate others. Figure 11 outlines the sample processing flow sheet for the recovery of indicator minerals. Samples were disaggregated and sieved to obtain the <2 mm (matrix) fraction ("Table feed"), and then, processed using a double-run across a shaking table to ensure a complete recovery of all indicator minerals. The table pre-concentrate was then panned to recover any gold, sulphide and platinum group minerals (PGM) and these minerals were then returned to the preconcentrate. After tabling and panning, the pre-concentrate was further refined using heavy liquid (methylene iodide - SG 3.2) and ferromagnetic (FM) separations. The <2 mm non-ferromagnetic (NFM) heavy mineral concentrates (HMC) were screened at 0.25 mm. The 0.25-2 mm fraction was used for indicator mineral picking. The total number of gold and PGM grains recovered, and the weights of table feed, table pre-concentrates, NFM- and FM- HMCs are presented in Appendix 10.

Indicator mineral picking

Prior to indicator mineral examination and selection, the 0.25-2 mm NFM-HMCs recovered from till samples were dry sieved to 0.25-0.5 mm, 0.5-1 mm and 1-2 mm. The 0.25-0.5 mm fraction of the samples was further refined using a Carpco® electromagnetic separator to produce fractions with different paramagnetic characteristics to help reduce the volume of concentrate to be visually examined (Averill and Huneault, 2006). All fractions were examined under a stereoscopic microscope at ODM to determine the abundance of potential kimberlite indicator minerals (KIMs) and metamorphosed or magmatic massive sulphide indicator minerals (MMSIM®), and any other mineral indicating the presence

of potential mineralization. For each sample, the entire concentrate in each of the three size fractions was examined. ODM performed checks on selected grains using SEM-energy dispersive x-ray spectrometer (EDS) to confirm mineral identification. Selected grains considered having possible KIM and MMSIM affinities were removed from the concentrate and mounted for further study. Because of their high abundance in some samples, only a few representative grains (20-30) of certain mineral species were picked for analysis (i.e. forsterite, fluorite, chromite). Appendix 10 includes all raw grain counts from the visual identification of possible indicator minerals for the 0.25-2 mm NFM-HMCs in worksheets "KIM Data" and "MMSIM".

Eleven blank sand samples consisting of weathered Silurian-Devonian granite (grus) (Plouffe et al., 2013a, 2013b) were inserted by the GSC at the beginning and through the sample batches to monitor potential cross-contamination introduced during heavy mineral separation. Data for the blank samples are listed in Appendix 10 and are highlighted in yellow. Expected hornblende/titanite-zircon assemblages with no specific indicator minerals were found in the blanks. No sulphides, PGMs, KIMs or MMSIMs were found in the blank samples except for one single grain of pyrite in the pan concentrate of sample 11MOB-M096B01 at the end of the batch in 2011.

Comparisons of the gold grain abundance data for the field duplicate samples indicate that gold grain counts were reproducible in 2010, 2011 and 2012. Field duplicates collected in 2011 returned comparable KIMs and MMSIMs grain counts while within site variability was more important in the two field duplicate samples collected in 2010, especially for olivine (18 grains versus 0, and 18 versus 5), and in three field duplicates collected in 2012 (4 olivine grains versus 0; 11 olivine versus 1; 5 olivine versus 2 and 1 chromite versus 0). The variability of the indicator mineral content between the original and duplicate samples reflects a combination of sediment heterogeneity and the precision of the mineral separation and identification method. To verify the reproducibility of the indicator mineral grain counts (i.e. Plouffe et al., 2013a), re-picking of NFM-HMCs was completed on eight random samples of the 2012 batch samples (all 3 size fractions) after all picked grains were poured back into the vials with the original NF-HMC fractions. Results of the replicate grain counts indicate that in 2012, mineral grain counts were generally reproducible except for olivine which was significantly overpicked or underpicked in 4 of the 8 replicate samples. Chalcopyrite, fluorite and gahnite were slightly underpicked in a few replicate samples. All picking results for the blank and field duplicate samples, as well as re-picking results (samples 12MOB-R-001 to 008 in worksheets "KIM Data" and "MMSIM"), are reported in Appendix 10.

Electron microprobe analysis

Selected, visually identified, potential indicator minerals and some background grains (total of 305 grains from 2010, 745 grains from 2011 and 1466 grains for 2012) were mounted for probe work on 25-mm epoxy stubs at SGS Mineral Services, Lakefield, ON (2010 samples) and at Geoscience Laboratories, Sudbury, ON (2011 and 2012 samples). The mounts were carbon coated. The following mineral species were picked for mounting: low Cr-diopside, forsterite, enstatite, Cr-pyrope, Cr-grossular, spessartine, zoisite, Mn-epidote, spinel, gahnite, chalcopyrite, rutile, chromite, ruby corundum, leucosapphire corundum, sapphire, topaz, corundum, diopside, and almandine. Fluorite grains were mounted (74 grains from 2011; 69 grains from 81 picked in 2012) on stubs but not probed because of beam decomposition issues at the time of analysis; these mounted grains were archived for further studies. A few scheelite, loellingite and molybdenite grains picked from the 2011 and 2012 samples were

mounted but not probed.

Grains were analyzed at Geoscience Laboratories to confirm their identity and quantify their chemical composition using a CAMECA SX-100 Electron Probe Micro Analyzer (EPMA). Major elements were analyzed under normal operating conditions (20 kV and 20 nA), whereas minor/trace element analyses were carried out using a higher beam current (20 kV and 200 nA) and, where possible large surface area crystals (LLIF and LPET) were employed, to improve the limits of detection. Quality control data including standards, analyzing crystals, counting times, operation voltage, beam current, limits of detection, and limits of quantifications are given in Appendix 11. The analyzed grains were classified (or re-classified when necessary) by Dave Crabtree (Geoscience Laboratories) and the project geologists on the basis of their chemical composition. 25% of the 1423 visually identified forsterite were determined not to be olivine; 269 were re-classified as Cpx (19%), 36 as Opx, 17 as epidote, 15 as corundum, 6 as garnet, 4 as amphibole, 1 as titanite, and 10 as potentially feldspar, siderite or unknown. Of the classified 1065 olivine grains (75% of the potential "forsterite"), 1009 have $>Fo_{84}$ and as many as 658 (62%) are bona fide forsterite ($\geq Fo_{90}$). Forty grains picked as "Low Cr-diopside" were determined to be Cr-diopside with >0.5 wt.% Cr_2O_3. The final mineral classification and chemical data for the 0.25-2 mm probed grains are provided in Appendix 11. "Picked I.D." refers to the visual mineral identification and "Mineral classification" to the identification based on EPMA analysis provided by the Geoscience Laboratories. A table reporting the total number of indicator minerals per sample and by species is also provided in Appendix 11. Based on the proportion of representative olivine and chromite grains confirmed after probing ("Confirmed" column), a total number of grains per sample was estimated ("Total estimated").

RESULTS AND INTERPRETATIONS

Glacial landscapes and surficial sediments

Field observations, surficial geology compilation by air photo interpretation and remote predictive mapping based primarily on Landsat TM7 imagery have revealed diverse glacial landscapes and Quaternary sediments with distinct landform-sediment assemblages, and provided new insights into the glacial dynamics and deglacial history of the north Wager Bay area. Of particular interest are the relict and cold-based landscapes over the highlands of the Wager Plateau, the glacially scoured U-shaped valleys northwest of Wager Bay, the striking northward-trending streamlined landforms in the central part of the study area, the north-flowing and east-flowing glaciofluvial meltwater corridors, the exotic carbonate-rich and fossiliferous till in streamlined landforms south of Repulse Bay, and the extensive areas of exposed and gullied marine silts along the Committee Bay coast. A summary description and interpretation of these distinctive landscapes is provided below.

Relict and cold-based landscapes

Weathered bedrock and till surfaces are found in patchy areas on the uplands north of Ford and Brown lakes (Figs. 12 and 13). These restricted zones are characterized by subdued topography, subtle to no evidence of glacial erosion, scarcity of lakes, and lack of or poorly developed patterned ground; the surface material consists of extensive to patchy weathered bedrock and felsenmeer, weathered blocky till (weathered, angular granitic to gneissic local rock fragments in an oxidized stony, granular sand matrix), coarse residuum (regolith), and rare weathered erratics (Dredge et al., in prep.). These deposits provide

evidence of a pre-Late Wisconsinan relict terrain developed during a weathering interval, and reflect relatively intense or long cold-based conditions and preservation during, or at least parts of, the last glaciation and deglaciation. A similar weathered landscape is observed in the highlands south of Wager Bay (Dredge and McMartin, 2007) and on Melville Peninsula to the northeast (Dredge, 2002; Tremblay and Paulen, 2012).

Figure 12. Relict terrain north of Ford Lake showing: a) weathered felsenmeer and outcrops; and b) weathered till with local granitic clasts and oxidized matrix.

Further north near the National Park's boundary (McMartin et al., 2015; Dredge et al., in prep.), an atypical hummocky till with gently rolling topography and subdued kettles is present; the surface is commonly characterized by a regular, rectilinear, giant presumably ice-wedge, polygon network developed in a bouldery, compact and relatively unoxidized till (Figs. 13 and 14). For the most part, this terrain is found on the top of uplands. The polygons are generally orthogonal and range from 60 to 200 m across. Their sides can be aligned for long distances, creating linear depressions over 1000 m, with the dominant sets trending east-west normal to the regional ice flow direction. The thermal-contraction cracks (fissures) are 1-2 m wide and lined or filled with boulders. At several locations, the presence of water in the fissures indicates melting of underlying ice. The till over this terrain can be streamlined but in general there is subtle to no evidence of glacial scouring. These surfaces are thought to represent a till plain of unknown age preserved under cold-based conditions that occurred throughout the last glaciation and/or during downwasting of ice remnants in the uplands. On the Melville Peninsula Plateau, similar giant fissures partly filled with a boulder lag developed in ablation till were thought to represent ice crevasse patterns or some other late-glacial aspect of a remnant ice cap, possibly underlain by relict glacial ice (Dredge, 2002). Dyke et al. (1992) also reported similar features developed in hummocky end moraines on Prince of Wales Island. They concluded that the scale and regularity of the fissures indicate the presence of buried ice cores beneath the active layer in the till from which the fissures propagated.

Within the upland till plateaus of the Repulse Bay and Wager Bay drainage basins, single and nested lateral meltwater channels cross-cut the northward streamlined till on northern and southern-facing slopes (i.e. Smith, 1990; McMartin et al., 2015; Dredge et al., in prep.). Most channels indicate meltwater flowing east (Fig. 15a), controlled by the longitudinal gradient of the ice margin. Some channels have deltas and/or gravel alluvial fans at their eastern ends where meltwater accumulated in or near ice marginal lakes, now largely occupied by modern lakes. Other channels are filled with flat-top transverse eskerine and channel-fill deposits (Fig. 15b). The lateral meltwater channels are interpreted to represent retreating cold-based ice margins (cf. Dyke, 1993) along remnant ice masses centered in the highlands

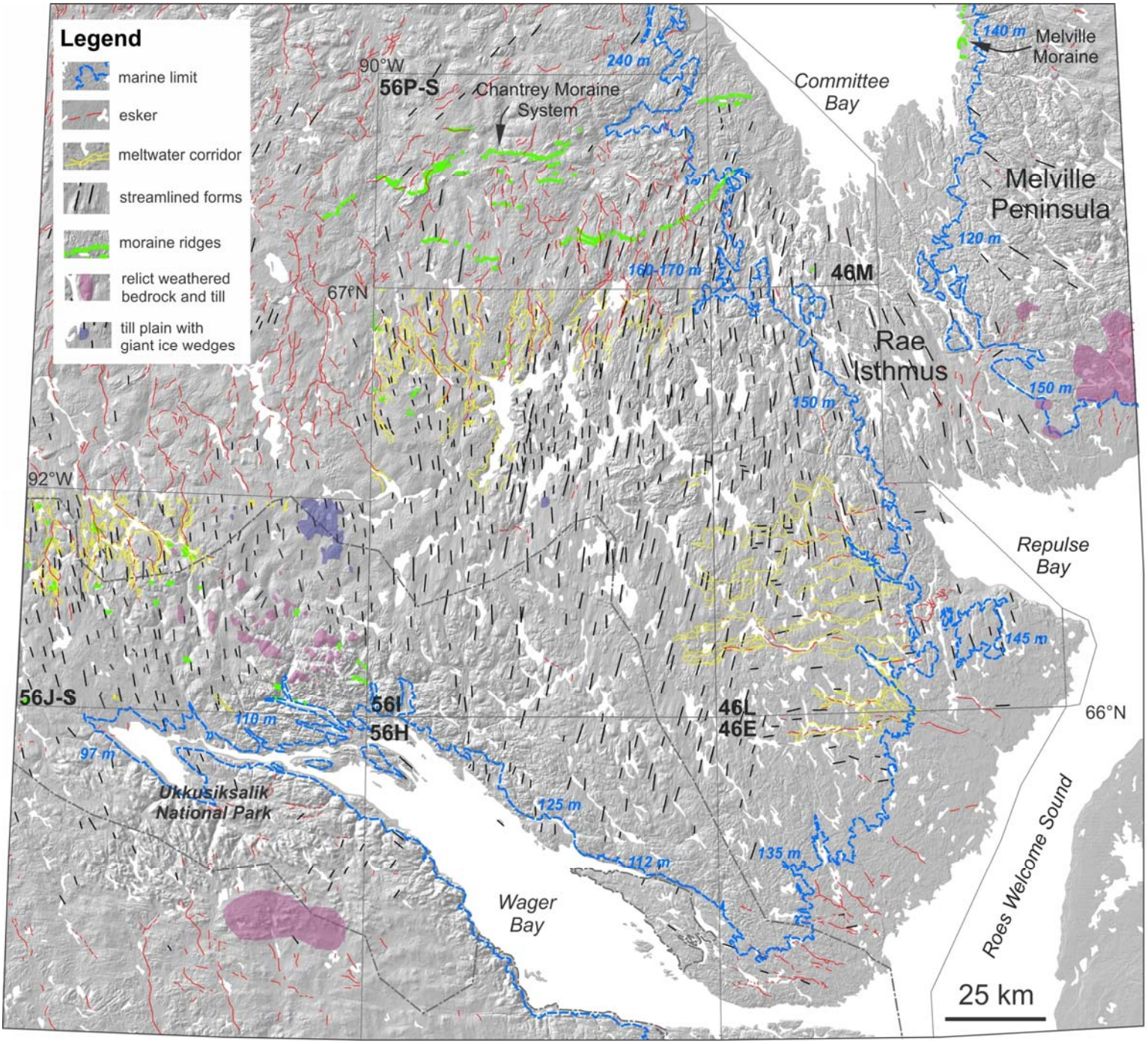

Figure 13. Generalized landform map for the North Wager Bay area. The trend of streamlined landforms was generalized using surficial geology maps (published or in press), a 30 m resolution floating point DEM, and satellite imageries (Landsat 742, SPOT 10). The marine limit, meltwater corridors, moraine ridges and relict terrains are derived from existing maps and field observations (see Appendix 1). The marine limit outside the study area is from Dredge (2002), Giangioppi et al. (2003) and Dredge and McMartin (2007). Melwater corridors were not compiled outside the study area. All eskers are from Ayslworth and Shilts (1987a), except for Melville Peninsula (Dredge, 2002).

north of Wager Bay. The orientation of some of the channels indicates that the last discrete ice remnants occupied many of the major lake basins (e.g. Curtis Lake, Qamanialuk Lakes).

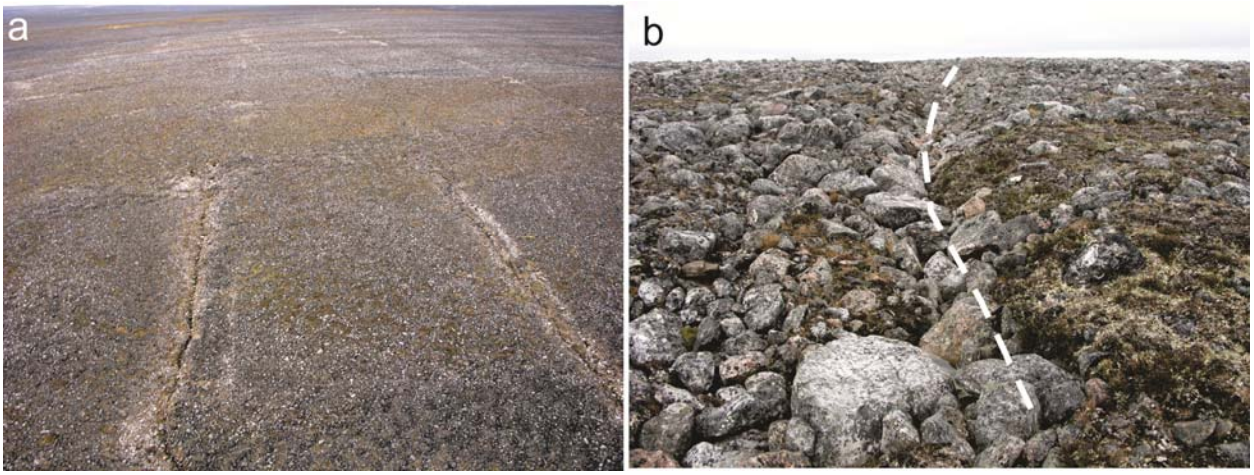

Figure 14. Regular spaced, giant ice-wedge polygon network developed in bouldery till in the uplands near the northern National Park's boundaries: a) view from the air (sides of polygons are about 100 to 200 m in length); b) view from the ground of boulder-filled ice wedge developed in bouldery till. Boulder in front is 1 m wide.

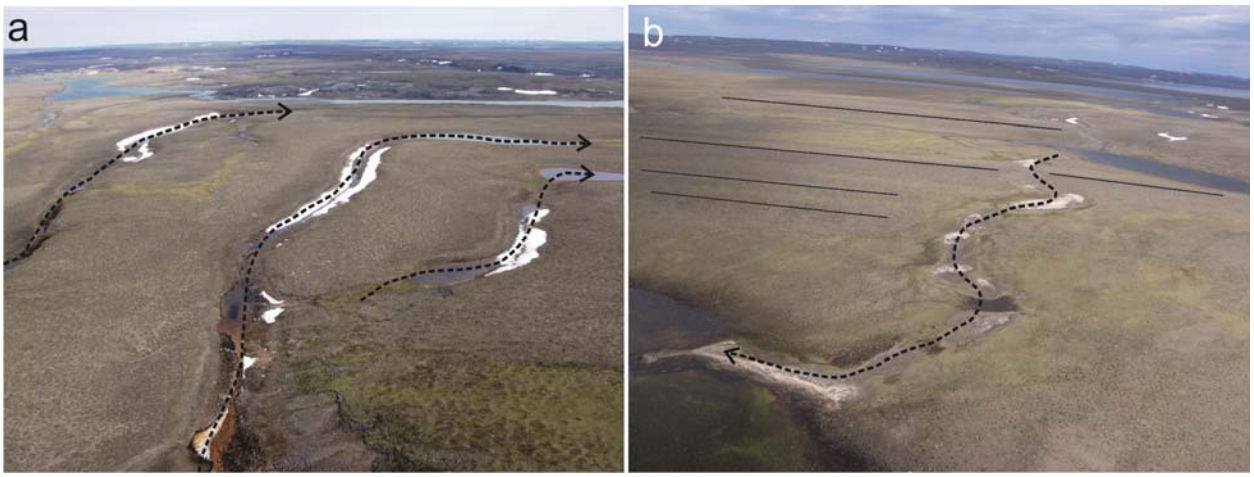

Figure 15. Lateral meltwater channels were maximized by frozen margins in the highlands north of Wager Bay: a) view from the air of nested channels cut into till, 2-3 km in length and 500 m in spacing, indicating meltwater drainage towards the east (away from the viewer); b) view from the air of a single ice-marginal channel incised in streamlined till and filled with flat-topped sand and gravel deposits, perpendicular to ice-flow direction.

Glacially scoured U-shaped valleys

Within the National Park north of Ford Lake and northwest of Wager Bay, deeply incised U-shaped valleys (Fig. 16) indicate selective linear erosion separated by upland plateaus (McMartin and Dredge, 2005; Dredge and McMartin, 2005; Dredge et al., in prep.). Although the predominant ice flow recorded on the uplands in this area is north-northwestward, glacial erosion into Wager Bay was apparently intense during one or several glaciations, developing fjordic lakes and deep glacial troughs. In addition to southward-flowing esker segments and small end moraines indicating northward retreat, late south and southeast ice-flow indicators were recorded at the bottom of some of these valleys, and along the north shores of Wager Bay. These indicators suggest that as the ice sheet thinned during deglaciation, ice-flow became focused into topographical troughs, resulting in a reverse ice flow into proto-Wager Bay.

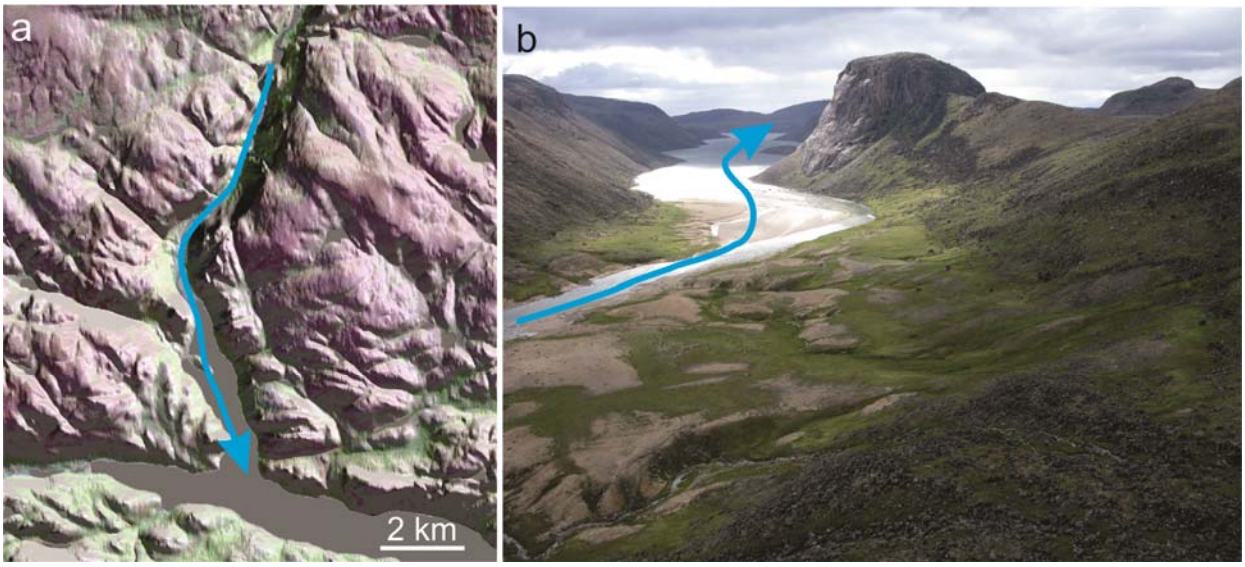

Figure 16. Glacial trough north of Ford Lake indicating selective linear erosion into proto-Wager Bay: a) Map showing hill-shaded DEM underlain by transparent SPOT 10 and Landsat 742 imageries; b) ground view of U-shaped valley looking south with marine sediments in the foreground. Arrow indicates direction of ice flow.

Till streamlined landforms

Conspicuous northward-trending crag-and-tail landforms and other streamlined landforms (drumlins and drumlinoid ridges, flutings, pre-crag ridges) are found mostly in the central part of the study area (NTS 46L-west, 56I, 56H-north). The largest landforms, which can be detected clearly on digital elevation models and consist mainly of impressive crag-and-tail landforms (Figs. 13 and 17a), converge northward (north-northeast to north-northwest) into Committee Bay, and are presumably related to active ice streaming in Rae Isthmus and Committee Bay during the last glaciation (Dredge, 2002; Margold et al., 2015). More subtle but pervasive north to north-northwesterward streamlined landforms of various shapes, lengths and spacing overprint a large portion of the study area (e.g. Fig. 13: NTS 56I-N). Most of these later, subparallel landforms are not detectable on the available DEM but are obvious on air photos. They are thought to have formed during deglaciation as the ice retreated from the Chantrey Moraine System southward into the study area (i.e. McMartin et al., 2015). In the east towards Repulse Bay, Roes Welcome Sound and further south along the shores of Wager Bay, weakly fluted till landforms indicating ice flow towards the east and east-southeast are superimposed on the various northerly oriented landforms (Fig. 13). These late streamlined landforms are associated with major shifts and reversal in ice flow towards open waters in the Tyrrell Sea during the late stages of deglaciation.

Hand dug pits in the streamlined landforms indicate that the surface material is composed of a poorly sorted, massive, silty sand diamicton (till), with a variable clast content. The few natural exposures in the streamlined landforms observed from the air suggest the landforms are composed of till. Permafrost features on these landforms include frost boils, sorted nets, and some ice-wedge polygons. While boulder cover is variable (Fig. 17b), it is quite dense (>60 %) in some areas especially where the till is thin or has been affected by meltwater erosion.

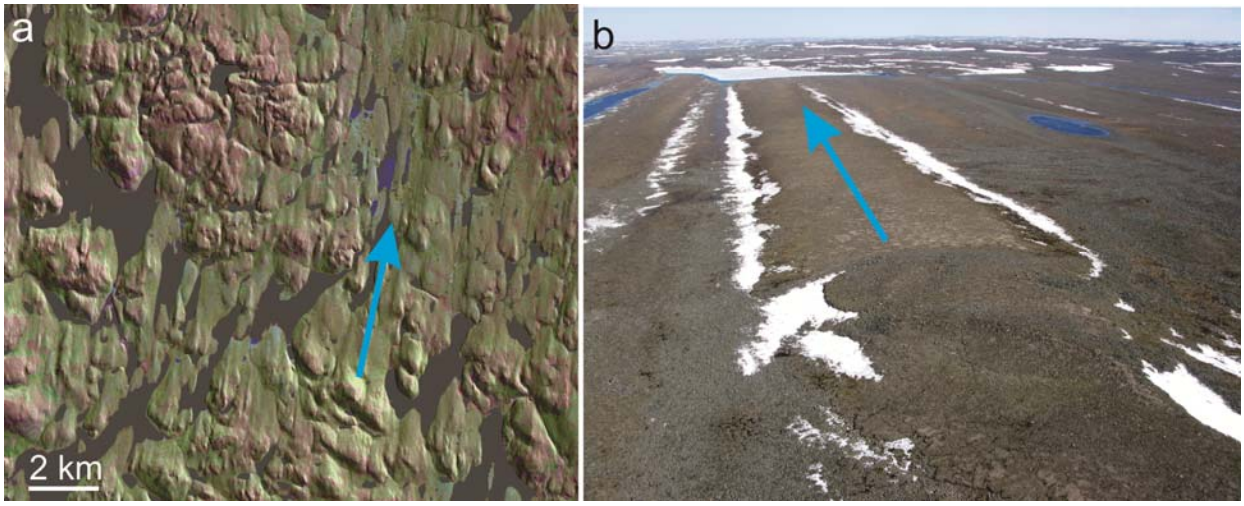

Figure 17. Prominent north-northeasterly trending crag-and-tail landforms north of Wager Bay: a) Map showing hill-shaded DEM underlain by transparent SPOT 10 and Landsat 742 imageries; b) aerial view looking north of a bedrock crag and well-developed till tail with frost boils. Arrow indicates direction of ice flow.

Subglacial meltwater corridors

Two subglacial meltwater drainage corridor systems, which have distinct and complex landform-sediment assemblages and divergent orientations, originate in the uplands close to modern topographic drainage divides (Fig. 13). In the northern parts of NTS 56I and 56J-South, near the head of the Arctic Ocean drainage basin (cf. Fig. 2), prominent north-flowing meltwater corridors with thick packages of sediments occur in subglacial ice-contact landforms (eskers, kames, aprons, crevasse fills, transverse ridges, hummocks), and terraced and kettled proglacial outwash plains (Fig. 18). These deposits typically fill 1-4 km wide valleys that form a large dendritic system, and occur in association with small end moraines and glaciolacustrine sediments deposited in short-lived glacial lakes trapped by the topographic divide. The north flowing corridors reflect southward ice retreat and a succession of depositional environments related to subglacial and proglacial meltwater erosion and deposition. Surface materials in these corridors vary considerably and include sand and gravel, boulders, eroded tills, glacial diamictons, and glacial lake sediments (sand and minor silts).

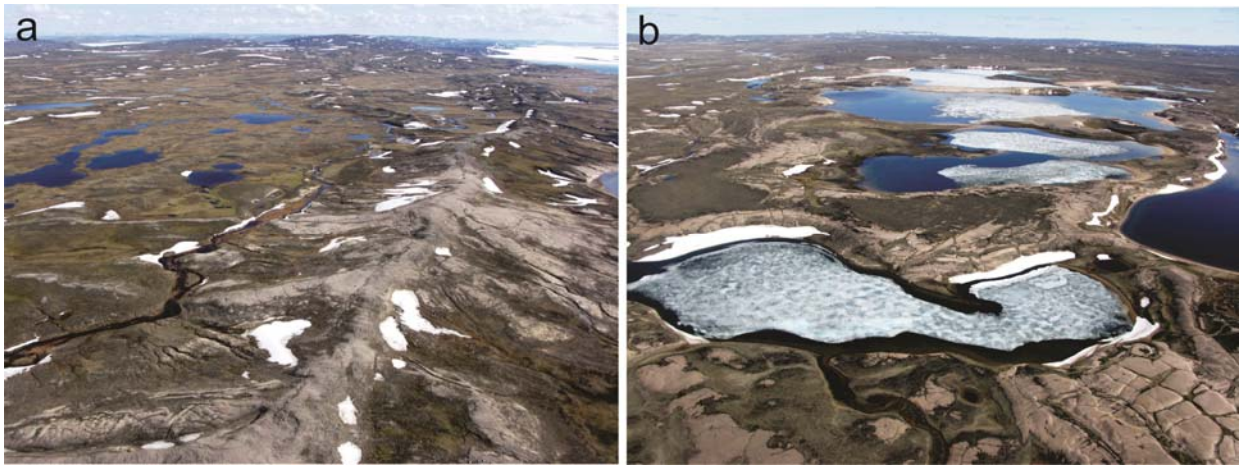

Figure 18. Thick sediment packages in north-flowing meltwater corridors: a) Aerial view looking south towards Curtis Lake showing esker complex and straight crevasse-fill ridges bordered by subaqueous outwash fan sediments and glaciolacustrine veneers; b) kettled outwash plain with ice wedge polygons in large meltwater corridor northwest of Curtis Lake.

East-flowing meltwater corridors, located within the Repulse Bay drainage basin (Fig. 13), form broad, 0.5 to 2 km wide, shallow channels characterized primarily by erosional features and subglacial sediment-landform assemblages including discontinuous scarp margins, exposed bedrock, boulder lags and eroded tills, variously shaped small hummocks, transverse ridges (pseudo-ribbed), and small subglacial ice-contact (eskers/kames) deposits (Fig. 19). These subglacial corridors cut across the topography in their higher portions while their lower portions follow wide topographic lows controlled by bedrock and form a quasi-distributed drainage network. They crosscut northward-trending streamlined landforms near the map border with NTS 56I and indicate a westward retreating ice margin in NTS 46E-north and 46L-south. Their eastern extents are coincident with the marine limit and several marine deltas which suggest these corridors actively drained subglacial meltwater during the marine incursion around Repulse Bay. Surface materials include eroded till, glacial diamictons, boulders, and sand and gravel. Both the northward and eastward meltwater corridors are intimately linked to the deglacial ice-flow history and dynamics, and are thought to have formed in a time-transgressive manner in relatively small segments near the retreating ice margins (i.e. Campbell et al., 2013).

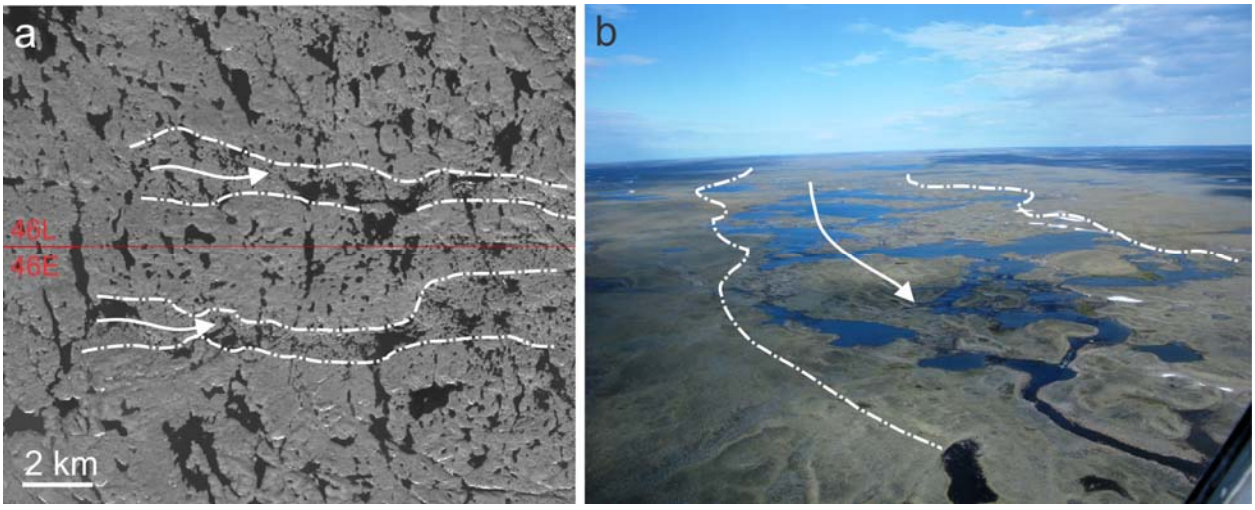

Figure 19. East-flowing meltwater corridors: a) air photo showing extent of two meltwater corridors above the marine limit near the boundary between NTS 46L and 46E; b) aerial view looking west showing a shallow, well-defined glacial conduit in NTS 46L-east. The dashed white lines delimit the margin of the corridors and the arrows indicate the direction of meltwater flow.

Exotic carbonate and fossiliferous streamlined till

An exotic carbonate-rich, fossiliferous, sandy silty till underlain by glacially-scoured Archean gneisses was discovered on low-relief upland terrain south of Repulse Bay in 2011 (NTS 46L-Southeast) (Fig. 20). The presence of carbonate till in this area was previously unknown but remote predictive mapping (RPM) predicted its occurrence prior to field checking in 2011 (Wityk et al., 2011). The fine-grained calcareous till forms large frost boils and solifluction stripes with exposed sediments and is spectrally distinct in RPM classification using Landsat TM7 imagery (i.e. Wityk et al., 2013). The carbonate-rich till contains Paleozoic carbonate debris and occurs in association with north-northwestward oriented streamlined landforms and striations. The presence of carbonate till in this area extends the southern limit of the Rae Isthmus Ice Stream south of Repulse Bay, indicating that the source area was in Roes Welcome Sound, not in Foxe Basin as previously suggested (e.g., Dredge, 2002).

Figure 20. Thick carbonate-rich till south of Repulse Bay: a) sandy silt calcareous till with exposed sediments in large frost boils and solifluction stripes; b) frost-shattered Paleozoic dolomite clasts on the surface of the carbonate till.

Furthermore, above the Holocene marine limit at 145 m asl, the carbonate till contains small but robust pieces of marine shells present as glacial erratics. These shells were likely scooped up from the floor of Roes Welcome Sound or with pre-Holocene raised coastal marine sediments, transported and redeposited with the Paleozoic debris inland by northward flowing ice. Detailed work on these shells, including radiocarbon age determinations, is ongoing (e.g. McMartin et al., 2013; also see discussion under Marine incursion section).

Marine limit and cover sequence

In the study area, the limit of postglacial sea inundation is 240 m asl in the area west of Committee Bay, falling to about 145-150 m asl west of Repulse Bay, 130-135 m asl at the mouth of Wager Bay, and 100-110 m asl inland north of Ford Lake (Fig. 13). The marine limit is indicated by high-level trimlines defined by wave-washed till surfaces exposing bedrock below, sandy terraces or wave-cut notches in till (Fig. 21a), and glaciomarine deltas at the distal end of meltwater corridors and channels. The southward declining elevation of the marine limit suggests the ice remained much longer over the Rae Isthmus and to the south, relative to areas in the northern part of the study area west of Committee Bay. The proto-Committee Bay must have been open and stable over a significant time period while the ice margin stood at the Chantrey Moraine System since the marine limit elevation drops significantly from 240 m asl north of the Chantrey moraines down to 170-160 m in the Quusluk River area just south of the moraines (Campbell and McMartin, 2014; McMartin et al., 2015). The marine limit also drops to 140 m along the east side of Committee Bay east of the Melville Moraine, probably equivalent in age to the Chantrey moraines (about 8000 radiocarbon years ago – see Dredge, 2002). Furthermore, the westward declining marine limit elevations in Wager Bay suggest that a late ice mass remnant persisted longer in the inner portions of Wager Bay, relative to the mouth of the bay near Roes Welcome Sound.

The marine cover sequence includes, from the limit of marine incursion to the present day coastline, thick deposits of deltaic sands and gravels, marine offshore clayey silts, marine offlap sands and silts, and sand and gravel littoral sediments. Particularly thick accumulations of marine silts, clays and minor fine sands, often exposed by extensive gullying and rilling, dominate the west coastal plain of Committee Bay in NTS 46M-southwest (Fig. 21b) (Campbell and McMartin, 2014). These fine-grained marine sediments extend up valleys into NTS 56P-south, reaching elevations up to 170 m above sea level

(Giangioppi et al., 2003; Campbell et al., 2013d). Evidence for marine reworking, to varying degrees, such as sand veneers and patches of wave-washed tills, is present at all elevations below marine limit. In particular, coastal plains along Roes Welcome Sound are sediment poor and dominated by bedrock outcrop, reworked till veneers and littoral deposits.

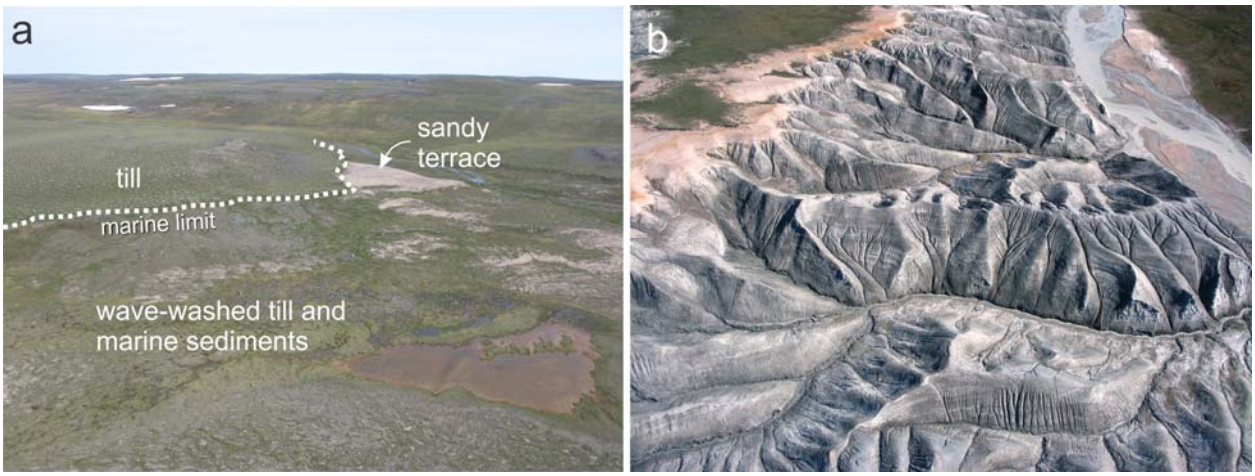

Figure 21. Aerial views of marine deposits in the study area: a) wave-washed till and sandy patches below marine limit marked by a trimline and a sandy apron at 112 m asl north of Douglas Harbour; b) rhythmically bedded and gullied marine clayey silt deposits capped by offlap nearshore sands along Committee Bay.

Summary of glacial and deglacial histories

The results from mapping of glacial flow indicators measured on bedrock, as well as glacial streamlined landforms and retreat features (moraines, eskers, corridors, channels), suggest a complex history of past ice flow and a time-transgressive deglaciation. To help interpret this complex glacial record, three sub-regions having similar trends and relative ages of glacial striations, and for the most part comprising analogous glacial landforms, meltwater corridors and glacial retreat features, were defined for the study area (Fig. 22). In region A, old striations ranging from northeastward to northwestward are superimposed by pervasive late north-northwestward striations associated with ice-marginal retreat positions from the various Chantrey moraine segments and other smaller end moraines further south. Streamlined landforms in this region trend north-northwestward in the west to north-northeastward in the east where the influence of ice streaming into Committee Bay was more important. This region also comprises most of the north-trending meltwater corridors and eskers, relict weathered landscapes and till plains with giant ice wedges (Fig. 13). Region A' represents a central high plateau around Pearce Lake dominated by north trending striations with no obvious older striation patterns and relatively few streamlined forms. In region B, centered over large lakes on the Wager Plateau (Curtis, Stewart, Qamanialuk lakes), striations and large crag-and-tail landforms converging to the north are cross-cut by late northward striations and superimposed by a multitude of parallel elongated streamlined landforms. Region C surrounds Repulse Bay as far as 80 km inland from the coast and includes northward to north-northwestward trending striations and landforms superimposed by late oblique to reverse striations and flutings indicating ice flow towards Repulse Bay and Roes Welcome Sound. This region includes all of the east-trending meltwater corridors. Region C' surrounds Wager Bay and is characterized by northeastward and northward striations and some streamlined landforms, cross-cut by late striations and the presence of small esker segments and end moraines indicating ice flow into and down the bay.

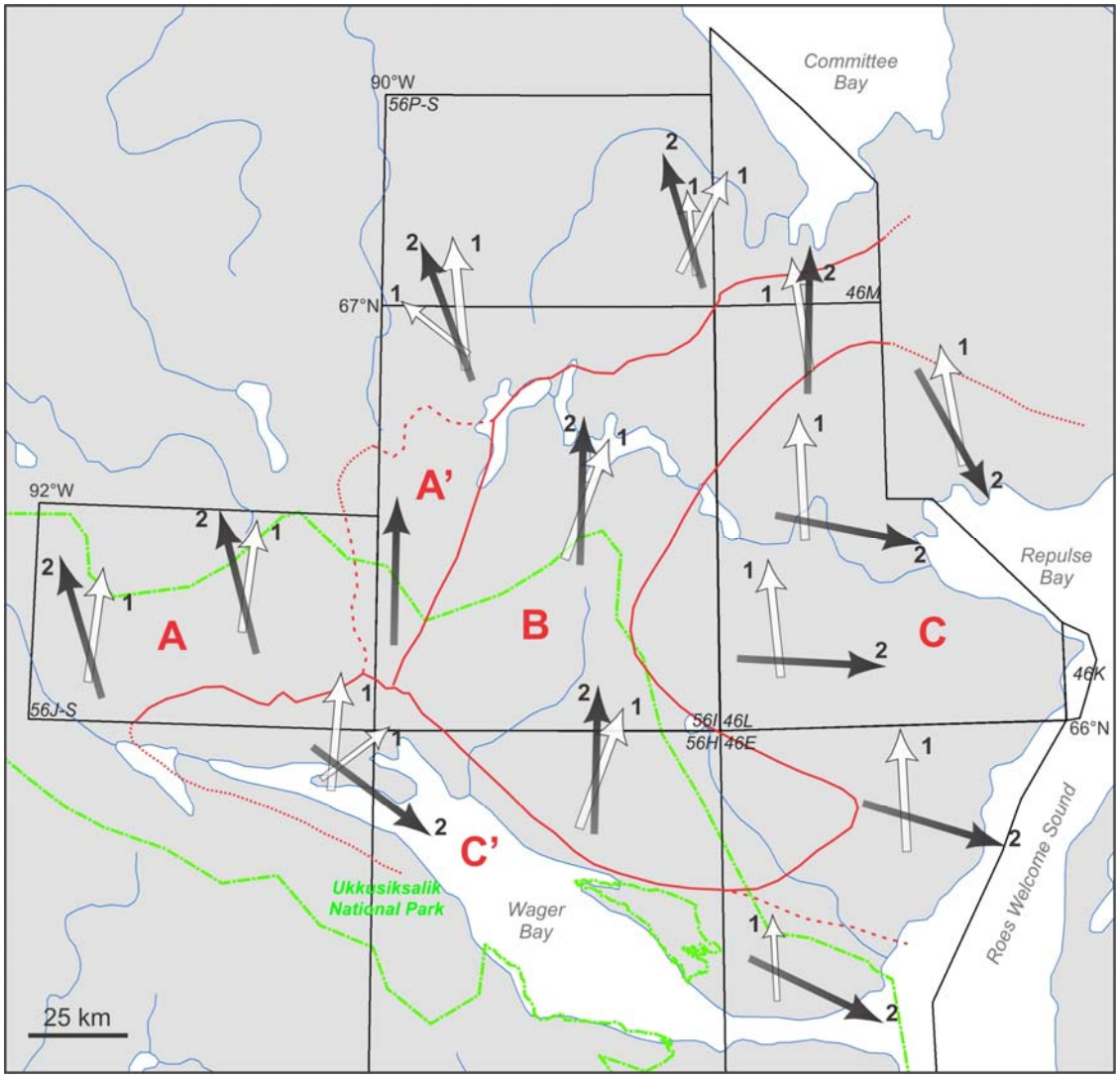

Figure 22. Generalized glacial flow trends within sub-regions A to C are shown by large arrows (darker arrow represents latest flow; 1=oldest). The sub-regions are defined by having similar trends and relative ages of glacial striations, and analogous glacial landforms, meltwater corridors and glacial retreat features. Boundaries of sub-regions are well defined (solid), approximate (dashed) or extrapolated outside the study area (dotted).

The interpretation of the glacial ice directional patterns described above is given in Figure 23. The earliest, regionally-distributed striations and largest streamlined landforms indicate the area was influenced primarily by ice flowing north (north-northeast to north-northwest), from an ice mass centered within and/or immediately south of Wager Bay during the last glaciation (Fig. 23a). Keewatin Sector ice converged with Foxe Sector ice towards the lowlands of the Rae Isthmus and flowed rapidly towards Committee Bay as part of the Rae Isthmus Ice Stream (i.e. Dredge, 2002), a tributary feeding into the larger Gulf of Boothia Ice Stream (i.e. Dyke, 2004; Margold et al., 2015). West of the ice stream bedform imprint, a northward ice flow, mainly documented in the TGI-1 area and tentatively attributed to the LGM (Phase I of McMartin et al., 2003b), may have been contemporaneous with the ice stream flow during this time. Patches of cold-based ice, mainly located outside the ice stream terrain, likely preserved relict weathered glacial landscapes during parts, if not all, of the last glaciation. Earlier flows (pre-LGM?) towards the north and northeast occurring sporadically across the study area are not depicted here. At the beginning of the last deglaciation, the ice stream continued to be active but the direction of ice flow in the

western part of the study area shifted to the northeast, converging into opening proto-Committee Bay marine waters as a result of thinning and drawdown into the bay (Fig. 23b; Phase II of McMartin et al., 2003b). As ice retreat continued inland, the ice margin became reoriented in a more east-west configuration and paused at the Chantrey Moraine System at approximately 8.2 ka BP (Dyke, 2004), resulting in a northward to north-northwestward ice flow across the study area (Fig. 23c; Phase III of McMartin et al., 2003b).

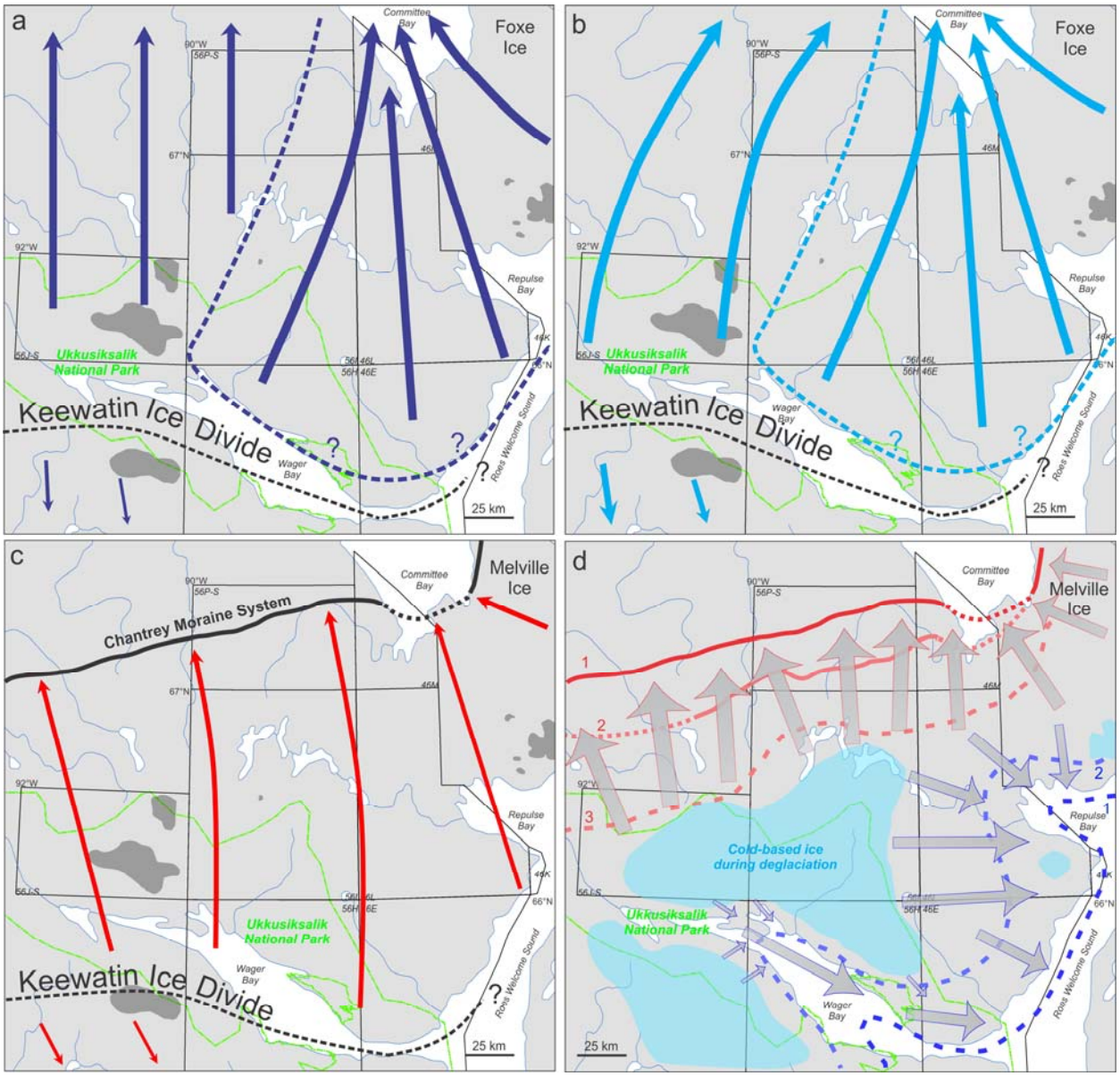

Figure 23. Generalized ice-flow sequence maps for areas north of Wager Bay based on glacial and deglacial record from study area and surrounding areas (see Figs 6, 12 and 21). Arrows indicate trends of dominant ice flows during: a) the last glaciation (LGM?) with ice streaming towards Committee Bay; b) early deglaciation and opening of Committee Bay; c) retreat to the northernmost Chantrey Moraine segments; d) last deglacial patterns. In a and b, dashed lines in blue are approximate margins of the ice stream. The minimum extent of cold-based ice preserving relict weathered and fresh landscapes are shown in dark grey in a-b-c. In d, zones in light blue were probably underlain by cold-based deglacial margins; recession lines represent successive ice marginal positions during ice retreat (1=earliest), from the Chantrey moraines (red) and from an unknown position in Hudson Bay (blue). These retreat positions were not contemporaneous.

Late during deglaciation, a major switch and reversal in ice-flow direction occurred all around the coast of Repulse Bay and Roes Welcome Sound (Fig. 23d). This late convergent ice flow is associated with marine incursion into Hudson Bay and opening of Repulse Bay (Tyrrell Sea). Influence of subglacial bed topography on ice-flow dynamics increased as the ice thinned. Further opening of Roes Welcome Sound and Wager Bay in late deglacial time, and drawdown into Wager Bay, resulted in the separation of remnant ice centers on either side of Wager Bay and ice flow into deep glacial troughs. As remnant ice masses thinned in the highlands north of Wager Bay, retreat was accompanied by the expansion of a cold-based zone to the margins, preserving the northward streamlined glacial landscape. The absence of warm-based deglacial features and sediments related to southward and northward retreat over a large portion of the plateau, except for lateral ice-marginal channels cross-cutting north-trending landforms, provide evidence that the thermal ice regime was cold-based during the final deglaciation.

Marine incursion

New radiocarbon dates on marine shells collected in the study area are reported in Table 1 and plotted on Figure 24 (red dots). The dates were all corrected for isotopic fractionation (norm to -25 o/oo), and a marine reservoir of 630 and 740 years for Foxe Basin and Arctic Basin sites respectively – see McNeely et al. (2006). The Holocene ages indicate a minimum deglaciation age and concurrent marine incursion at approximately 5.41 to 6.87 kyr ^{14}C BP for the Rae Isthmus-Repulse Bay-Roes Welcome Sound area. Marine shells lying on the surface north of the Chantrey moraines was dated at 8.448 ka (see Giangioppi et al., 2003 for description; age reported in Little, 2006 but uncorrected for isotopic fractionation). The 1500-2000 radiocarbon year difference between ages north and south of the Chantrey Moraine System indicates a significant still stand during ice retreat at this morainic system. The age of 6.87 kyr south of Rae Isthmus on the mainland suggests the ice had disappeared from the entire isthmus by 7.0 kyr, and probably earlier. The westward declining marine limit reported in Wager Bay is compatible with the radiocarbon ages that indicate the presence of late ice remnants in the inner portion of Wager Bay during deglaciation (e.g., Dredge and McMartin, 2005).

Table 1. Radiocarbon ages on marine mollusks (AMS dating). Ages in blue are from samples collected at the same site, both analyzed at BETA ("field duplicates"); ages in red are "laboratory" duplicates analyzed at Keck Laboratory.

Elevation (m)	GSC sample ID	LAB ID	$^{13}C/^{12}C$ o/oo	Conventional ^{14}C age (BP)	Corrected ^{14}C age (BP) for marine reservoir	Species
50	10MOBI063A01	Beta-293257	+1.5	6750 +/- 40	6010 +/- 40	*Hiatella arctica*
108	10MOBI051A01	Beta-293256	+1.3	6930 +/- 40	6300 +/- 40	Unidentified
44	10MOBI038A02	Beta-293255	+0.4	6150 +/- 40	5410 +/- 40	*Hiatella arctica*
121	11MOBM045A02	Beta-315077	+1.7	6720 +/- 30	6090 +/- 30	Unidentified
30	11MOBC087A02	Beta-315075	+2.2	7260 +/- 40	6630 +/- 40	*Hiatella arctica*
60	11MOBC033B01	Beta-315074	-0.6	7250 +/- 40	6620 +/- 40	*Hiatella arctica*
87	11MOBC029B01	Beta-315073	+0.4	6940 +/- 40	6310 +/- 40	*Mya truncata*
111	11MOBM023A01	Beta-315072	-1.1	6890 +/- 40	6150 +/- 40	*Macoma calcarea*
78	12MOBC089A01	Beta-339719	+2.1	6530 +/- 30	5900 +/- 30	*Mya truncata?*
57	12MOBC044A02	Beta-339714	+0.1	6490 +/- 30	5860 +/- 30	*Hiatella arctica*
95	12MOBC004A02	Beta-339712	-0.8	7500 +/- 40	6870 +/- 40	Unidentified
167	11MOB-M044A02	Beta-315076	+1.4	39820 +/- 460	39190 +/- 460	Unidentified
168	12MOBC087A01	Beta-339718	+3.6	39450 +/- 460	38820 +/- 460	Unidentified
168	12MOBC087A01	Keck-122338	+2.5	32290 +/- 210	31660 +/- 210	Unidentified
172	12MOBC086A01	Beta-339717	+0.1	36590 +/- 350	35960 +/- 350	Unidentified
172	12MOBC086A01	Keck-122480	+1.4	36950 +/- 590	36320 +/- 590	Unidentified
184	12MOBC085A01	Beta-339716	+1.8	33950 +/- 270	33320 +/- 270	Unidentified
147	12MOBC084A01	Beta-339715	+1.2	38240 +/- 410	37610 +/- 410	Unidentified
187	12MOBC005A02	Beta-339713	+1.2	38000 +/- 400	37370 +/- 400	Unidentified

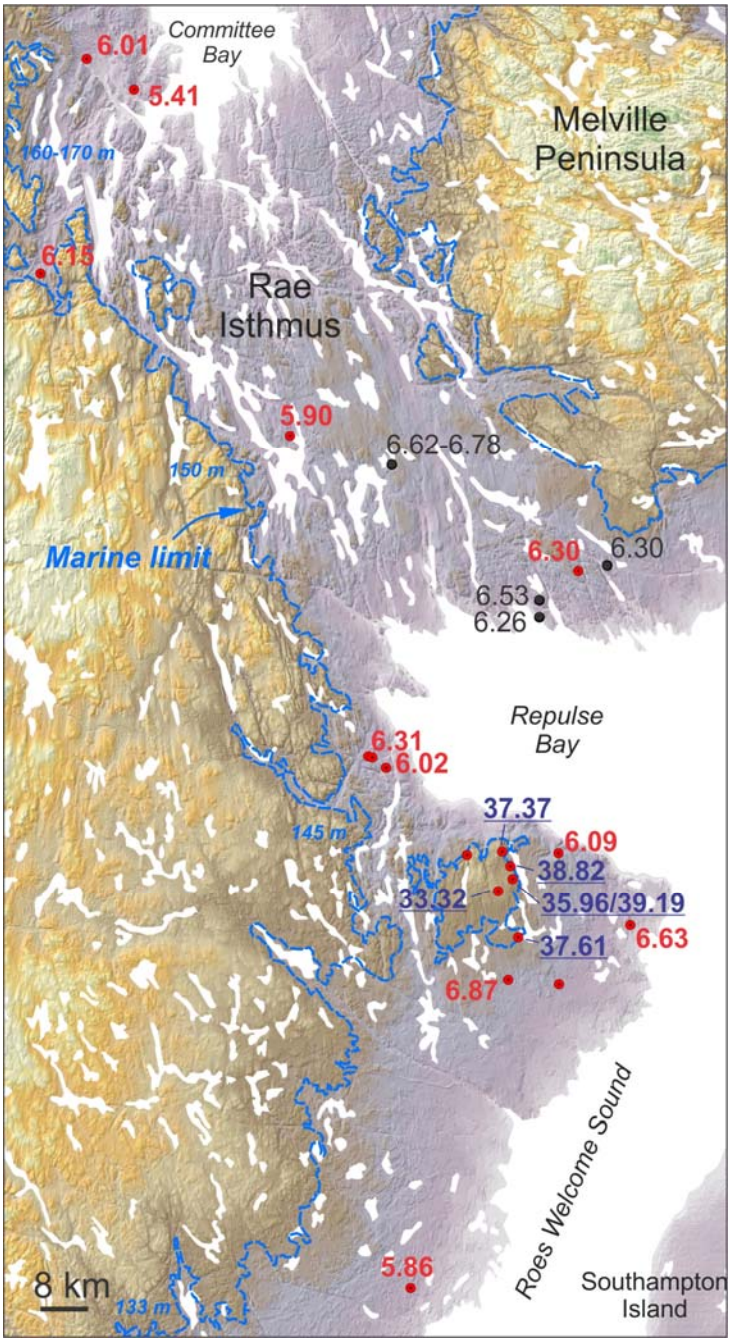

Figure 24. New radiocarbon ages (red dots) determined on marine molluscs in the study area (in ^{14}C kyr BP). All ages were corrected for isotopic fractionation and marine reservoir (see text for details). Holocene ages are shown in red and mid-Wisconsinan ages are shown in dark blue. Radiocarbon ages determined on shells from Dredge (2002) in the same area are also shown (black dots). Legend to DEM elevations are given in Figure 2.

Mid-Wisconsinan ages were determined for the small but robust marine shell fragments found within the carbonate-rich till south of Repulse Bay, with corrected finite ages varying between 31,660 ± 210 BP ^{14}C yr BP and 39,190 ± 460 ^{14}C yr BP at five separate sites (Table 1). Radiocarbon ages for field duplicate samples collected at one of these sites and for laboratory duplicates analyzed at two different laboratories (Beta and Keck) confirm the reproducibility of the mid-Wisconsinan age for these shells. Implications for these findings are significant. In contrast to most paleogeographic models of the LIS that suggest full ice conditions in Hudson Bay during marine isotope stage 3 (i.e. Dyke et al., 2003; Stokes et al., 2012; Tarasov et al., 2012), the pre-Late Wisconsinan ages of the marine shells in the streamlined till suggest the northwestern part of Hudson Bay through Roes Welcome Sound or Repulse Bay was ice-free for a minimum of 7530 radiocarbon years (McMartin et al., 2013b; Helmens et al., submitted).

Till provenance

Results show that till in the Wager Bay north area is mainly derived from the south and that glacial transport distances are relatively long (~10 to >100 km), in contrast to areas south of Wager Bay where short (~<1 to 10s km) distances were interpreted as the result of proximity to the Keewatin Ice Divide during the last glaciation (Dredge et al., 2005; McMartin et al., 2013c). The lithological composition of till (8-30 mm pebble fraction) does not vary significantly at the regional scale (Fig. 25): 1) high contents of felsic to intermediate intrusive rocks averaging ~96% are found throughout the area, ranging from ~48 to 100%; 2) generally low contents of metavolcanic and metasedimentary (supracrustal) rocks averaging ~2% characterize the till, ranging from 0 to 42%; and, 3) Paleozoic carbonate clasts are found exclusively in the eastern part of the study area north and south of Repulse Bay, with concentrations averaging 19% and ranging from ~2 to 38%. No Dubawnt Supergroup clasts or any other distinctive lithologies that could be traced to specific sources were found in surface till.

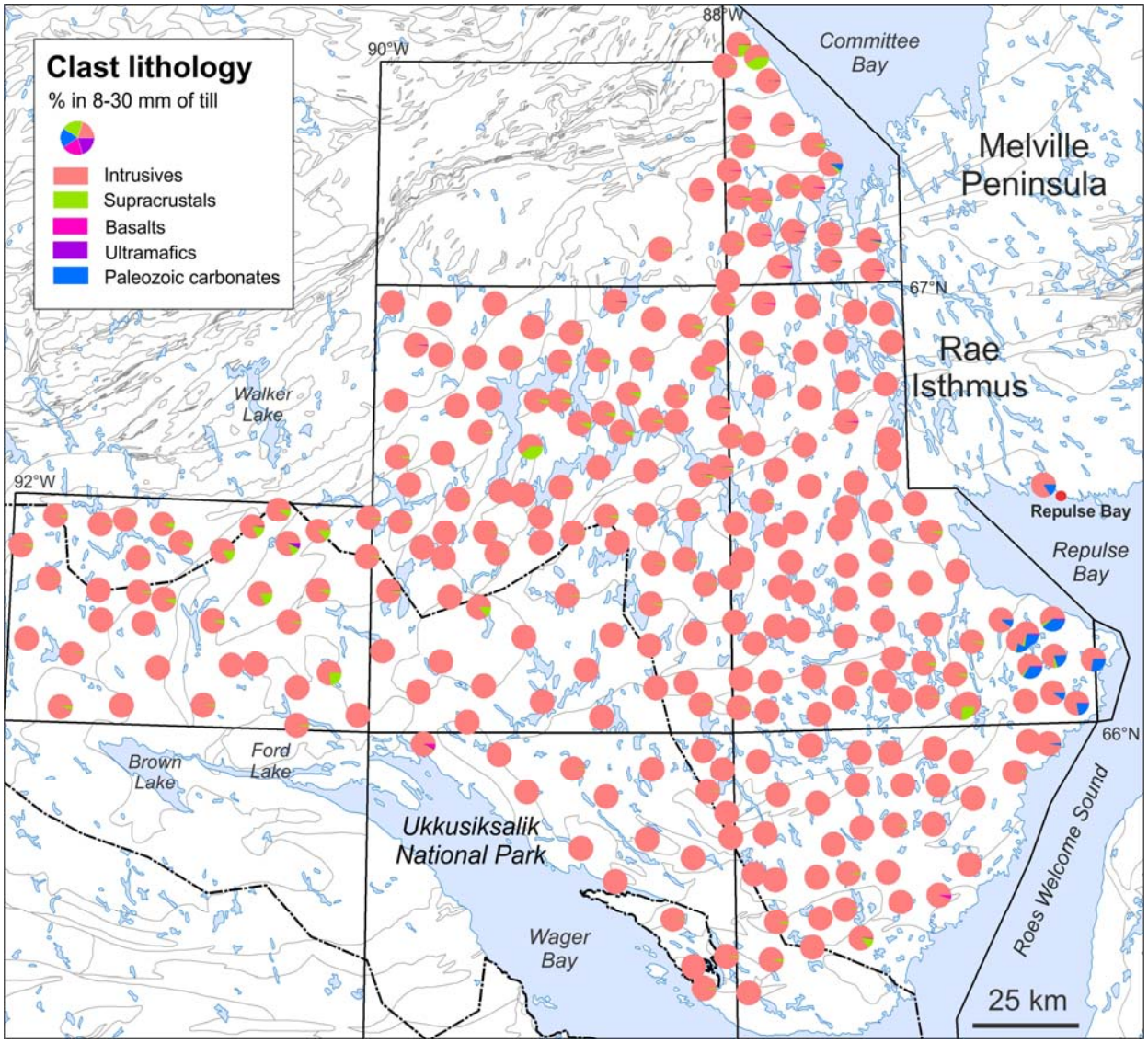

Figure 25. Distribution of the main lithological classes in till displayed as pie charts for each till sample. Bedrock geology polygons from Figure 3 are outlined in grey.

Dispersal of carbonate material

The carbonate-rich till south of Repulse Bay is considered part of the large expanse of calcareous till centered within a 40-50 km-wide corridor over Rae Isthmus and extending for 150 km long to the shores of Committee Bay (cf. Dredge, 2002). The calcareous till is found in association with north-northwestward streamlined landforms and striations that converge into Rae Isthmus (Fig. 26). The fine-grained till has a calcareous matrix (6 to 32%; see Appendix 8) and contains 1 to 12 % Ca (cf. map in Appendix 4) for GEM1 samples. Carbonate clast contents are up to 56% within the plume (Dredge, 2004; <4 cm clasts). The boundaries between areas covered by thick carbonate-rich till and thinner shield-derived till are discontinuous but sharp, although the carbonate plume does not precisely follow the lowlands of the Rae Isthmus nor does it occur exclusively below the marine limit (Fig. 26). The nearest up-ice (south-southeastern) carbonate bedrock sources are Paleozoic platform rocks lying under Repulse Bay and Roes Welcome Sound and on Southampton Island. The distribution of exotic carbonate-rich till is interpreted as glacial dispersal by a topographically-controlled ice stream originating south of Repulse Bay. The carbonate plume does not exhibit obvious decreasing carbonate debris concentrations until the shores of Committee Bay where clasts contents are down to 2%, typical of Boothia-type dispersal found in ice streams (i.e. Dyke and Morris, 1988). Noteworthy is the absence of carbonate debris in till along the west coast of Roes Welcome Sound, even if abundant northward indicators of ice flow were recorded as far south as the mouth of Wager Bay (cf. Fig. 6). Perhaps faster-flowing ice concentrated in the main trunk zone over Rae Isthmus for a sustained period of time provided the highest rate of sediment delivery and long-range transport of carbonate material in this area. The beginning of the ice stream onset zone in Roes Welcome Sound as depicted in Fig. 23 may also explain the restricted distribution of carbonate till south of Repulse Bay.

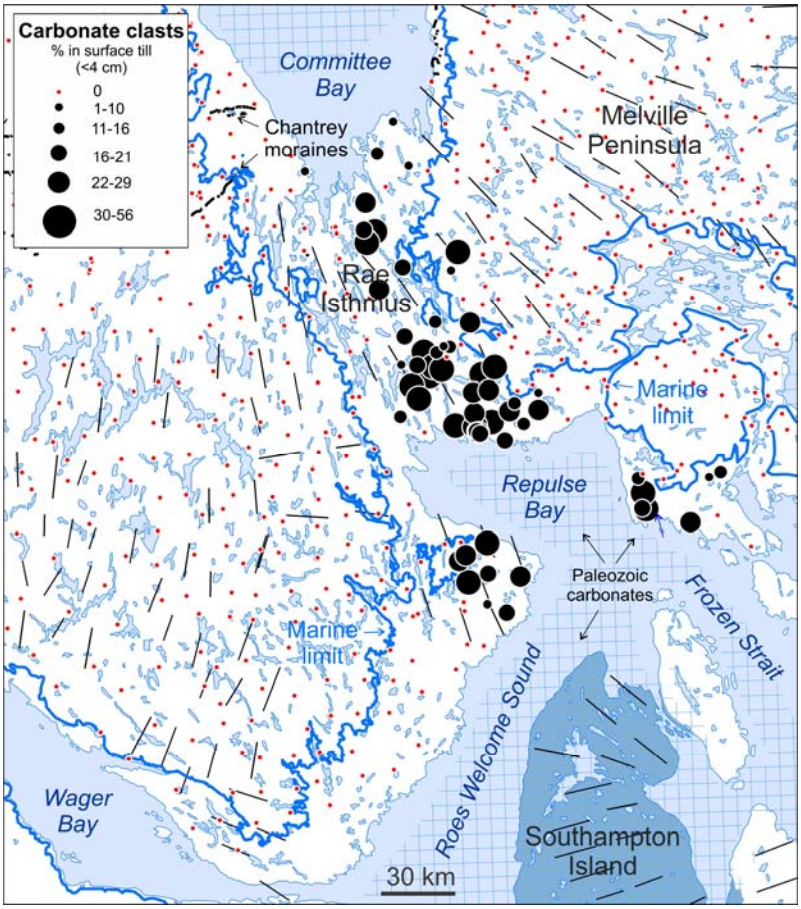

Figure 26. Regional distribution of carbonate clasts in till (<4 cm). Data from GEM-1 study (this Report: 8-30 mm), Dredge (2004:<4 cm) and McMartin et al. (2003: 4-8 mm). Short black lines are streamlined forms (from Fulton, 1995). Paleozoic carbonate platform rocks are shown on Southampton Island in blue and in offshore areas as a blue hatch pattern.

Dispersal of supracrustal clasts

The northward converging ice-flows (cf. Fig. 23a-b) appear to be responsible for the majority of glacial dispersal across the study area, not only in Rae Isthmus but over a large portion of the Wager Plateau. The distribution of supracrustal clasts in till indicates significant northward dispersal in four main areas (Fig. 27). In NTS 56I-north, supracrustal pebbles are found in till over a large area, stretching at least 55 km down-ice (north) of the nearest known outcrops of supracrustal rocks of the Penhryn Group. This wide dispersal train extends to the north-northeast and appears to begin 10 km north of the closest known contact with intrusive rocks perhaps indicating the presence of large unmapped strands of supracrustal rocks in the area. Several sites in NTS 46M-SW also have high counts of supracrustal pebbles which are likely derived from known and suspected outcrops of Prince Albert Group metasediments along Committee Bay (Tom Skulski, per. com.). In NTS 56J-south, a dispersal fan is observed over and north of undifferentiated supracrustal rocks of possible Archean age (PAG?). The northward component of this train extends 30 km further into the TGI Committee Bay project area (cf. McMartin et al., 2003b). The material is also dispersed, although not as extensively, to the latest north-northwest ice-flow direction. Similar fan-shaped dispersal trains in Cr and As in the till matrix (McMartin et al., 2003b) and in distinctive anorthosite clasts in till (McMartin et al., 2003a) were documented in the TGI project area to the west and interpreted as palimpsest glacial dispersal from two ice-flow directions.

A few sites having high counts of supracrustal clasts are thought to indicate local dispersal from previously unmapped but small outcrops of supracrustal rocks (cf. Fig. 27: e.g. 12MOB-C048 and C174). Some of these sites were visited in the field; at site 12MOB-M131 in NTS 56I-south, calcium silicate and orthoquartzite boulders and outcrops of suspected Penhryn Group rocks were observed near the edge of intrusive rock outcrops. Two previously unknown outcrops of supracrustal rocks were found in an area that corresponds to sharp aeromagnetic patterns in NTS 46L-south (12MOB-C093 and C96): magnetite-rich silicate BIF intermixed with volcanics at the first site and weathered outcrops of garnetiferous anthophyllite at the second site. Glacial dispersal from these two previously unmapped supracrustal rock outcrops or from other unknown outcrops of similar lithologies may explain the distribution of clasts west of the Beach Pt area as shown on Fig. 27.

Major oxide concentrations

Major oxide concentrations also indicate till provenance and glacial transport patterns. For example, the distribution of Al_2O_3 forms a remarkable northward converging, long-range dispersal train extending possibly as far as 125 km from unidentified bedrock sources located in a poorly mapped terrain along the coasts of Wager Bay and Roes Welcome Sound in NTS 56H and 46E (Fig. 28). LREEs, K_2O, Na_2O (cf. data and/or maps in Appendix 6) concentrations are also relatively high in this area. The Al_2O_3 pattern is coincident with converging streamlined landforms thought to result from ice streaming into Committee Bay (cf. Fig. 23a-b). Potential sources in bedrock from the south Roes Welcome Sound – outer Wager Bay area include paragneiss and derived paraluminous granite and supracrustal metasedimentary rocks. Also the boundary with higher Al_2O_3 contents in the west corresponds to the presumed ice stream margin in NTS 56I (cf. Fig. 23a-b).

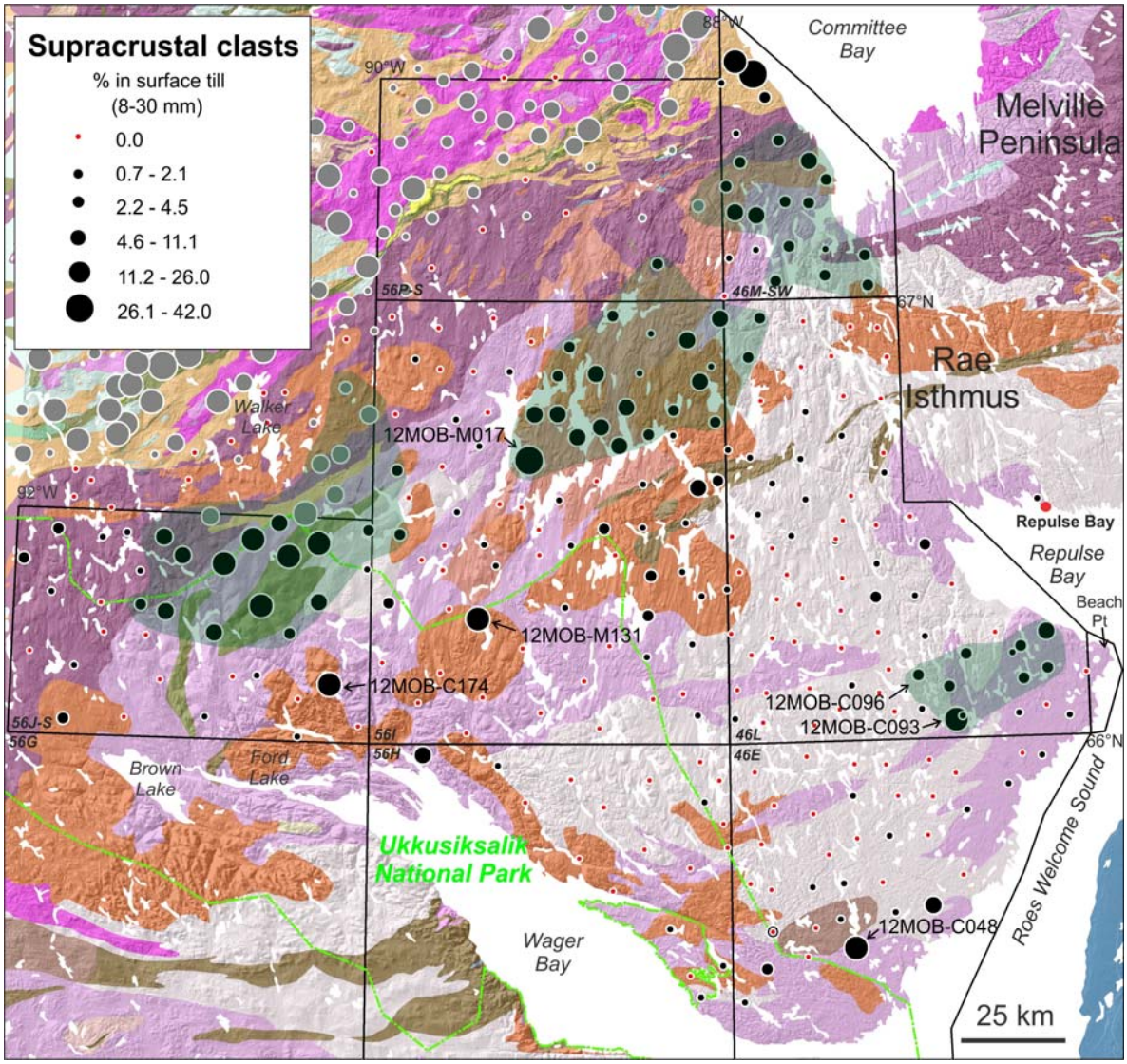

Figure 27. Distribution of supracrustal clasts in till (includes basalt and ultramafic rocks). Pebble counts from the TGI till samples (4-8 mm fraction) are shown in grey using the same classes (data from McMartin et al., 2003a). Green areas are dispersal fans of supracrustal rocks discussed in the text. Specific sample sites are also discussed throughout the report. Figure 3 provides legend for the underlying bedrock geology.

Despite the observation of weathered till at site 12MOB-C162 and preserved weathered/altered crust on bedrock at site 12MOB-C177 over the highlands north of Ford Lake, all till samples (excluding the carbonate samples) have low chemical index of alteration (CIA) values, ranging between 46.8 and 54.5. CIA values use molar proportion of oxides to evaluate the extent at which surface tills have weathered (Refsnider and Miller, 2010). These rather low CIA values suggest warm-based conditions and erosion from mostly unweathered bedrock sources were prevalent during most if not all of the last glaciation. The higher Al_2O_3 values in the western part of the study area may reflect erosion of primary Al-rich minerals (i.e. plagioclase, K-feldspar, biotite, etc.) rather than clay minerals derived from weathering. However mixing of fresh bedrock-derived silt and clay-sized material with previously weathered material can significantly dilute the CIA value therefore lower values are expected in polythermal settings (Refsnider and Miller, 2013). Additional samples in suspected patches of cold-based terrains north of Wager Bay are needed to properly evaluate the geochemical signatures of potentially preserved weathered till.

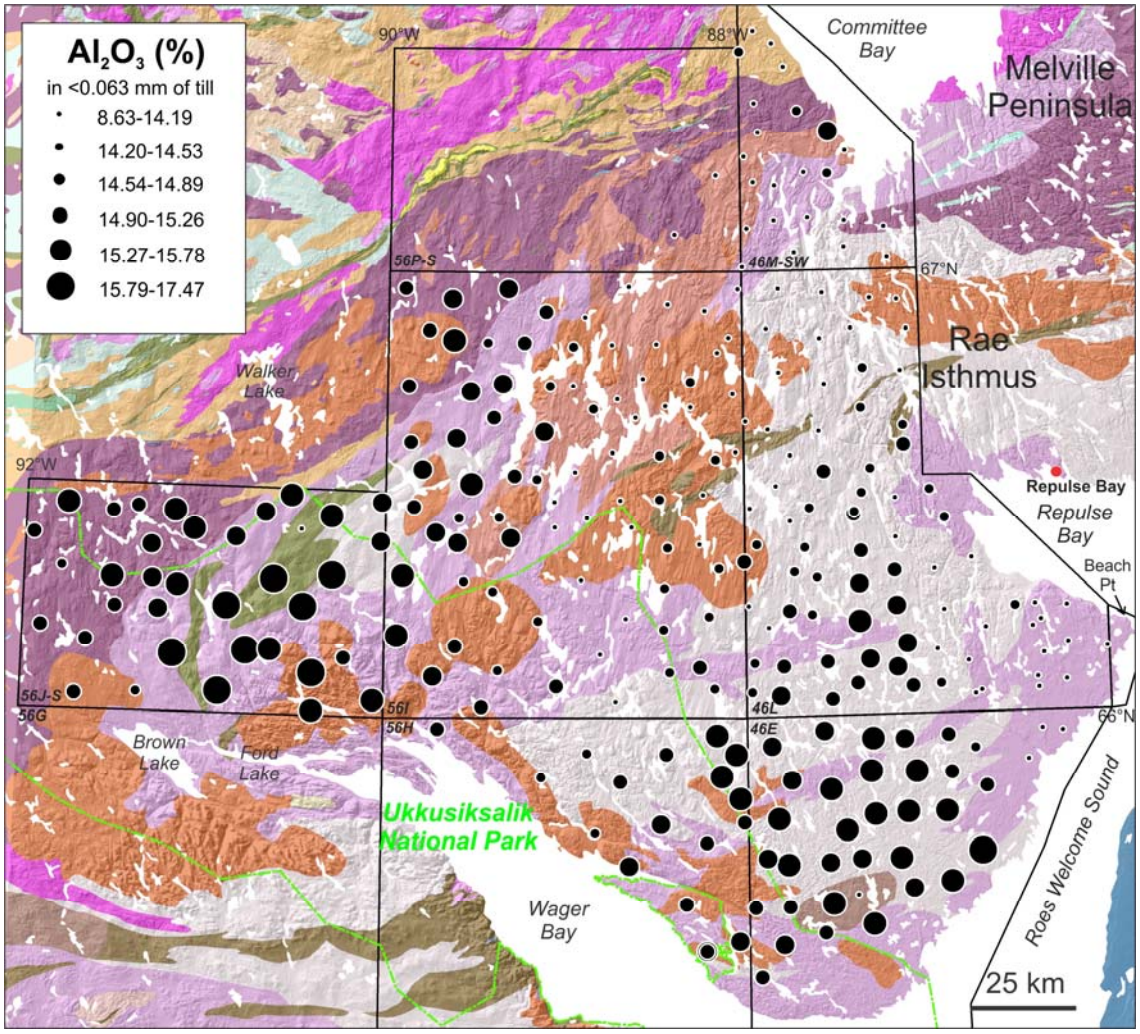

Figure 28. Distribution of Al_2O_3 in the <0.063 mm fraction of till (by ICP-ES after quenched fusion). Figure 3 provides legend for the underlying bedrock geology.

Economic implications

Diamond potential

Diamondiferous kimberlite bodies are located southwest (Nanuq) and east (Qilalugaq) of the study area (Pell, 2008; Kupsch and Farrow, 2012). The kimberlites were discovered by a combination of reconnaissance till sampling for heavy minerals, followed by airborne geophysical surveys, ground geophysical grids and further detailed till sampling, and drilling. At Nanuq, located in the Wager Bay map sheet (NTS 56G), several southeast-trending glacial dispersal trains dominated by either Cr-pyrope, eclogitic garnet and Cr-diopside, or by forsteritic olivine, were reported by Peregrine Diamonds Ltd (Pell, 2008). The indicator mineral chemistry showed evidence of sampling within the diamond stability field highlighted by the presence of pyrope garnets (both G10s and G9s) and diamond inclusion field eclogitic garnet and chromite. Dredge et al. (2006), reported the presence of KIMs in several till samples within, near, or down-ice from dispersal trains documented by industry. McMartin et al. (2013c) suggested that some of the observed forsteritic olivine grains south of Wager Bay could be derived from olivine-rich crustal rocks or from multiple kimberlite sources outside the Nanuq kimberlite field. At Qilalugaq, regional till sampling by industry yielded mantle-derived garnet, ilmenite, chromite and rare Cr-diopside forming discrete dispersal trains with variable indicator mineral abundances and mineral chemical

signatures (Kupsch and Farrow, 2012). Stornoway Diamonds Corp. (ibid) reported that regionally the indicator mineral dispersal plume has a northwest trend, parallel to predominant glacial striations, streamlined rock and till landforms. However, on a local scale, south-directed indicator mineral dispersal trains were noted within the south-central portion of the Project area near Repulse Bay. These south-trending dispersal trains were interpreted to result from the late convergent ice-flow reversal into Repulse Bay (Kupsch and Farrow, 2012, p. 23).

Examination of indicator minerals in the GEM-1 Wager Bay North project till samples and EPMA of selected olivine grains from these samples show a significant number of Mg-rich olivine grains ($>Fo_{74}$), with many of them having $> Fo_{90}$ (Figs. 29 and 30). The data indicate a large cluster of Mg-rich grains (Fo_{87-93}) with high NiO contents (0.2 and 0.6 wt. %), suggesting an origin from ultramafic rocks, potentially including mantle xenoliths (Fig. 30). The distribution of these grains shows a large zone of particularly high counts in southern NTS 56I within an area dominated by north and north-northeast ice flows (sub-region B shown in Fig. 22). Although these samples do not contain any other potential indicators of mantle xenoliths (e.g. pyrope garnet, Cr-diopside, chromite)(e.g. Fig. 31) or high concentrations of elements in the <0.063 mm fraction that would suggest a kimberlitic source (e.g. Fig. 33), a significant portion of the Mg-rich olivine grains in this area are forsteritic, relatively coarse-grained (many >0.5 mm in size with a few 1-2 mm grains) and have particularly high NiO contents (>0.45%), which may indicate kimberlite-derived macrocrysts. This area also contains site 12MOB-M131 (cf. Fig. 29) where a frost-shattered ultramafic lamprophyre boulder was found at the surface in a boulder field 80 m to the NW of the till sampling site (Fig. 34). The till sample at this site contains 13 forsteritic olivine grains and is moderately enriched in REEs (See data in Appendices 4-5-6).

The lithology of the boulder can be described as a macrocrystal carbonate-rich ultramafic lamprophyre. The rock contains disaggregated biotite-hornblende granitic xenoliths, completely altered olivine macrocrysts, partly altered glimmerite xenoliths and complexly zoned phlogopite crystals set in a fine-grained phlogopite-carbonate-rich groundmass containing clinopyroxene and abundant Fe-Ti-Cr oxides, including atoll spinels, Nb-rutile, and minor apatite and REE minerals. Granite xenoliths and xenocrysts derived from them were incorporated into the host magma at high crustal levels from rocks of the Ford Lake plutonic suite (LeCheminant et al., 1987). The sample location is within one of the largest of these composite plutons. EPMA of minerals in a thin section of the boulder shows REEs-rich phases, Cr-poor clinopyroxene, oxide phases (chromite), and a Fe-Mg carbonate matrix. One hand sample was disaggregated with an Electric Pulse Disaggregator (EPD) for heavy mineral separation and indicator mineral picking at ODM (cf. Appendix 12). The heavy mineral concentrate of this sample contains chromite and tremolite grains, and abundant apatite in the 0.25-0.5 mm fraction (cf. color photos in Appendix 12). The Nanuq kimberlites are located under and south of the Keewatin Ice Divide, and associated KIMs in the local till are distinct from those recovered from the ultramafic lamprophyre boulder. This boulder was found north of the ice divide, >100 km northeast from Nanuq, in an area dominated by northward flows at the margin of a major ice stream flow. The boulder is at the boundary of Ukkusiksalik National Park, therefore the bedrock source likely lies south, within the Park but north of Wager Bay. Location of the boulder, its distinct composition, and the regional glacial transport direction, suggest a bedrock source distinct from all known kimberlite fields in the region.

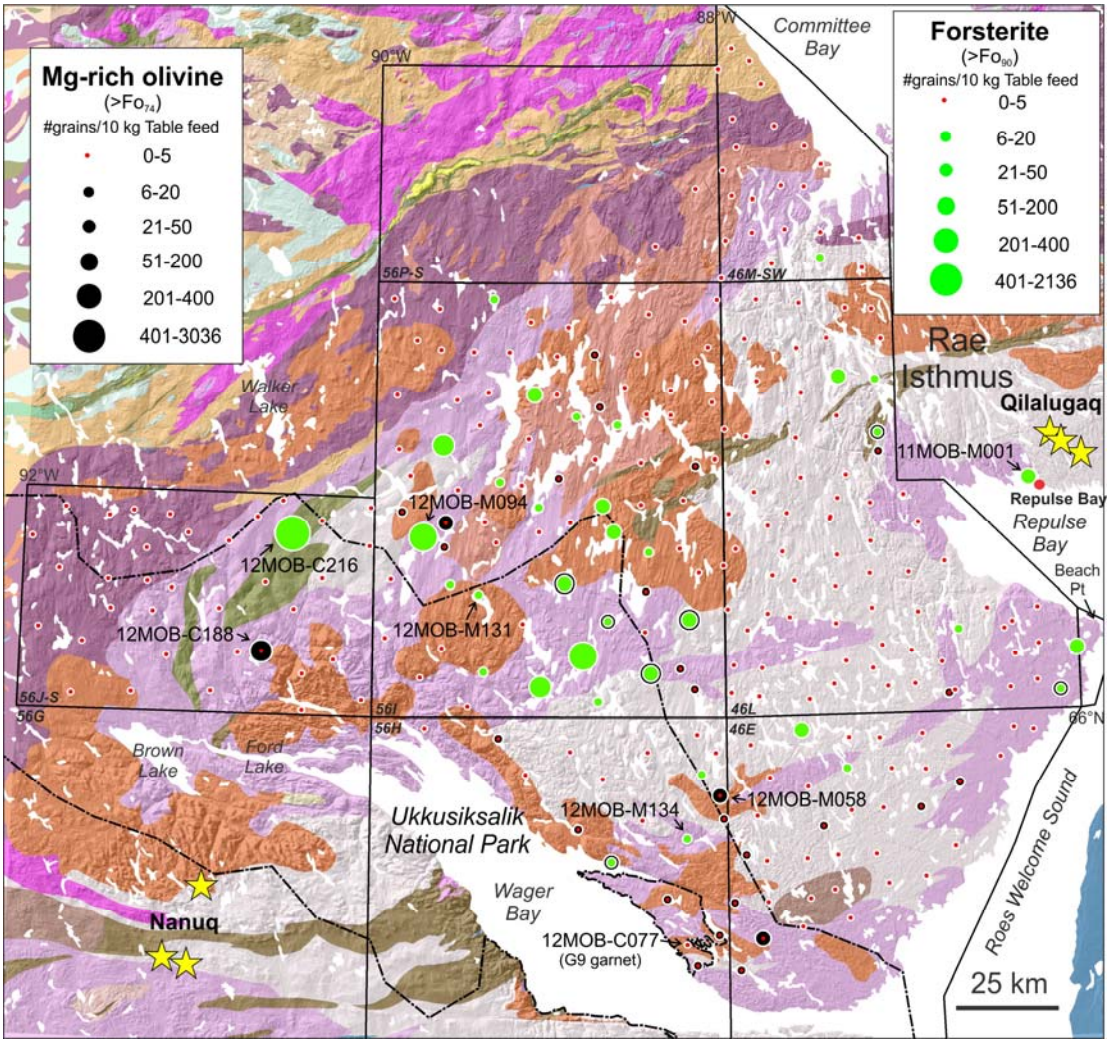

Figure 29. Distribution of total Mg-rich olivine grains in surface till (0.25-2 mm), estimated based on confirmed grains after probing. Grains with >Fo_{90} are mapped as green dots. Kimberlite fields are shown as yellow stars. Sites discussed in text are indicated. Figure 3 provides legend for the underlying bedrock geology.

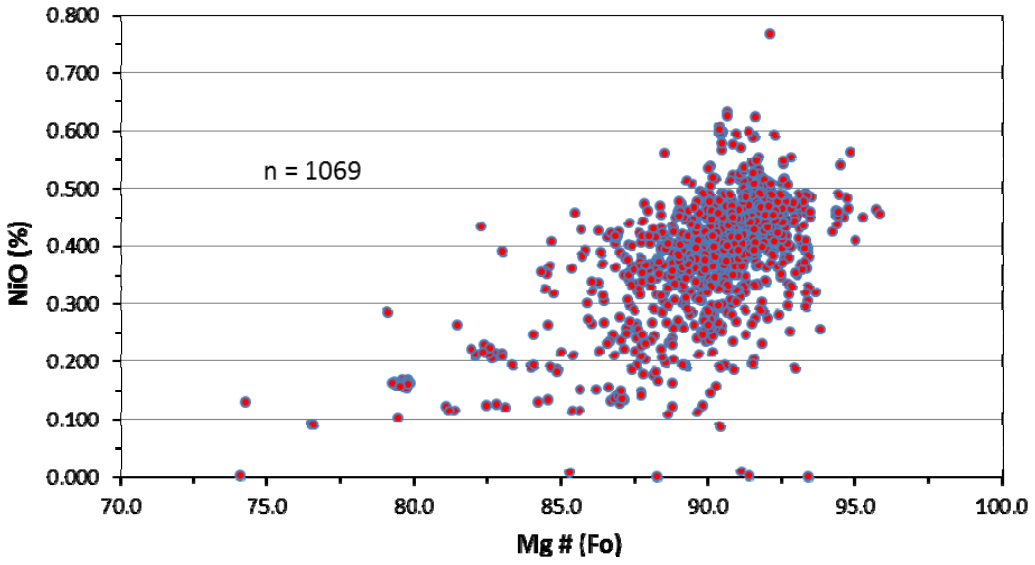

Figure 30. NiO versus Mg# (Fo) in olivine grains from all till samples.

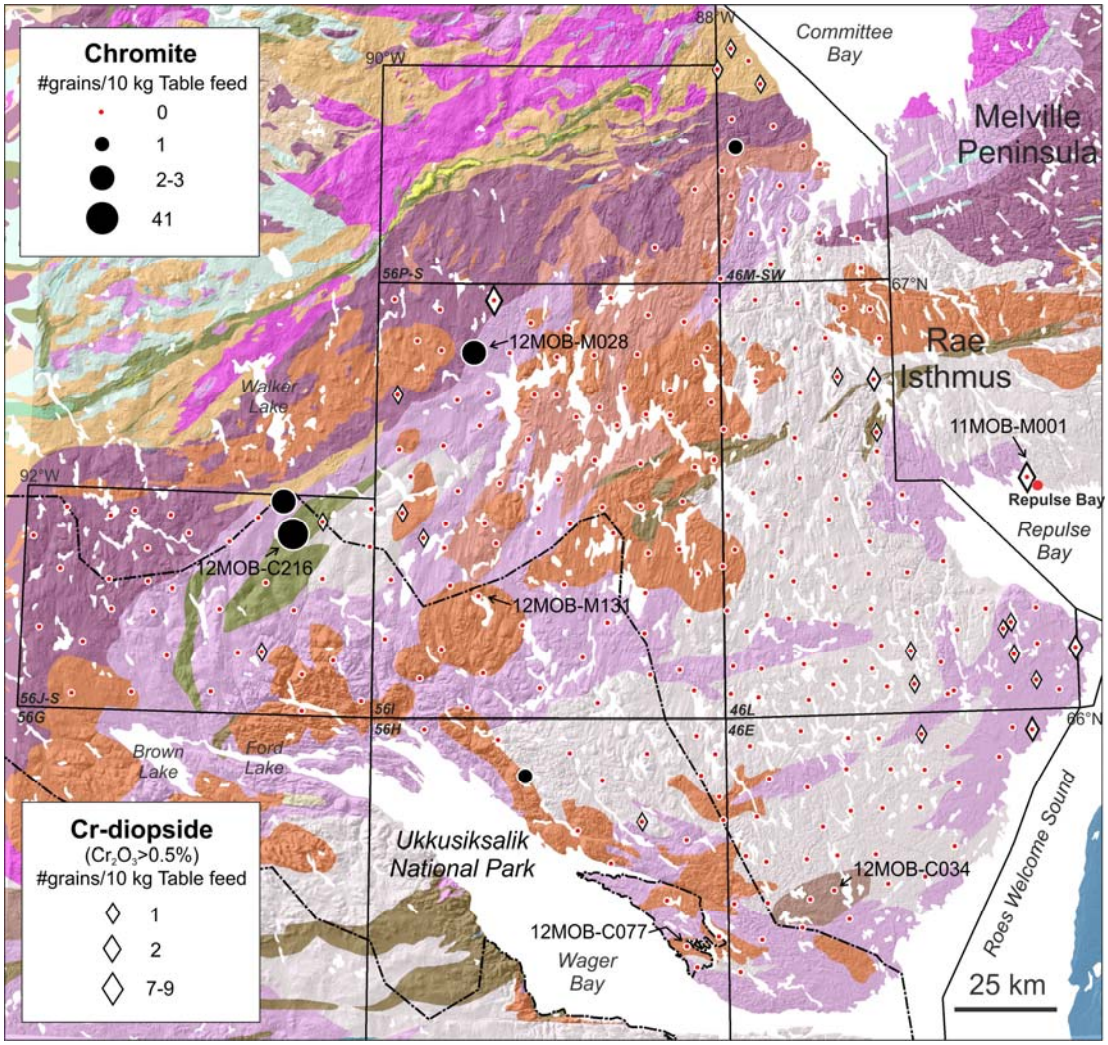

Figure 31. Distribution of chromite and Cr-diopside grains in surface till (0.25-1 mm), estimated based on confirmed grains after probing. All samples with chromite grains contain no Cr-diopside. Figure 3 provides legend for the underlying bedrock geology.

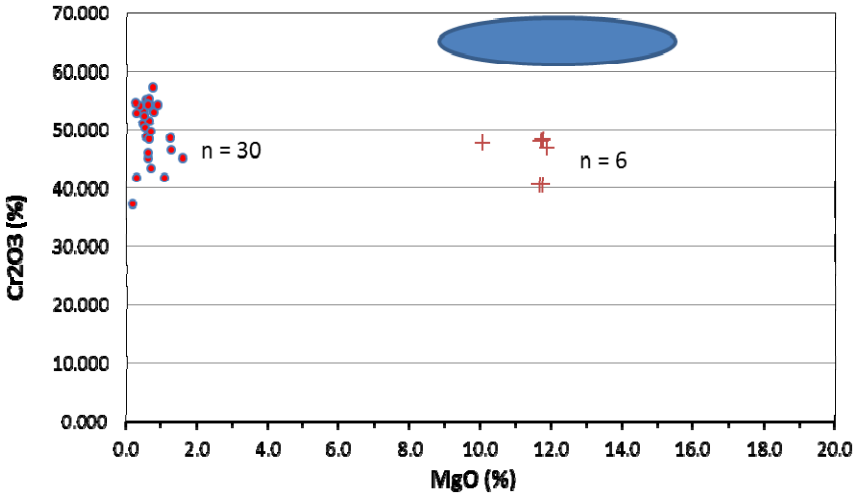

Figure 32. Cr_2O_3 versus MgO in chromite grains from till confirmed after probing (circles) and in chromite grains from the ultramafic lamprophyre boulder sample at site 12MOB-M131 (crosses). Blue field for chromite inclusions in diamonds is generalized after Fipke et al. (1995).

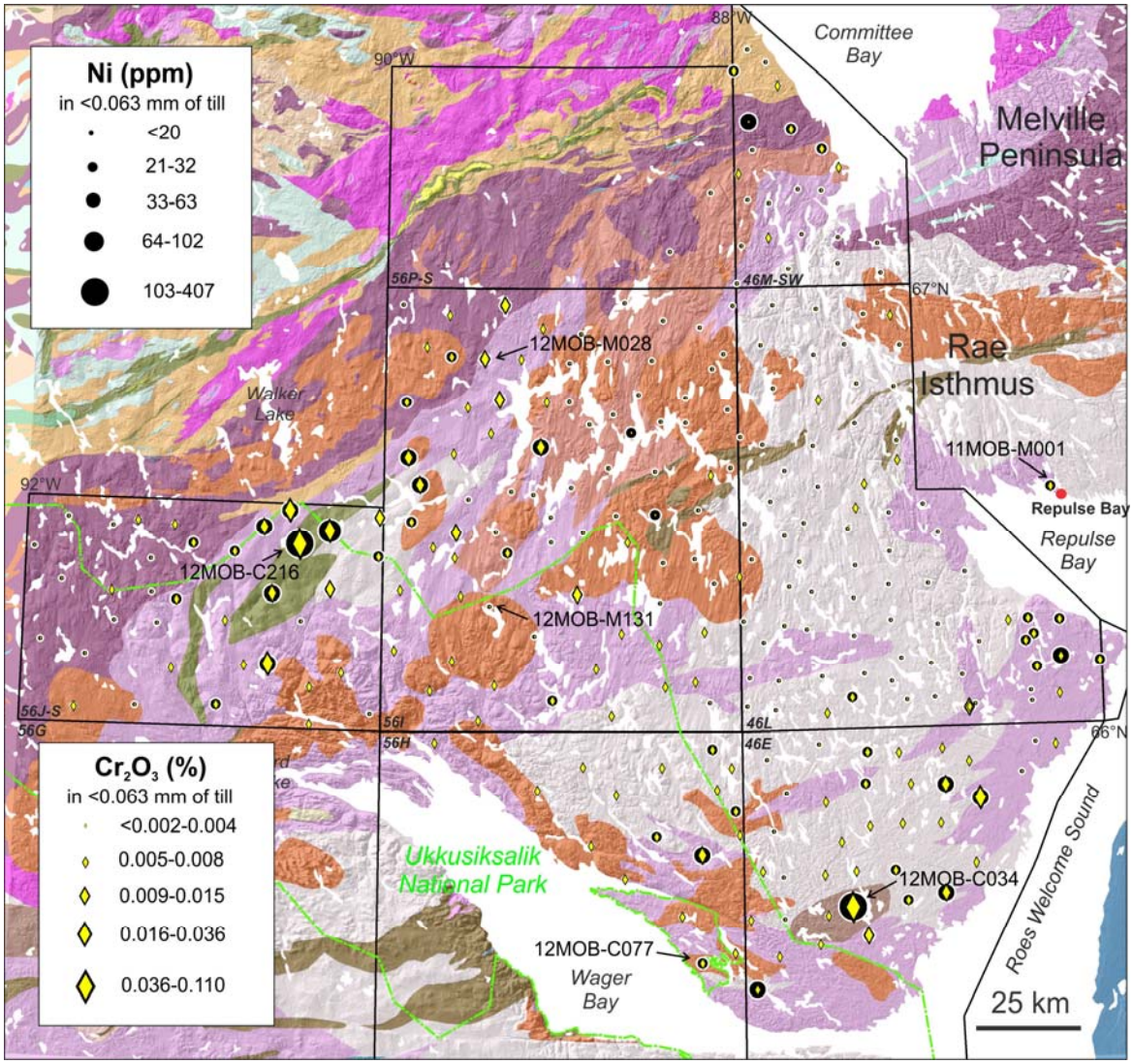

Figure 33. Distribution of Ni and Cr_2O_3 in the <0.063 mm fraction of till (by ICP-ES after quenched fusion)

Another area of relatively high counts of Mg-rich olivine (most with >Fo_{90}) in till is located in west-central 56I within an area dominated by northward ice flows (Fig. 29). Till samples from this area and from an area further north near the boundary with NTS 56P also contain some Cr-diopside, chromite (Fig. 31) and chalcopyrite grains, and show slightly elevated Ni and Cr contents in the <0.063 mm fraction (Fig. 33). Apart from sample 12MOB-M094 which contains coarse-grained (0.5-1 mm) olivine (Fig. 29), in general the Mg-rich olivine grains from this area are 0.25-0.5 mm in size and they have slightly lower NiO contents as compared with till in the large area in NTS 56I-south discussed above. Chromite composition from one till sample located in this area (12MOB-M028: Fig. 31) indicates insufficient Cr_2O_3 and MgO contents to plot in the diamond inclusion field (Fig. 32 and Appendix 11).

Two samples (12MOB-C188 and 12MOB-C216) with high counts of Mg-rich olivine grains are located in 56J-south (Fig. 29). Both samples show elevated Cr_2O_3 and Ni contents in the <0.063 mm of till (Fig. 33), especially the northern most sample (12MOB-C216) that also contains a significant number of chromite grains (n=41) (Fig. 31). Chromite composition, matrix composition and the discovery of coincident ultramafic boulders suggest a crustal mafic or ultramafic source rather than a kimberlite source for this sample.

Figure 34. Distinctive, orange-weathering colored ultramafic lamprophyre boulder at site 12MOB-M131: a) frost-shattered boulder found at the surface; b) photograph of hand-specimen.

Between the west side of Committee Bay and Beach Pt, scattered samples have a low to moderate number of forsterite and Cr-diopside grains, including sample 11MOB-M001 located outside the study area near Repulse Bay which contains 25 NiO-rich (0.28-0.55%) olivine grains (Fo_{88-92}), nine Cr-diopside and 10 low-Cr diopside grains (Fig. 29 and 31). The distribution of these KIMs indicates long-range northwestward dispersal as part of the ice stream and local reworking from the kimberlite field at Qilalugaq or from other unknown kimberlite sources.

The rest of the Mg-rich olivine grains have lower Mg# and slightly lower Ni contents (Fig. 30). The group of grains with the lowest Mg# are mainly from till samples located in the southeast part of the study area that contain no chromite or Cr-diopside grains, suggesting a distinct source from the forsteritic olivine clusters. A single G9 Cr-pyrope garnet that plots above the 85% line of Gurney (1984), indicating a source from lherzolitic mantle xenoliths found in kimberlite, was recovered from one till sample collected along Wager Bay in this general area (Fig. 29).

Base- and precious-metal potential

Several significant regional geochemical trends and local anomalies are recognized in the till data that suggests a potential for base metal mineralization. Elevated Cr_2O_3-Ni-Cr-Co-Cu-Zn-Pt±Mg±V±Mn concentrations in the <0.063 mm fraction of till, as well as high chromite and forsterite grain counts, and rare Cr-diopside, are found in a few samples collected in the western part of the region south of Walker Lake (Figs. 29, 31, 33). Large ultramafic boulder erratics varying from slightly altered to heavily weathered pyroxenite, peridotite and dunite with talc-actinolite-tremolite±magnetite±chlorite alteration, were found within this area at site 12MOB-C216 (Fig. 35). The forsterite grains (Fo_{88-92}) have moderate amounts of NiO (0.15-0.37%) and the chromite grains have a fairly limited range in composition with 0.2 to 1.6 wt.% MgO, 0.18 to 0.43 % MnO and <55 wt.% Cr_2O_3 (Appendix 11). The northward Ni-Cr-Co-Cu-chromite dispersal train mapped in the TGI Committee Bay project area immediately north of the anomalous samples (McMartin et al., 2003b) represents the down-ice part of a north-northeast-trending, 35 km-long ultramafic dispersal train originating in the present study area (Fig. 36). One of the sources of this dispersal train may be located within 100s of metres of the boulder occurrence in undifferentiated supracrustal rocks as suggested by the total airborne magnetic field map (Fig. 36). Other potential sources are located up-ice and down-ice of the boulder occurrence. The till composition, the ultramafic boulders and underlying bedrock suggest that an ultramafic source with a potential for carving stone and/or Ni-Cu-PGE mineralization lies in the area of the boulder occurrence, within and/or just north of the National Park.

Along the eastern boundary of NTS 56H, an outcrop of ultramafic rocks with tremolite-talc-serpentine±magnetite±chlorite alteration was observed as part of the regional till sampling and prospecting activities in 2012 (site 12MOB-M134: Fig. 29). Remarkable green tremolite needles are present at the outcrop surface. Huge ultramafic boulders of similar lithology were first found 14 km northeast from this outcrop (12MOB-M058) and followed up-ice to discover the outcrop site. Till at the outcrop is moderately enriched in Cr_2O_3, Ni and Cr (total) and contains 11 forsterite grains (Fo_{90-93}). The outcrop lies within the National Park and has potential as a carving stone.

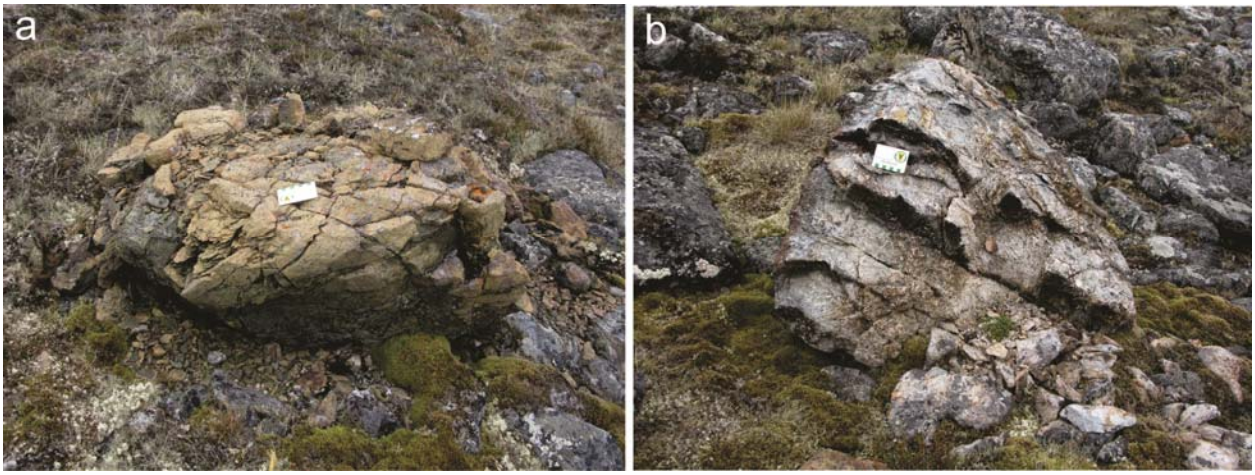

Figure 35. Ultramafic boulders found at site 12MOB-C216: a) serpentinized dunite; b) with talc alteration.

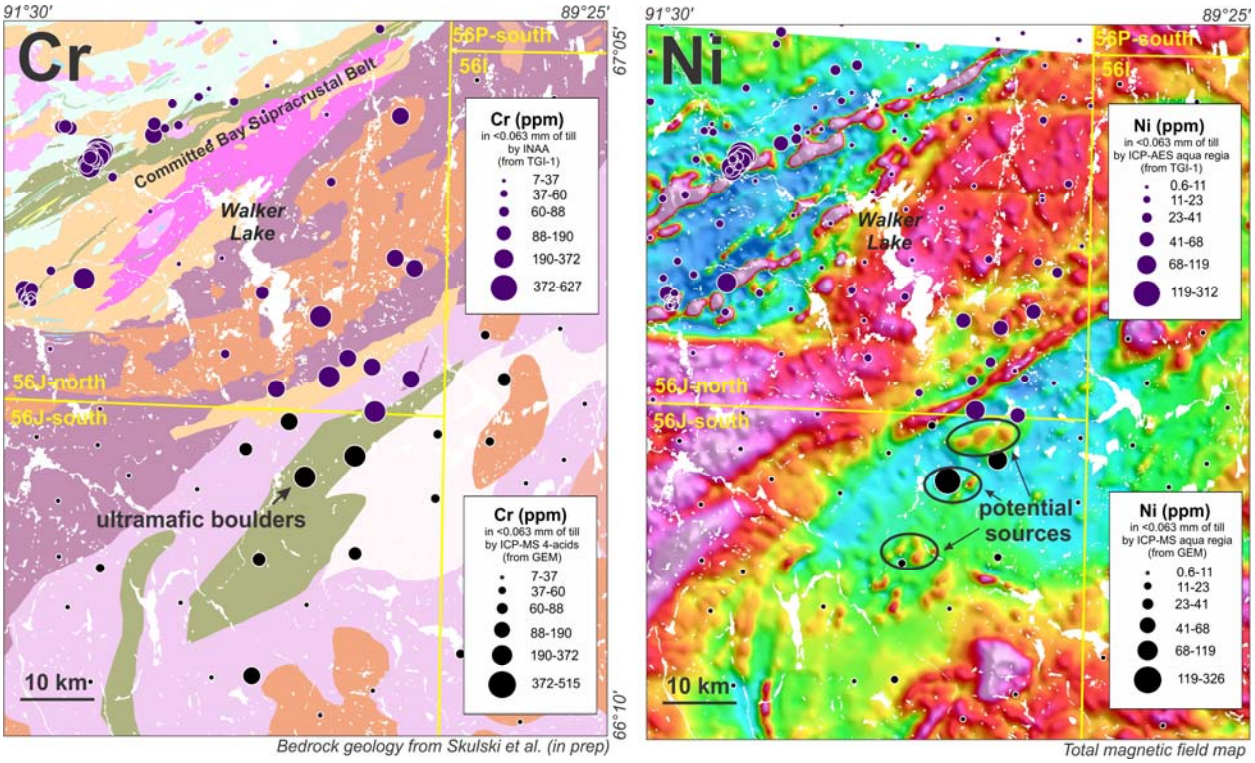

Figure 36. Distribution of Cr and Ni in the <0.063 mm fraction of surface till, Walker Lake area. TGI project results outside the study area are shown in purple (from McMartin et al., 2003a). Bedrock geology is from Fig. 3. Ni map is underlain by an airborne total magnetic field map with highly magnetic (red) to non-magnetic rocks (blue).

Moderately elevated Cr-Ni-Co-Mg-Cu-Zn-Fe concentrations, sulphide, gahnite and gold grains, and moderate counts of supracrustal clasts are found in scattered non-carbonate till samples as far as 30-35 km inland from the shores of Roes Welcome Sound and outer Wager Bay. Sample site 12MOB-C034 for example (Figs. 37 and 38), is located over suspected supracrustal rocks in an area with sharp aeromagnetic patterns, and mapped as granulite (paragneiss, migmatite, diatexite and/or mafic gneiss) by Skulski et al. (unpublished). The sample contains one chalcopyrite grain and about 800 pyrite grains in the 0.25-0.5 mm fraction, as well as two sperrylite ($PtAs_2$) grains and one gold grain in the pan concentrate. Heywood (1967) indicates a Py showing just west of 12MOB-C034 (Fig. 3). Sample 12MOB-C048 located 8 km south-southeast of 12MOBC034, directly down-ice (east-southeast) of

potential supracrustal rocks, contains 14 chalcopyrite, one molybdenite, one loellingite, six gahnite and two gold grains (Fig. 37). Other sites with variable amounts of chalcopyrite, pyrite and gahnite (e.g. 11MOB-C092, 12MOB-M144C) and variably enriched in base metals are located nearby. This area, where suspected enclaves of supracrustal gneisses spatially associated with quartzite, banded iron formation (BIF), amphibolite and ultramafic schist, has potential for base- and or precious-metal mineralization. However, more detailed till sampling, prospecting and bedrock mapping is required to better assess the mineral potential.

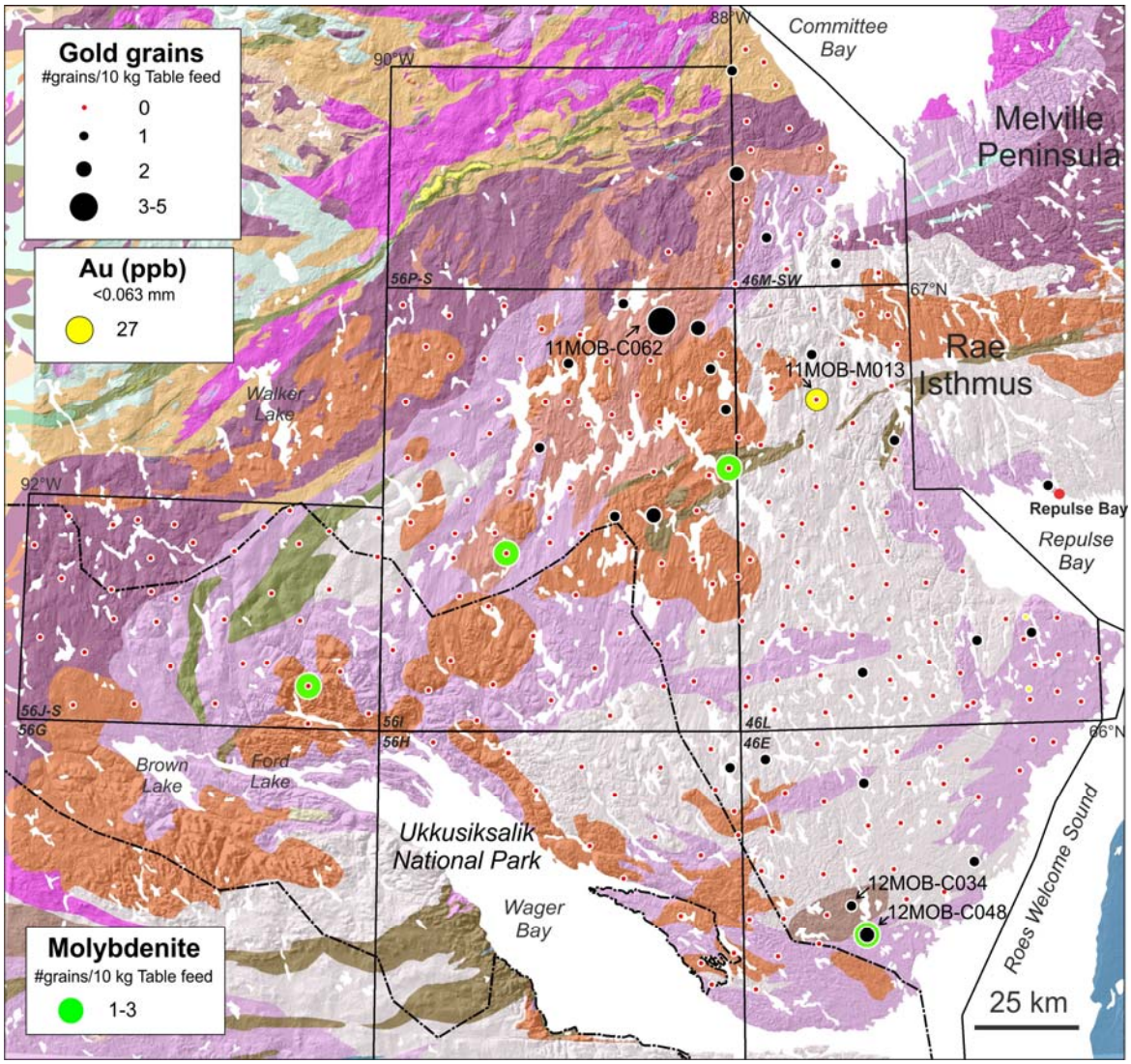

Figure 37. Distribution of gold and molybdenite grains in surface till. One sample with Au concentrations (ICP-MS, modified aqua regia) reaching 27 ppb is shown. All the other samples contained less than 5 ppb of Au.

In highly calcareous till, numerous base metals (e.g. Ag-As-Cu) as well as S concentrations south of Repulse Bay, are moderately elevated in the <0.063 mm fraction of till (Fig. 37 & cf. maps in Appendix 4). A few sulphide grains in the >0.25 mm are present as well. Relatively high contents of these chalcophile elements in the fine fraction of till suggest that the most labile minerals (i.e. sulphides) are less affected by leaching in alkaline soil conditions relative to non-carbonate till. Higher clay content for carbonate tills (4-16%) probably also reduces the rate of weathering of sulphide minerals. Therefore, the increased concentrations of certain metals in calcareous till are not related to provenance or source, but to variations in trace element mobility (e.g., Tremblay and Paulen, 2012).

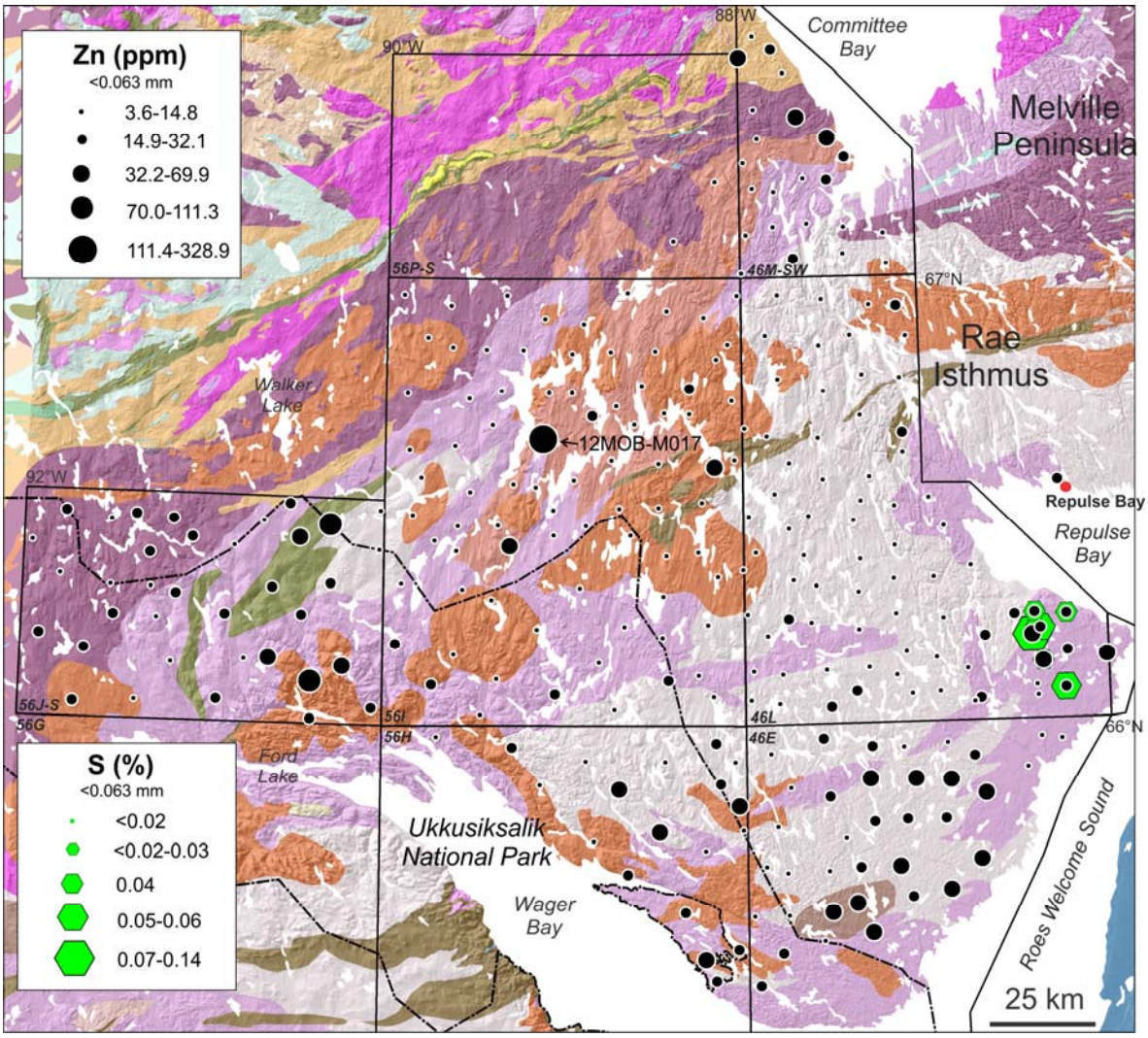

Figure 38. Distribution of Zn and S concentrations in the <0.063 mm fraction of surface till (ICP-MS, modified aqua regia). Bedrock geology is from Fig. 3.

Directly over and down-ice of known outcrops of Penhryn Group rocks and possible extents of this belt to the southwest, scattered samples contain a few gold, molybdenite (Fig. 37) and pyrite grains, and one sample (site 11MOB-M013) has an elevated gold content (27 ppb) in the <0.063 mm fraction (Fig. 37). he presence of a few gossans is known in these Paleoproterozoic rocks and into Archean tonalite gneisses west of Qamanialuk Lakes (cf. Fig. 3); at least one gossan was visited and sampled for till (Fig. 38: 12MOB-M017). Gossanous till at this site has elevated Ag-Cd-Cu-Fe-Pb-Zn concentrations but contains only a few sulphide grains (chalcopyrite and pyrite), suggesting a highly acidic and oxidizing environment that resulted in intense leaching of soluble ions from the host rock, and adsorption/precipitation of these ions as part of hydrated Fe-oxides and sulfates (e.g. West et al., 2009). Site 12MOB-M031, located 10 km down-ice (north) of this gossan, has an interesting suite of indicator minerals including 17 chalcopyrite, 1 Mn-epidote, 1 red rutile and 1 gahnite (Appendix 10). Further north close to the boundary with NTS 56P, a sample contains 5 non-pristine gold grains (Fig. 37: 11MOB-C062). Till composition in the central part of the study area, underlain by known Penrhyn Group rocks and possible extensions of this belt to the southwest, and over poorly mapped tonalitic gneiss to the north of the main belt, suggest this area has some base- and precious-metal potential that should be assessed.

REE-U metal potential

Moderately elevated Pb-Zn-U-Mo-Sn-Ba-Th±REEs concentrations and significant sand-sized fluorite grains are found in scattered till samples (Fig. 39) over and down-ice (north) of a northeast-trending series of Hudsonian calc-alkaline plutons north of Ford Lake that extend towards Committee Bay (i.e. LeCheminant, 1986; Henderson and Broome, 1990). Concentrations are particularly high near the Ford Lake batholith and over and down-ice (north-northeast) of a large circular aeromagnetic anomaly, mainly consisting of a megacrystic fluorite-biotite syenogranite (cf. LeCheminant, 1986; LeCheminant, et al., 1987). Fluorite is marginally heavy (3.01-3.25 gm/cc; up to 3.56 if high in REEs) therefore grain counts could be inaccurate and/or even higher in some of the fluorite-rich samples. Furthermore, a cluster of samples east of Qamanialuk Lakes have significant uraninite grains in the pan concentrate (5 to 100 grains – Appendix 11). Elevated Pb-Zn contents have also been reported in the clay-sized fraction of till collected over the Ford Lake batholith (Jefferson et al., 1991). The results presented here indicate the various composite granitic batholiths in the area may have potential for hosting base-REE-U metals. Interestingly, although fluorite occurs in both Nueltin and Hudson Suite granites and can therefore not be used to distinguish these intrusions, fluorite can be coarse-grained and present in open cavities of Nueltin granites, making them a more likely source of fluorite grains in till (Tony Peterson, per. com). Some of the fluorite grains in till north of Wager Bay could therefore be sourced from unrecognized Nueltin rocks, which are associated with precious and base metal occurrences further south in Keewatin.

SUMMARY

As part of the Geo-mapping for Energy and Minerals (GEM-1) Program, the Geological Survey of Canada completed a surficial geological mapping activity in the Wager Bay region of mainland Nunavut north of Wager Bay. The results of this activity provide a Quaternary geological framework that will contribute to effective management of the terrain and evaluation of mineral and park resources. This Open File report presents an overview of the Quaternary geology and discusses the economic implications for surface mineral exploration in the North Wager Bay project area. It releases the complete field database and analytical results from the 2010, 2011 and 2012 field seasons. Quaternary field observations were recorded at 699 field stations; 345 of these included ice-flow indicator measurements. Regional surface till samples were collected at an average spacing of 10-km over 30,000 km^2 (n=298) primarily for matrix geochemistry, and indicator mineral analysis of the sand fraction. Marine mollusk shell samples were collected at 16 sites for radiocarbon age determination.

Analytical results include till matrix texture, color, carbon and carbonate contents, pebble count analysis, as well as till matrix geochemistry performed on the <0.063 mm fraction using ICP-MS modified aqua regia digestion, ICP-MS 4-acid digestion, and ICP-ES/MS lithium borate fusion. QA/QC analysis was determined using field and analytical duplicates as well as control reference samples (silica blanks and primary standards). The analytical and QA/QC procedures follow the protocols for till samples collected as part of GEM projects (Spirito et al., 2011; McClenaghan et al., 2013). Heavy mineral processing, precious metal grain counts and visual indicator mineral identification of potential KIM and MMSIM® were completed for each regional till sample. Contamination, grain carryover, reproducibility and site heterogeneity were evaluated using blanks and field duplicates. The chemical composition of selected visually identified indicator minerals was determined using electron microprobe through single point per grain analysis. All the field datasets and the complete analytical results are presented in a spreadsheet format easily importable in any geographic information system.

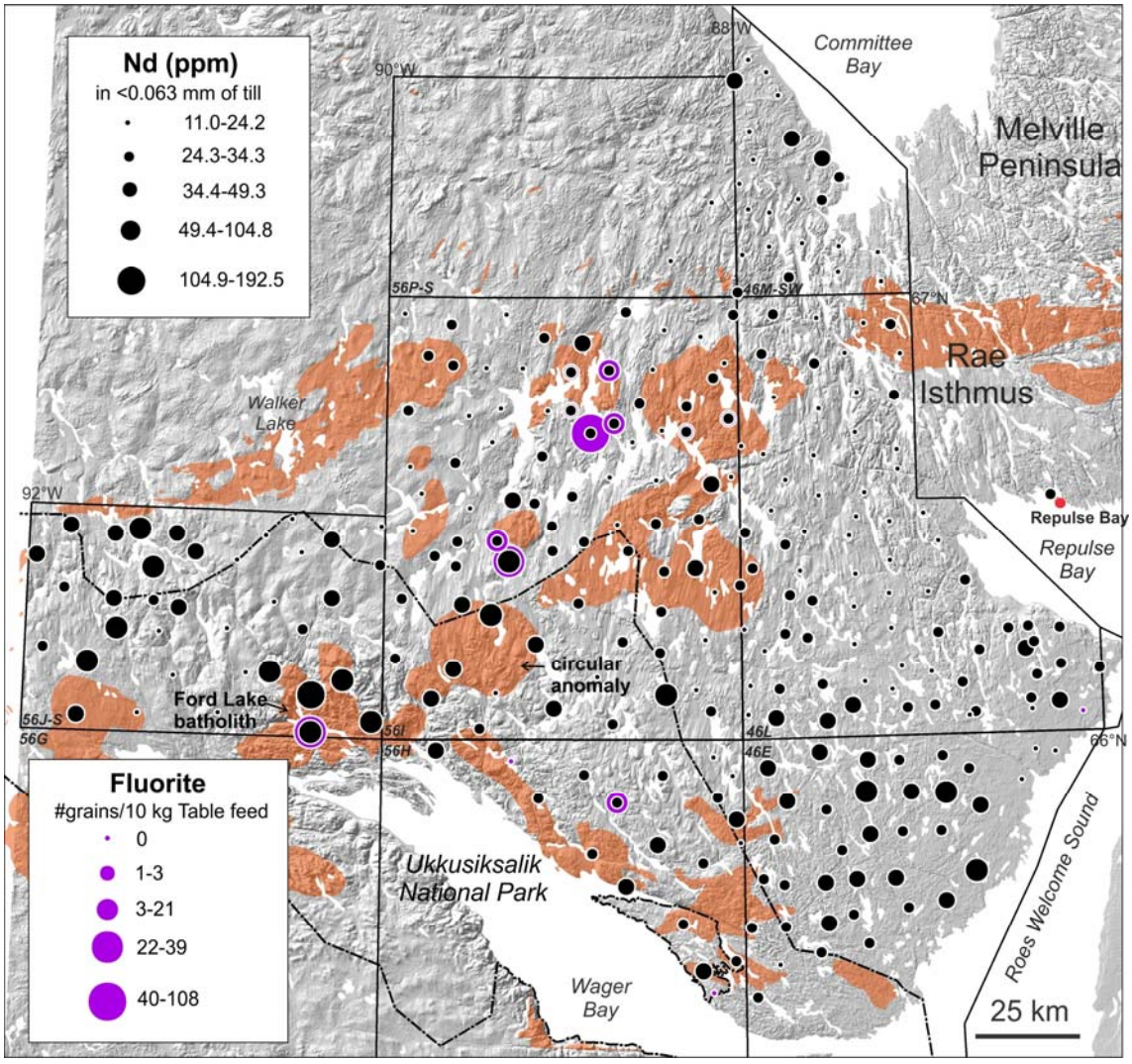

Figure 39. Distribution of Nd (by ICP-ES after quenched fusion) in the <0.063 mm fraction of till and fluorite grains in the 0.25-0.5 mm heavy mineral fraction of till. Nd is shown as an example of REE distribution. Hudsonian and possible Nueltin calc-alkaline granitic plutons are highlighted in orange from the bedrock map shown in Fig. 3.

Field observations indicate this region is key for the glacial history reconstruction of the northern part of Keewatin Ice Sector of the Laurentide Ice Sheet. Surficial mapping shows conspicuous northward-trending crag-and-tail and other streamlined landforms composed of a poorly sorted, massive, silty sand diamicton (till), with variable clast content. These landforms indicate a prevailing northward direction of ice flow from a centre of outflow lying immediately south of, or along Wager Bay. The largest landforms and early striations converge north into Committee Bay, and are thought to result from active ice streaming during the last glaciation. Early during deglaciation, Committee Bay started to open and the ice all around the bay started to converge as a result of drawdown into opened marine waters. As the ice retreated from the Chantrey Moraine System, more subtle but pervasive north to north-northwest streamlined landforms and associated striations overprinted the largest landforms. North-flowing meltwater corridors formed during deglaciation, infilling north-trending valleys near the head of the Committee Bay drainage basin. Lateral meltwater channels developed in the southern uplands at the margin of cold-based ice remnants. In the east towards Repulse Bay and Roes Welcome Sound, weakly fluted till, late striations and east-flowing meltwater corridors are associated with an ice-flow reversal and

drawdown into Repulse Bay-Roes Welcome Sound during late deglaciation. Patches of cold-based ice preserved relict, weathered and fresh glacial landscapes in the Wager Bay highlands throughout deglaciation.

Although there is evidence of multiple ice flow directions in the area, the main ice-flow trend, which converges north (NNE to NNW) towards Committee Bay, appears to be responsible for the most prominent streamlined forms and the predominant direction of glacial transport in the study area. With the exception of the cold-based highland terrains near Wager Bay, this suggests warm-based conditions during the last glaciation, with long-range dispersal under fast ice flow in Rae Isthmus and Committee Bay maintained by the convergence of ice from Keewatin Sector and Foxe Sector ice. The sharp boundary between shield-derived till and thick carbonate-rich till, as well as the weak indication of eastward dispersal, suggests that generally the late deglacial flows towards Repulse Bay had minor influence on surface till composition.

The area has potential to host diamondiferous kimberlites as shown by the significant number of Mg-rich olivines in till samples, with many of them having $>Fo_{90}$ and high NiO contents, and being coarse-grained, which may indicate kimberlite-derived macrocrysts. A frost-shattered ultramafic lamprophyre boulder was found at the surface in a boulder field within an area of high Mg-rich olivine counts. Location of the boulder, the known glacial transport history of that area, and its distinct composition, suggest a bedrock source distinct from known kimberlite fields in the region. The distribution of KIMs along the eastern side of the study area indicates long-range northwestward dispersal as part of the ice stream flow from the kimberlite field at Qilalugaq or from other unknown kimberlite sources.

The study area also has potential for base metal mineralization, particularly for Ni-Cu-PGE. A north-northeast trending, 35 km-long ultramafic dispersal train characterized by an ultramafic geochemical signature (mainly Ni-Cr-Co-Cu-Zn), high chromite and forsterite grain counts in till, and the presence of large ultramafic boulder erratics near its head, is found in the western part of the region near Walker Lake. The sources of this dispersal train may be located in undifferentiated supracrustal rocks close to the boulder occurrence, within and/or just north of the National Park. An outcrop of ultramafic rocks with striking green tremolite needles and showing potential as a carving stone was discovered within the Park north of Wager Bay as a result of boulder prospecting. A large area north of Roes Welcome Sound where poorly mapped strands of supracrustal belts are suspected, has potential for base- and or precious-metal mineralization but more detailed till sampling, prospecting and bedrock mapping is required to better assess its mineral potential. Known Penhryn Group rocks and extensions of this belt to the southwest show some base- and precious-metal potential. The REE-U metals potential of a northeast-trending series of Hudsonian calc-alkaline plutons that crosses the area remains to be determined.

ACKNOWLEDGEMENTS

This work was conducted as part of Wager Bay Surficial Geology Mapping Activity within the Melville Peninsula Multiple Metals Project of the GEM-1 Program. We are grateful to Ulanna Wityk (U. of Waterloo), Fiona Humber (Memorial U.), Sarah Hashmi (Simon Fraser U.) and Kerry Robillard (Carleton U.) for assistance in the field in 2010, 2011 and 2012; Ramsey Akkuardjuk and Lazari Katokra for bear monitoring in 2011; North Country Gold for logistical support at their Hayes River Camp in 2012; Shauna Madore and her team (GSC-Sedimentology Laboratory) for the management and analysis of the till samples; Guy Buller, Sean Eagles and Louis Robertson (GSC) for the GIS management of the

field datasets and production of field maps; Pat Hunt and Katherine Venance (GSC) for SEM and microprobe work; Dominique Paré (Consorminex Inc.) for the lithological analysis; Overburden Drilling Management (Stu Averill and Rémy Huneault) for the heavy mineral processing and indicator mineral counting; Dave Crabtree (Geoscience Laboratories, OGS) for electron microprobe analysis; Polar Shelf Continental Project for helicopter support, and Helicopter Transport Services for efficient air support during our field work. Ariane Castagner (U of Ottawa) helped to prepare figures and appendices, and completed some clast lithological analysis. We thank Tommy Tremblay (CNGO) and numerous colleagues from the GSC (David Corrigan, Art Dyke, Charlie Jefferson, Tom Skulski, Tony Peterson and Sally Pehrsson) for insightful discussions on various aspects of this work and Beth McClenaghan who provided a critical review.

REFERENCES

Averill, S.A. and Huneault, R. 2006. Overburden Drilling Management Ltd: Exploring heavy minerals; EXPLORE, Newsletter of the Association of Applied Geochemists, v. 133, p. 1-5.

Aylsworth, J.M. and Shilts, W.W. 1989a. Glacial features around the Keewatin Ice Divide: Districts of MacKenzie and Keewatin; Geological Survey of Canada, Map 24-1987, scale 1:1 000 000.

Aylsworth, J. M. and Shilts, W. W. 1989b. Glacial features around the Keewatin Ice divide: Districts of MacKenzie and Keewatin; Geological Survey of Canada, Paper 88-24, 21 p.

Bostock. 1967. Physiographic Regions of Canada. 1254A; Scale 1:5M compiled by H.S.; Geological Survey of Canada.

Boulton, G.S. and Clark, C.D. 1990. A highly mobile Laurentide ice sheet revealed by satellite images of glacial lineations; Nature, 346: 813-817.

Campbell, J.E. and McMartin, I. 2010. Surficial geological mapping in the Wager Bay area, Nunavut - filling in the gaps; 38th annual Yellowknife Geoscience Forum, Abstracts of talks and posters (Palmer, E. ed.), Northwest Territories Geoscience Office, Yellowknife Geoscience Forum Abstracts Volume 2010, p. 6-7.

Campbell, J.E. and McMartin, I. 2011. Regional glacial patterns in the Repulse Bay - Wager Bay area, Nunavut; Geohydro 2011, Proceedings of the joint meeting of the Canadian Quaternary Association and the Canadian Chapter of the International Association of Hydrogeologists, Quebec City, Quebec, August 2011, Doc. 2156.

Campbell, J.E. and McMartin, I. 2014. Surficial geology, Lefroy Bay (southwest), Nunavut; Geological Survey of Canada; CGM-P152, 1: 100 000 scale.

Campbell, J.E., Little, E.C, Utting, D. and McMartin, I. 2013a. Surficial geology, Nanuraqtalik Lake area, Nunavut; Geological Survey of Canada, CGM-P60, 1: 50 000 scale.

Campbell, J.E., Little, E.C, Utting, D. and McMartin, I. 2013b. Surficial geology, Kinngalugjuaq Mountain area, Nunavut; Geological Survey of Canada, CGM-P61, 1: 50 000 scale.

Campbell, J.E., Little, E.C, Utting, D. and McMartin, I. 2013c. Surficial geology, Atorquait River area, Nunavut; Geological Survey of Canada, CGM-P62, 1: 50 000 scale.

Campbell, J.E., Little, E.C, Utting, D. and McMartin, I. 2013d. Surficial geology, Curtis River area, Nunavut; Geological Survey of Canada, CGM-P63, 1: 50 000 scale.

Campbell, J.E., McMartin, I., Tremblay, T., Wityk, U. and Dredge, L.A. 2011. New insights on the surficial geology of the Repulse Bay area, Nunavut: implications for mineral exploration; in Fischer, B.J. and Watson, D.M. (eds), 39th annual Yellowknife Geoscience Forum Abstracts, Northwest Territories Geoscience Office, Volume 2011, p. 24-25.

Campbell, J.E., Harris, J.R., Huntley, D., McMartin, I., Wityk, U., Dredge, L.A. and Eagles, S. 2013e. Remote Predictive Mapping of Surficial Earth Materials: Wager Bay North Area, Nunavut; Geological Survey of Canada, Open File 7118.

Campbell, J.E., McMartin , I. and Dredge, L.A. 2013f. Morphology, architecture and associated landform-sediment assemblages of meltwater corridors north of Wager Bay, Nunavut; in 2013 CANQUA-CGRG Biennial Meeting, August 18-22, 2013 Edmonton, AB, Abstracts, p. 71.

Chandler, F.W., Jefferson, C.W., Nacha, S., Smith, J.E.M., Fitzhenry, K. and Powis, K. 1993. Progress On Geology and Resource Assessment of the Archean Prince Albert Group and Crystalline Rocks, Laughland Lake Area, Northwest Territories; Current Research, Part C, Canadian Shield/Recherches En Cours, Partie C, Bouclier Canadien, Geological Survey of Canada, Paper no. 93-1C, p. 209-219.

Clark, C.D. 1997. Reconstructing the evolutionary dynamics of former ice-sheets using multi-temporal evidence,

remote sensing and GIS; Quaternary Science Reviews, 16: 1067-1092.
De Angelis, H. 2007. Glacial geomorphology of the east-central Canadian Arctic; Journal of maps: 323-341.
De Angelis, H. and Kleman, J. 2005. Palaeo-ice streams in the northern Keewatin sector of the Laurentide ice sheet; Annals of Glaciology, 42: 135-144.
De Angelis, H. and Kleman, J. 2007. Palaeo-ice streams in the Foxe/Baffin sector of the Laurentide Ice Sheet; Quaternary Science Reviews, 26: 1313-1331.
De Angelis, H. and Kleman, J. 2008. Palaeo-ice-stream onsets; examples from the north-eastern Laurentide ice sheet; Earth Surface Processes and Landforms, 33: 560-572.
Deyell, C. and Sherlock, R.L. 2003. Iron-formation hosted gold occurrences in the Ellice Hills area, Committee Bay belt, Nunavut; Geological Survey of Canada, Current Research, no. 2003-C16, 11 pages.
Dredge, L.A. 1990. The Melville Moraine: sea-level change and response of the western margin of the Foxe Ice Dome, Melville Peninsula, Northwest Territories; Canadian Journal of Earth Sciences, 27 (9): 1215-1224.
Dredge, L.A. 1995. Quaternary geology of northern Melville Peninsula, Northwest Territories; Geological Survey of Canada, Bulletin 484, 114 p.
Dredge, L.A. 2000. Carbonate dispersal trains, secondary till plumes, and ice streams in the west Foxe Sector, Laurentide Ice Sheet; Boreas, 29: 144-156.
Dredge, L.A. 2001. Late Pleistocene and Holocene glaciation and deglaciation of Melville Peninsula, Northern Laurentide Ice Sheet; Géographie physique et Quaternaire, 55: 159-170.
Dredge, L.A. 2002. Quaternary geology of southern Melville Peninsula, Nunavut; Geological Survey of Canada Bulletin, 561, 110 p.
Dredge, L.A. 2004. Till geochemistry, and results of carbonate, lithological and textural analyses, southern Melville Peninsula, Nunavut; Geological Survey of Canada, Open File 4636.
Dredge, L.A. 2009. Till geochemistry, and results of lithological, carbonate and textural analyses, northern Melville Peninsula, Nunavut (NTS 47A,B,C,D); Geological Survey of Canada, Open File 6285.
Dredge, L.A. and McMartin, I. 2005. Postglacial marine deposits and marine limit determinations, inner Wager Bay area, Kivalliq region, Nunavut; Geological Survey of Canada, Current Research no. 2005-B3.
Dredge, L.A. and McMartin, I. 2007. Surficial geology, Wager Bay, Nunavut; Geological Survey of Canada, "A" Series Map 2111A, 1 sheet, 1:250 000.
Dredge, L.A., McMartin, I. and Ford, K. 2005. Till geochemistry, gamma ray spectrometry, and gold grain counts, Wager Bay area, mainland Nunavut (NTS 56 G); Geological Survey of Canada, Open File 5014.
Dredge, L.A., McMartin, I. and Kjarsgaard, I.M. 2006. Kimberlite indicator minerals in till from the Wager Bay area, mainland Nunavut: data and interpretation (NTS 56G); Geological Survey of Canada, Open File 5087.
Dredge, L.A., McMartin, I. and Campbell, J.E. 2013a. Surficial geology, Yellow Bluff (west), Nunavut; Geological Survey of Canada, CGM-P145, scale 1:100 000.
Dredge, L.A., McMartin, I. and Campbell, J.E. 2013b. Surficial geology, Daly Lake (south), Nunavut; Geological Survey of Canada, CGM-P146, scale 1:100 000.
Dredge, L.A., McMartin, I. and Campbell, J.E. 2013c. Surficial geology, Daly Lake (north), Nunavut; Geological Survey of Canada, CGM-P147, scale 1:100 000.
Dredge, L.A., Campbell, J.E. and McMartin, I. in preparation. Surficial geology, Walker Lake (south), Nunavut; Geological Survey of Canada, CGM-P151, scale 1:100 000.
Dyke, A.S. 1993. Landscapes of cold-centred Late Wisconsinan ice caps, Arctic Canada; Progress in Physical Geography, 17: 223-247.
Dyke, A.S., Moore, A. and Robertson, L. 2003. Deglaciation of North America; Geological Survey of Canada, Open File 1574.
Dyke, A.S. 2004. An outline of North American deglaciation with emphasis on central and northern Canada; In J. Ehlers and P.L. Gibbard, eds., Quaternary Glaciations: Extent and Chronology, Part II. Elsevier, Amsterdam, p. 373-424.
Dyke, A.S. and Morris, T.F. 1988. Drumlin Fields, Dispersal Trains, and Ice Streams in Arctic Canada; The Canadian Geographer, 32, no. 1: 86-90.
Dyke, A.S., Morris, T.F., Green, D.E.C. and England, J. 1992. Quaternary geology of Prince of Wales Island, Arctic Canada; Geological Survey of Canada Memoir 433, 142p., 2-1:250 000 scale maps
Dyke, A. S. and Prest, V. K. 1987. Late Wisconsinan and Holocene history of the Laurentide Ice Sheet; Géographie physique et Quaternaire, 41: 237-263.
Filzmoser, P., Hron, K., Reimann, C. 2009. Univariate statistical analysis of environmental (compositional) data: problems and possibilities; Science of the Total Environment, 407, pp. 6100-6108.
Fipke, C.E., Gurney, J.J., and Moore, R.O. 1995. Diamond exploration techniques emphasizing indicator mineral geochemistry and Canadian examples; Geological Survey of Canada, Bulletin 423, 86 p.
Garrett, R.G. 1969. The determination of sampling and analytical errors in exploration geochemistry; Economic

Geology, 64: 568-569.
Garrett, R.G. 1983. Sampling Methodology; *In* R.J. Howarth (ed) Statistics and Data Analysis in Geochemical Prospecting, Handbook of Exploration Geochemistry, Vol. 2, (G.J.S. Govett, series ed), Elsevier, Amsterdam, Chapter 4, p. 83-110.
Garrett, R.G. 2013. The 'rgr' package for the R Open Source statistical computing and graphics environment - a tool to support geochemical data interpretation; Geochemistry: Exploration, Environment, Analysis, v. 13, p.355-378.
Garrett, R.G. 2015. The GSC Applied Geochemistry EDA Package, http://cran.r-project.org/web/packages, 17 March 2015.
Giangioppi, M., Little, E.C., Ferbey, T., Ozyer, C.A. and Utting, D.J. 2003. Quaternary glaciomarine environments west of Committee Bay, central mainland Nunavut; Geological Survey of Canada, Current Research, 2003-C5.
Girard, I, Klassen, R.A. and Laframboise, R.R. 2004. Sedimentology laboratory manual, Terrain Sciences Division; Geological Survey of Canada, Open File 4823.
Helmens, K., Väliranta, M., McMartin, I., Campbell, J., Eskola, T. and Sarala, P. submitted. Global ice volume during MIS 3: substantial or insignificant?; INQUA 2015 session P16: MIS 3 glaciation. Abstract submitted as consideration for poster.
Henderson, J.R. and Broome, J., 1990. Geometry and kinematics of Wager shear zone interpreted from structural fabrics and magnetic data; Canadian Journal of Earth Sciences, v. 27, p. 590-604.
Heywood, W.W. 1967. Geology, northeastern District of Keewatin and southern Melville Peninsula, District of Franklin; Geological Survey of Canada, Preliminary Map 14-1966.
Jefferson, C.W., Smith, J.E.M. and Hamilton, S.M. 1991. Preliminary Account of the Resource Assessment Study of Proposed National Park, Wager Bay - Southampton Island Areas, District of Keewatin; Geological Survey of Canada, Open File 2351.
Jefferson, C.W., Chandler, F.W., Hulbert, L.J., Smith, J.E.M., Fitzhenry, K. and Powis, K. 1993. Assessment of mineral and energy resource potential in the Laughland Lake terrestrial area and Wager Bay marine area, N.W.T.; Geological Survey of Canada, Open File 2659.
Kleman, J., Fastook, J. and Stroeven, A.P. 2002. Geological and geomorphologically constrained numerical model of Laurentide Ice Sheet inception and build-up; Quaternary International, v. 95-96: 87-98.
Kleman, J., Jansson, K.N., De Angelis, H., Stroeven, A.P., Hättestrand, C., Alm, G. and Glasser, N.F. 2010. North American Ice Sheet build-up during the last glacial cycle, 115–21 kyr; Quaternary Science Reviews, 29: 2036-2051.
Kupsch, B. and Farrow, D. 2012. Technical report on the Qilalugaq Diamond Project, Nunavut, Canada: http://www.stornowaydiamonds.com/_resources/Qilalugaq_43-101_Technical%20Report_Jun%208-2012.pdf. Stornoway Diamond Co. NI 43-101 Technical Report, 2012.
LeCheminant, A.N. 1986. Part I: Megacrystic granite and granodiorite, Ford Lake; *In* Preliminary Account of the Geology Around Wager Bay, District of Keewatin, Henderson, J.R., LeCheminant, A.N., Jefferson, C.W., Coe, K. and Henderson, M.N., Current Research Part A, Geological Survey of Canada, Paper no. 86-1A, p. 160-164.
LeCheminant, A.N., Roddick, J.C., Tessier, A.C. and Bethune, K.M. 1987. Geology and U - Pb Ages of Early Proterozoic Calc - Alkaline Plutons Northwest of Wager Bay, District of Keewatin; Current Research Part A/Recherches En Cours Partie A, Geological Survey of Canada, Paper no. 87-1A, p. 773-782.
Lee, H.A., Craig, B.G. and Fyles, J.G. 1957. Keewatin Ice Divide; Geological Society of America, Bulletin 68, p. 1760-1761.
Little, E.C. 2004. Results of kimberlite indicator mineral analyses on till and esker samples from the Committee Bay project: Laughland Lake (56 K), Walker Lake (56 J north), Arrowsmith River (56-O south) and Ellice Hills (56 P); Geological Survey of Canada, Open File 4602.
Little, E.C. 2006. Surficial geology, Ellice Hills (north), Nunavut; Geological Survey of Canada, Open File 5016, scale 1:50 000, 5 sheets.
Little, E.C., Sherlock, R.L. and Sandeman, H.A. 2003. Evaluation of till prospecting as an exploration tool for precious and base metal mineralization in Prince Albert supracrustal rocks, central mainland Nunavut; *In* J.E. Udd and G. Bekkers (eds.) Mining in the Arctic, Proceedings of the 7th International Symposium on Mining in the Arctic, Iqaluit, Nunavut, March 30-April 1 2003, p. 35-49.
Margold M., Stokes C.R. and Clark C.D. 2015. Ice streams in the Laurentide Ice Sheet: a new mapping inventory; Earth-Science Reviews, 143: 117-146.
McClenaghan, M.B., Plouffe, A., McMartin, I., Campbell, J.E., Spirito, W.A., Paulen, R.C., Garrett, R.G., and Hall, G.E.M., 2013. Till sampling and geochemical analytical protocols used by the Geological Survey of Canada; Geochemistry, Exploration, Environment, Analysis, 13: 285-301.

McClenaghan, M.B., Parkhill, M.A., Pronk, A.G., Boldon, G.R., Pyne, R.M., and Rice, J.M., 2015. Till geochemical signatures of the Mount Pleasant Sn-W-Mo-Bi-In deposit, New Brunswick; Geological Survey of Canada, Open File 7722.

McMartin, I. and Henderson, P.J. 2004. Evidence from Keewatin (Central Nunavut) for paleo-ice divide migration; Géographie physique et Quaternaire, 58: 163-187.

McMartin, I., and Dredge, L. A. 2005. History of ice flow in the Shultz Lake and Wager Bay areas, Kivalliq Region, Nunavut; Geological Survey of Canada Current Research, 2005-B2, 10 p.

McMartin, I., Utting, D.J., Little, E.C., Ozyer, C.A. and Ferbey, T. 2003a. Complete results from the Committee Bay drift prospecting survey, central Nunavut; Geological Survey of Canada, Open File 4493.

McMartin, I., Little, E.C., Ferbey, T., Ozyer, C.A. and Utting, D.J. 2003b. Ice flow history and drift prospecting in the Committee Bay belt, central Nunavut: results from the Targeted Geoscience Initiative; Geological Survey Canada, Current Research 2003-C4, 11 p.

McMartin, I., Campbell, J.E., Dredge, L.A., Corrigan, D. and Huntley, D. 2012. Glacial history and dispersal patterns north of Wager Bay, Nunavut; *In* Watson, D.M. (compiler), 40th Annual Yellowknife Geoscience Forum Abstracts, Northwest Territories Geoscience Office, Yellowknife, NT. YKGSF Volume 2012, p. 29.

McMartin, I., Campbell, J.E., Dredge, L.A., and McCurdy, M.W., 2013a. Till composition and ice-flow indicators West of Repulse Bay: 2010 and 2011 results from the GEM Wager Bay Surficial Geology Activity; Geological Survey of Canada, Open File 7288.

McMartin, I., Campbell, J.E. and Dredge, L.A. 2013b. Pre-Late Wisconsinan shells in Rae Isthmus Ice Stream tills: implications for LIS dynamics and deglaciation of northwestern Hudson Bay; in 2013 CANQUA-CGRG Biennial Meeting, August 18-22, 2013 Edmonton, AB, Abstracts, p. 167.

McMartin, I., Wodicka, N., Bazor, D., and Boyd, B. 2013c. Till composition across the Rae craton south of Wager Bay, Nunavut: results from the Geo-mapping Frontiers' Tehery-Cape Dobbs project; Geological Survey of Canada, Open File 7417.

McMartin, I., Campbell, J.E. and Dredge, L.A. 2015. Surficial geology, Curtis Lake (north), Nunavut; Geological Survey of Canada, CGM-P204, scale 1:100 000.

McNeely, R., Dyke, A.S and Southon, J.R. 2006. Canadian marine reservoir ages, preliminary data assessment; Geological Survey of Canada, Open File 5049.

Ozyer, C.A. and Hicock, S.R. 2002. Glacial landforms and preliminary chronology of ice-movement in the Arrowsmith River map area, Nunavut; Geological Survey of Canada, Current Research, 2002-C10.

Pell, J., 2008. Technical report on the Nanuq property, Kivalliq region, Nunavut: http://www.pdiam.com/i/pdf/Nanuq-43-101-2008.pdf. Peregrine Diamonds Ltd. NI 43-101 Technical Report, 2008.

Peterson, T.D., Van Breemen, O., Sandeman, H. and Cousens, B. 2002. Proterozoic (1.85-1.75 Ga) igneous suites of the Western Churchill Province: granitoid and ultrapotassic magmatism in a reworked Archean hinterland; Precambrian Research, 119: 73-100.

Plouffe, A., McClenaghan, M.B., Paulen, R.C., McMartin, I., Campbell, J., and Spirito, W. 2013a. Processing of unconsolidated glacial sediments for the recovery of indicator minerals: protocols used at the Geological Survey of Canada; Geochemistry, Exploration, Environment, Analysis, 13: 303-316.

Plouffe, A., McClenaghan, M.B., Paulen, R.C., McMartin, I., Campbell, J.E., and Spirito, W.A. 2013b. Quality assurance and quality control measures applied to indicator mineral studies at the Geological Survey of Canada; in New frontiers for exploration in glaciated terrain, Paulen, R.C. and McClenaghan, M.B. (eds.), Geological Survey of Canada, Open File Report 7374, p. 13-19.

Prest, V.K., Grant, D.R. and Rampton, V.N. 1968. Glacial Map of Canada; Geological Survey of Canada, Map 1253A, Scale 1:5 000 000.

Refsnider K.A and Miller G.H. 2010. Reorganization of ice sheet flow patterns in arctic Canada and the mid-Pleistocene transition. Geophysical Research Letters, 37:L13502.

Refsnider, K.A, Miller, G.H. 2013. Ice-sheet erosion and the stripping of Tertiary regolith from Baffin Island, eastern canadian Arctic. Quaternary Science Reviews, 67: 176-189.

Sandeman, H.A.I., Skulski, T. and Sanborn-Barrie, M. 2004. Geology, Ellice Hills, Nunavut; Geological Survey of Canada, Open File 1794, 2 sheets, 1:100 000 scale.

Shaw, J., Sharpe, D. and Harris, J. 2010a. A flowline map of glaciated Canada based on remote sensing data; Canadian Journal of Earth Sciences, 47: 89-101.

Shaw, J., Sharpe, D.R., Harris, J., Lemkow, D. and Pehleman, D. 2010b. Digital landform patterns for glaciated regions of Canada - a predictive model of flowlines based on topographic and LANDSAT 7 data; Geological Survey of Canada, Open File 6190.

Sherlock, R.L. and Deyell, C. 2003. Geochemical and assessment report compilation for the Committee Bay region, central mainland, Nunavut; Geological Survey of Canada, Open File 1554.

Skulski, T., Paul, D., Buckle, J., Sandeman, H., Berman, R., Chorlton, L., Pehrsson, S., Rainbird, R., Davis, W. and Sanborn-Barrie, M. *in prep.* Bedrock geology and regional synthesis of the north-central Rae domain, western Churchill Province, Nunavut, Canada; Geological Survey of Canada, Open File 5577, 1:550,000 scale.

Smith, J.E.M. 1990. The glacial history of the Wager Bay area, District of Keewatin, N.W.T.; unpublished M. Sc. Thesis, Carleton University, Ottawa, 107 p.

Spirito, W.A., McClenaghan, M.B., Plouffe, A., McMartin, I., Campbell, J.E., Paulen, R.C., Garrett, R.G. and Hall, G.E.M. 2011. Till Sampling and Analytical Protocols for GEM Projects: from field to archive; Geological Survey of Canada Open File 6850.

Stokes, C.R., Tarasov, L. and Dyke, A.S. 2012. Dynamics of the North American Ice Sheet Complex during its inception and build-up to the Last Glacial Maximum. Quaternary Science Reviews, 50: 86-104.

Tarasov, L., Dyke, A.S., Neal, R.M. and Peltier, W.R. 2012. A data-calibrated distribution of deglacial chronologies for the North American ice complex from glaciological modeling; Earth and Planetary Science Letters, 315-316: 30–40.

Tremblay, T. and Paulen, R. 2012. Glacial geomorphology and till geochemistry of central Melville Peninsula, Nunavut; Geological Survey of Canada, Open File 7115.

Tremblay, T., Corrigan, D. and Paulen, R. 2010. The GEM-Minerals program on the Melville Peninsula: project summary and preliminary report: Surficial geology and exploration geochemistry; Nunavut Mining Symposium, Iqaluit, April 13-15, 2010, computer file, 24 pages.

Utting, D.J., Ward, B.C. and Little, E.C. 2009. Genesis of hummocks in glaciofluvial corridors near the Keewatin Ice Divide, Canada; Boreas, 38: 471–481.

West, L., McGown, D.J., Onstott, T.C., Morris, R.V., Suchecki, P. and Pratt, L.M. 2009. High Lake gossan deposit: An Arctic analogue for ancient Martian surficial processes?; Planetary and Space Science, 57: 1302-1311.

Wityk, U. 2014. Surficial Materials Mapping using Remote Sensing and Classification Methods: A Geological Knowledge and Statistical Approach; MSc Thesis, University of Waterloo, 116 p.

Wityk, U., Ross, M., McMartin, I., Campbell, J.E, Grunsky, E. and Harris, J.R. 2011. Developing and testing surficial materials classification using remote predictive mapping methods: preliminary results near Repulse Bay, Nunavut; Geological Association of Canada-Mineralogical Association of Canada, Joint Annual Meeting, Abstracts Volume vol. 36, Ottawa, Ontario, May 2011, p.235.

Wityk, U., Ross, M., McMartin, I., Campbell, J.E., Grunsky, E. and Harris, J.R. 2012. Developing and testing surficial sediments classification methods using remote predictive mapping, Repulse Bay area, Nunavut; *In* Proceedings of the 33rd Canadian Symposium on Remote Sensing, Abstract #1057, p. 57.

Wityk, U., Harris, J.R., McMartin, I., Campbell, J.E., Ross, M. and Grunsky, E., 2013a. Remote Predictive Mapping of Surficial Materials West of Repulse Bay, Nunavut (NTS 46M-SW, 46L-W and 46K-SW); Geological Survey of Canada, Open File 7357.

Wityk, U., Ross, M., McMartin, I., Campbell, J.E., Grunsky, E. and Harris, J.R. 2013b. Surficial materials mapping using remote sensing and classification methods, Repulse Bay area, Nunavut - geological knowledge vs. statistical approach; CANQUA-CGRG Biennial Meeting, August 18-22, 2013 Edmonton, AB, Abstracts, p. 258.